DIFFERENT MODES OF ACTIVATION OF THE FOUR REGULATORY

PYRUVATE DEHYDROGENASE KINASES BY THE E2 AND E3 BINDING

PROTEIN COMPONENTS OF THE HUMAN PYRUVATE DEHYDROGENASE

COMPLEX

by

ELENA LUISA GUEVARA

A Dissertation submitted to the

Graduate School - Newark

Rutgers, The State University of New Jersey

in partial fulfillment of the requirements

for the degree of

Doctor of Philosophy

Graduate Program in Chemistry

written under the direction of

Professor Frank Jordan

and approved by

_____

_____

_____

_____

Newark, New Jersey

May, 2017

ABSTRACT OF THE DISSERTATION

Different Modes of Activation of the Four Regulatory Pyruvate Dehydrogenase Kinases

by the E2 and E3 Binding Protein Components of the Human Pyruvate Dehydrogenase

Complex

By

Elena Luisa Guevara

Dissertation Director: Professor Frank Jordan

The focus of this study is on the human pyruvate dehydrogenase complex (PDC) consisting of six proteins including thiamin diphosphate (ThDP)-dependent pyruvate dehydrogenase (**E1p**, $\alpha_2\beta_2$-heterotetramer), the dihydrolipoamide transacetylase (**E2p**, with two lipoyl domains), dihydrolipoamide dehydrogenase (**E3**), a unique E3-binding protein (**E3BP**) and two regulatory enzymes, the pyruvate dehydrogenase kinases (**PDK1-4**) and phosphatases (**PDP1-2**). The flux of pyruvate through PDC is regulated via reversible phosphorylation (inactivation) at E1 by PDK1-4 and reactivation by PDP1-2. Up-regulation of gene expression of PDK isoforms is involved in several forms of cancer, and PDKs may be further activated by PDC by binding to the E2•E3BP core. Therefore, the PDK: E2•E3BP interaction provides new therapeutic targets. In this thesis functional kinetic studies were carried out to demonstrate significant differences in the activation of PDK isoforms by binding to E2•E3BP core: (i) PDK2 does not need activation by E2•E3BP for its efficient functioning, while PDK4 was the least effective of the four isoforms, and could not be further activated by E2•E3BP. Hence, development of inhibitors to the interaction of

PDK2 and PDK4 with PDC core is not promising. (ii) The approach to design inhibitors, which interfere with interaction with PDC is indeed promising for PDK1 and PDK3. PDK3 needs E2•E3BP core for activation, an activation best achieved by synergistic combination of E2-derived catalytic domain and tridomain.

Recently the Jordan group successfully identified the interaction loci between PDK1 or PDK2 with the E2•E3BP core. The studies described here interrogate the sites on E2•E3BP identified to interact with PDK1 or PDK2 (Glu35, Val198, Glu153, Glu209), in addition to the lipoyl-lysine sites found on L1 (Lys 46) and L2 (Lys 173). Site-directed mutagenesis was employed on the above amino acids, or 'hot spots', and E1 phosphorylation by PDK1, PDK2 or PDK3 in the presence of the constructed L1L2S mutants were tested to identify the resulting effects on overall PDC activity. These measurements will confirm whether the 'hot spots' interrogated indeed are important for the interaction of E2•E3BP with the PDKs, and will identify 'real' hot spots, against which rational drug design could be undertaken.

Additionally, the E1o component of 2-oxoglutarate dehydrogenase complex (2-OGDHc), which belongs to the super-family of the 2 oxo acid dehydrogenase multienzyme complexes, was studied in this thesis for its potential application to chiral synthesis. Specifically, the *E. coli* and human E1o were used to catalyzed chiral synthesis of α-hydroxy ketones by varying both the 2-oxo acid donor and aldehyde acceptor substrates in a carboligase-type reaction.

ACKNOWLEDGEMENTS

To my lab mates in the Dr. Jordan laboratory, Jieyu Zhou, Joydeep Chakraborty, Luying Yang, and Dr. Pradeep Nareddy, for their support and friendship during my time as a graduate student. I would also like to acknowledge Dr. Edgardo Farinas for his support and guidance during our weekly group meetings.

To my previous lab mates, Evrim Arslan, Rucha Shah and Aparna Argawal, for their friendship and support during the ups and downs of our graduate careers. I would also like to acknowledge my cousin, Vanessa Galindo, and my childhood friend, Christine Shamoon for their years of friendship and encouragement. I am forever grateful of your support and fortunate to call you my friends.

To Dr. Barry Komisaruk and all of my MBRS family for always being there for me and for the endless talks, advice and support. Thank you for always listening and helping me whenever I needed someone to talk to.

Also, I would like to acknowledge the chemistry department faculty and staff for their help and guidance during my time as a graduate student at Rutgers. Thank you to Dr. Fina Liotta, Dr. Roman Brukh, Ms. Maria Araujo, Mr. Paulo Vares, Ms. Judy Slocum, Ms. Monika Dabrowsky, and Ms. Lorraine McClendon for their continued help.

Finally, I would like to acknowledge my parents, Frank and Maria Elena Guevara, and brother, Frank L. Guevara, for their unconditional love and sacrifices without which I would not be here today. Thank you to my father, for passing down your love for science. To my aunts, uncles, and cousins who have always encouraged me to pursue my dreams. To my husband, Anthony Talarico, for always encouraging me to pursue my dreams and motivating me to never give up. To my in-laws, Anthony and Frances Talarico and the entire Talarico family, who have always supported and believed in me during this difficult journey. My sincerest gratitude and thanks to all.

DEDICATIONS

I would like to dedicate this work to my late grandparents: Francisco J. and Consuelo Guevara, Juan and Maria Paez, Manolo and Migdalia Verdura. My success would not be possible had it not been for their sacrifices as Cuban immigrants who came to the United States to provide a better life their children and grandchildren. I would also like to dedicate this work to my parents, Francisco D. and Maria Elena Guevara, and brother, Francisco L. Guevara, for their unconditional love and undeniable support during the pursuit of my doctorate degree and my entire life. As a first generation Cuban-American, I am proud to dedicate this work to my entire family as I know this is not only a milestone in my life, but in theirs as well. Last, but certainly not least, to my husband, Anthony C. Talarico, for always being my rock and, most importantly, for believing in me even when I didn't believe in myself.

TABLE OF CONTENTS

LIST OF SCHEMES

LIST OF FIGURES

LIST OF TABLES

ABBREVIATIONS

PDC, pyruvate dehydrogenase complex

E1p, pyruvate dehydrogenase, the first component of PDC

E2p, dihydroacetyllipoyl transferase, the second component of PDC

E3BP, the unique E3 binding protein of PDC

E3, dihydrolipoamide dehydrogenase, the third component of PDC and 2-OGDHc

L1, the outer lipoyl domain of E2p

L2S, the didomain (inner lipoyl and peripheral subunit-binding domains) of E2p

L1L2S, the tridomain (inner and outer lipoyl, and peripheral subunit-binding domains) of E2p

C, the E2p catalytic domain

L3S', the didomain (lipoyl and peripheral subunit-binding domains) of E3BP

PDK1-4, pyruvate dehydrogenase kinase isoforms 1-4

ThDP, thiamin diphosphate

NADH, nicotinamide adenine dinucleotide

CoA, coenzyme A

DCPIP, 2,6-dichlorophenolindophenol

iPTG, Isopropyl β-D-1-thiogalactopyranoside

Tris, tri(hydroxymethyl)aminomethane

DTT, dithiothreitol

2-OGDHc, 2-oxoglutarate dehydrogenase complex

E1o, the first component of 2-OGDHc

2-OG, 2-oxoglutarate

2-OV, 2-oxovalerate

2-OA, 2-oxoadipate

CD, circular dichroism

SDS-page, sodium dodecyl sulfate polyacrylamide gel electrophoresis

QQS, quinolone quorum sensing

HAQs, 4-hydroxy-2-alkylquinolines

HHQ, 4-hydroxy-2-heptylquinoline

PQS, 3,4-dihydroxy-2-heptylquinoline or the Pseudomonas quinolone signal

HMAQs, 4-hydroxy-3-methyl-2-alkylquinolines

HQNO, 2-alkyl-4-hydroxyquinolone N-oxides

*PA*01, *P. aeruginosa* 01 strain

FAD, Flavin adenine dinucleotide

HPLC, High-performance liquid chromatography

FTMS, Fourier-transform mass spectrometry

LC-MS, Liquid chromatography with mass spectrometry

CHAPTER 1

INTRODUCTION

1.1 HUMAN PYRUVATE DEHYDROGENASE COMPLEX (PDC)

The human pyruvate dehydrogenase complex (**PDC**) belongs to the super-family of the 2 oxo acid dehydrogenase multienzyme complexes which occupy key positions in the mitochondrial oxidation for energy production, and in the oxidation of the branched-chain amino acids[1-3]. Specifically, PDC catalyzes the conversion of pyruvate to Acetyl-CoA through irreversible oxidative decarboxylation, which links glycolysis to the citric acid cycle (Scheme 1.1)[4].
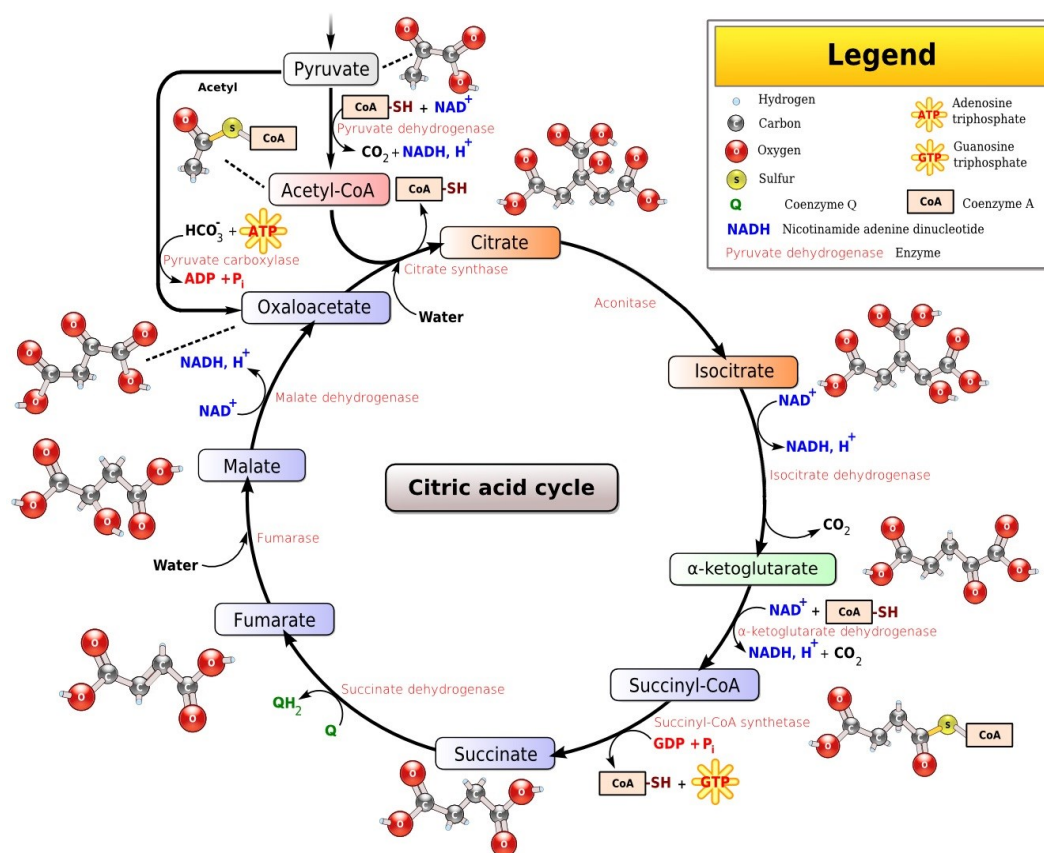
Scheme 1.1 Metabolic roles of PDC and OGDHc.

The human (or mammalian) PDC is composed of multiple copies of three principal catalytic components: 20-30 copies of the thiamin diphosphate (**ThDP**)-dependent pyruvate dehydrogenase (**E1**, an $\alpha_2\beta_2$-heterotetramer), 48 copies of the dihydrolipoamide acetyltransferase (**E2**), 12 copies of the FAD/NAD$^+$ dependent dihydrolipoamide dehydrogenase (**E3**) and two regulatory enzymes, pyruvate dehydrogenase kinase (**PDK**, four isozymes)[3,5-9] and pyruvate dehydrogenase phosphatase (**PDP**, two isozymes)[4,10,11]. In addition, there is in the mammalian PDC an E3-binding protein (**E3BP**) whose role appears to be communication between the E2 and E3 components. The 48 copies of E2 and 12 copies of E3BP form the core of the human PDC according to a "substitution" model, to which the peripheral components E1 and E3, PDKs, and PDPs are bound noncovalently[6,12]. The PDC catalyzes the oxidative decarboxylation of pyruvate with the formation of Acetyl-Coenzyme A (Acetyl-CoA) and NADH (H$^+$) according to equation 1.1 and Scheme 1.2.

Pyruvate + CoA + NAD$^+$ → Acetyl-CoA + CO$_2$ + NADH + H$^+$ **equation 1.1**

The E1 is a thiamin diphosphate (ThDP)-dependent enzyme and catalyzes two consecutive steps (Scheme 1.2): (i) the decarboxylation of pyruvate to CO$_2$ with the formation of C2α-hydroxyethylidene-ThDP (enamine) intermediate (k_2, k_3) and (ii) the reductive acetylation of the lipoyl groups covalently attached to the E2 (k_4, k_5). The E2 catalyzes the transfer of an acetyl moiety to CoA to form Acetyl-CoA (k_{-7}/k_7). The transfer of electrons from the dihydrolipoyl moieties of E2 to FAD and then to NAD$^+$ is carried out by E3.
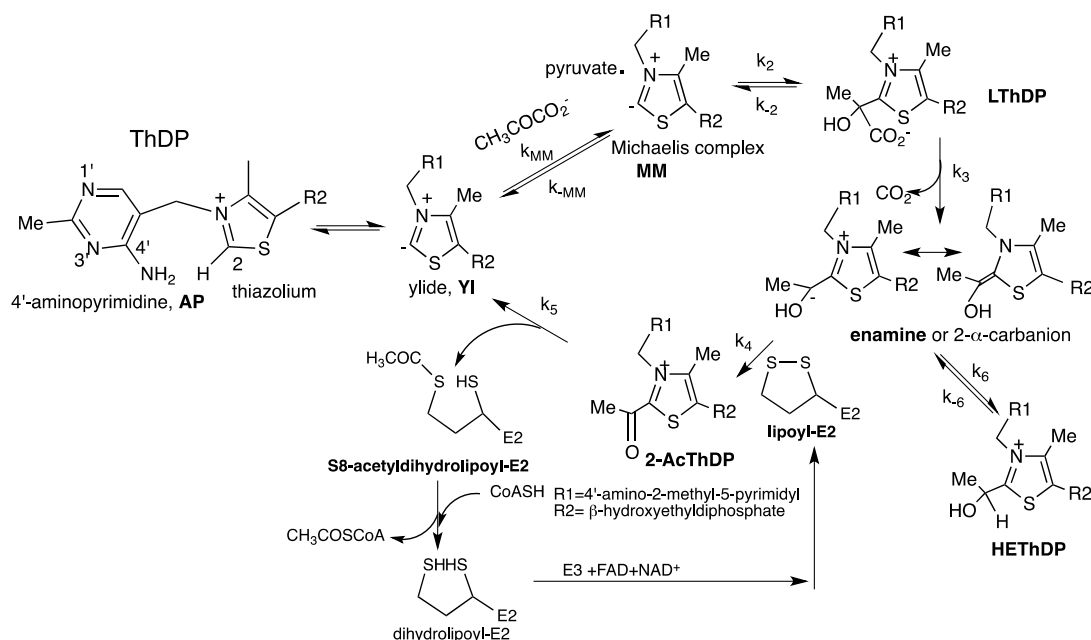
Scheme 1.2 Mechanism of Pyruvate Dehydrogenase Complex with role of ThDP and lipoic acid.

The E2 component has a multi-domain structure (Figure 1.1), comprising from the N-terminal end: two tandem lipoyl domains, the outer (**L1**) and the inner lipoyl domain (**L2**) approximately 9 kDa each, a peripheral subunit-binding domain (**PSBD**, or **S**, 4 kDa) and the acetyltransferase or catalytic domain (**C**) (28 kDa), all separated by 25-30 amino acid-long flexible linkers. The E3BP is composed of three linker-connected domains, similar but not identical to those in E2, a single lipoyl domain (**L3**), a variant of S, called **S'** to which E3 binds, and a catalytic domain **C'** that, unlike **C**, is incompetent to produce Acetyl-CoA.
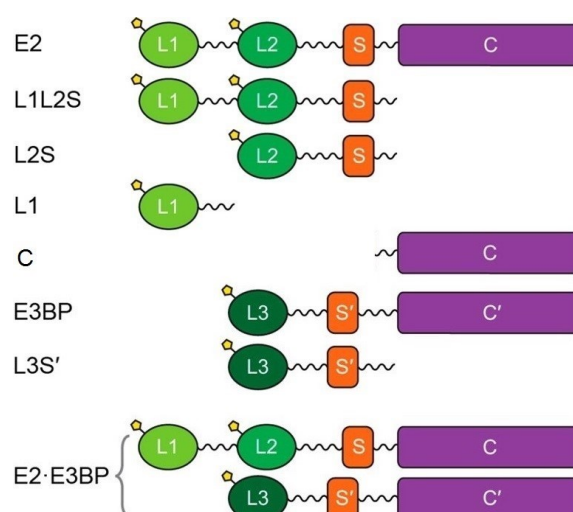
Figure 1.1 Schematic representation of the domains of the human pyruvate dehydrogenase E2•E3BP core.

1.2 2-OXOGLUTARATE DEHYDROGENASE COMPLEX (OGDHc)

The OGDHc catalyzes the rate-limiting step in the citric acid cycle (Scheme 1.1), which is the common pathway for the oxidation of fuel molecules, including carbohydrates, fatty acids, and amino acids, and catalyzes the formation of succinyl-coenzyme A (succinyl-CoA) according to equation 1.2 and Scheme 1.3[13,14].

2-oxoglutarate + CoA + NAD$^+$ → succinyl-CoA + CO$_2$ + NADH + H$^+$ **equation 1.2**

Scheme 1.3 Mechanism of 2-Oxoglutarate Dehydrogenase Complex.
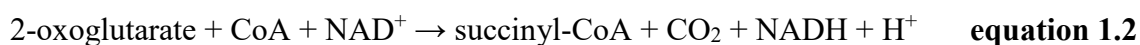
The OGDHc is composed of multiple copies of three components:[15-18] (1) thiamin diphosphate (ThDP)-dependent 2-oxoglutarate dehydrogenase (E1o), (2) dihydrolipoylsuccinyl transferase (E2o), and (3) dihydrolipoyl dehydrogenase (E3). The first two components carry out the principal reactions for succinyl-CoA formation, while the third reoxidizes dihydrolipoamide E2 to lipoamide E2. This mechanism is similar to those of other 2-oxoacid dehydrogenase complexes, including pyruvate dehydrogenase (PDC) and branched-chain 2-oxoacid dehydrogenase.

CHAPTER 2

Global View of Cognate Kinase Activation by the Human Pyruvate Dehydrogenase Complex

2.1 INTRODUCTION

The human pyruvate dehydrogenase complex (**PDC**) belongs to the super-family of the 2 oxo acid dehydrogenase multienzyme complexes which occupy key positions in the mitochondrial oxidation for energy production, and in the oxidation of the branched-chain amino acids[1-3]. The flux of pyruvate through PDC is tightly regulated by a reversible phosphorylation-dephosphorylation cycle involving the PDKs and PDPs (Figure 2.1)[3,4,19,20]. The cycle responds to NADH/NAD$^+$, Acetyl-CoA/CoA, and ATP/ADP ratios within the mitochondria. Additionally, certain effectors such as metabolites, nutritional states, and hormones influence active PDC.
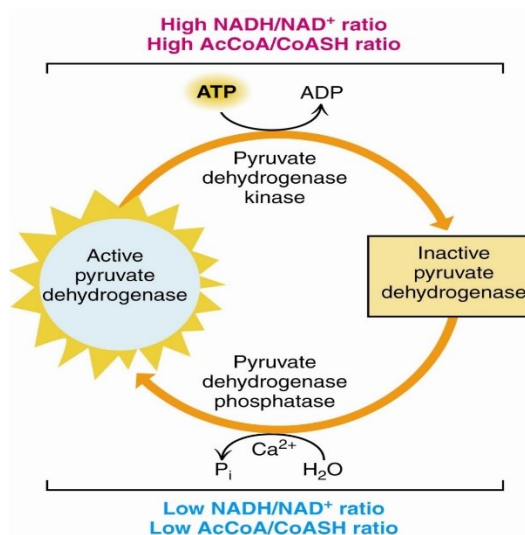
Figure 2.1 Phosphorylation-dephosphorylation cycle regulating human PDC.

The phosphorylation-dephosphorylation regulation of PDC occurs on the E1 component at three serine residues, involving the PDKs and PDPs[19,20]. The three serines in E1 are phosphorylated *in vivo* at different rates and with different specificities by the four PDKs[21-24] (Figure 2.2). Site 1 is preferentially phosphorylated, and sites 2 and 3 are sequentially phosphorylated[24,25]. Starvation and diabetes induce PDK2 and PDK4 activity in different tissues, inducing phosphorylation and inactivation of PDC[26-29].
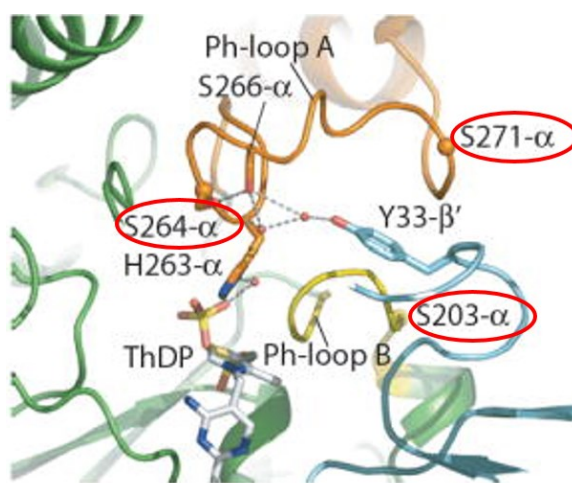
Figure 2.2 E1p Phosphorylation loops: A (259-α to 282-α in orange) and B (198-α to 205-α in yellow). Phosphorylation site 1 (S264), site 2 (S271) and site 3 (S203).

PDC is also implicated to play a role in neurodegenerative diseases, obesity, and other diseases[30-32]. More recently, PDC has been identified as a target for regulating glucose oxidation in cancer cells leading to the Warburg effect (aerobic glycolysis)[33-41], where the pyruvate is converted to lactate, partially because of upregulation of gene expression of PDK1[38,42-43], PDK2[44], and PDK3[22,45,46] (Figure 2.3).
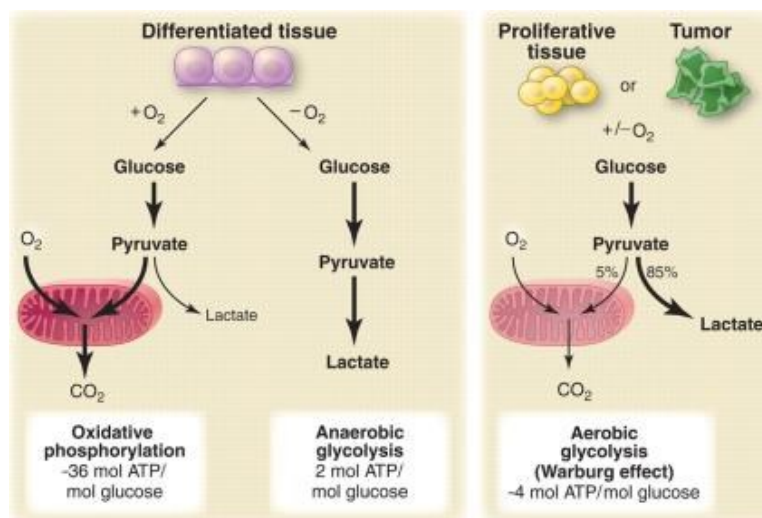
Figure 2.3 Human PDC and PDKs as gatekeeper of glucose oxidation in normal and cancer metabolism: Warburg effect in tumor cells.

Recent studies have also revealed that targeting of PDK could serve as a novel therapeutic approach in oncology. Among known inhibitors of PDKs, the glucose-lowering compound AZD7545 (AstraZeneca)[47], a mimic of dihydrolipoamide, exhibited efficient inhibition of PDK2 and PDK1 activities, but not of PDK4[48,49] (See Appendix C. for list of known inhibitors). Also, the secondary amides SDZ048–619 and their substituted analogues displayed efficient inhibition of PDKs, but these compounds did not lower glucose levels in diabetic animal models[50]. It was reported that the PDKs are activated upon binding to the E2•E3BP core: (a) The PDK2 was activated upon binding to E2[51], or to the L2S didomain, but not to the isolated L2[52]; (b) The PDK3 was activated on binding to E2, and to the isolated L2 equally well[10,51,53,54]. The availability of individually expressed PDK isozymes, E2•E3BP core and its derived domains enabled us to carry out H/D exchange mass spectrometric and NMR experiments to study the interactions of E2•E3BP with PDK1 and PDK2 in detail[55]. It became evident that there are domains on

E2, and on E3BP, in addition to the L2 that interact with PDKs[55]. Prompted by those results, we undertook this study to provide a global understanding of the role of the individual domains of the E2•E3BP core on the activation of all four PDK isoforms. For the first time, we carried out both functional kinetic and thermodynamic experiments to determine which of the domains of E2•E3BP each PDK isoform recruits to be activated. We developed two new tools to achieve these goals: (a) Monitoring the time course of PDC inactivation (according to the NADH assay of the overall PDC reaction) by a particular PDK isoform; (b) Determination of the binding affinity between E2·E3BP-derived domains labeled with a site-specifically introduced fluorophore and the four PDK isoforms. Results of these studies significantly alter our understanding of PDK activation by E2•E3BP. The significant differences in the functional activation and binding isotherms among the four PDK isoforms by PDC, suggest that interaction of PDC with PDK1 and PDK3, but not with PDK2 and PDK4, could be the targets for isozyme specific inhibitors.

2.2 MATERIALS AND METHODS

2.2.1 Materials. Ni-NTA agarose used for protein purification was purchased from GE Healthcare Life Sciences. Thiamin diphosphate (ThDP), dithiothreitol (DTT), isopropyl-β-D-thiogalactopyranoside (IPTG), NAD^+ and coenzyme A (CoA) were purchased from Affymetrix USB. Sodium pyruvate was purchased from Sigma Aldrich.

2.2.2 Wild type E1 and doubly substituted E1 variants: Bacterial Strains, Plasmids, Overexpression, and Purification.

Bacterial Strains, Plasmids and Overexpression. Recombinant wild-type E1 was overexpressed in *E. coli* BL21(DE3) cells harboring pET-28b-E1α/E1β (a co-expression

vector with coding sequences of both E1α and E1β subunits) and was purified using a Ni-NTA-agarose column as described previously[56,57]. Several doubly substituted (single phosphorylation site) E1α variants were used in this study: E1-Ser271Ala /Ser203Ala (serine residues at phosphorylation *site* 2 and *site* 3 replaced by alanine and only serine at *site* 1 available for phosphorylation), E1-Ser264Ala/ Ser203Ala (*site* 2 available) and E1-Ser264Ala/Ser271Ala (site 3 available)[23,24,58].

Wild type E1 cells were used to inoculate 5 tubes with 10 ml LB containing 35 μg/ml of kanamycin grown at 37 °C overnight. For the doubly substituted E1 variants, the cells were used to inoculate 5 tubes with 10 ml LB containing 25 μg/ml kanamycin and 100 μg/ml ampicillin grown at 37 °C overnight. The overnight culture, ~ 14 ml for a 20:1 dilution, was then used to inoculate 700 ml of LB medium containing the appropriate antibiotic, 1M $MgCl_2$ and 0.1 mg/ml thiamin chloride.   Cells were grown for about 2-2.5 h at 37 °C to OD_{600} = 0.60-0.70, then 0.50 mM IPTG was added and cells were grown overnight at 25 °C.   The cells were collected and washed with 20 mM KH_2PO_4 (pH 7.0) containing 0.15 M NaCl. Cell pellets were stored at -20 °C until purification.

Cell Disruption and Purification. Cells were dissolved in 40-50 ml of the sonication buffer containing 50 mM KH_2PO_4 (pH 7.5), 0.3 M KCl, 5 mM $MgCl_2$, 2 mM ThDP, 20 mM imidazole and 1 mM PMSF. Lysozyme was added to a final concentration of 0.60 mg/ml, and cells were incubated for 20 min on ice. Nuclease and DNase were added at 1,000 units each and cells were incubated for 20 min on ice. Then sonication was performed by using 20" on/ 20" off for 10 min and centrifugation at 16,000 rpm for 30 min. To avoid DNA contamination, 0.8 % streptomycin sulfate was added to the clear extract and cells were incubated an additional 20 min on ice with stirring to digest the DNA. Lastly, the cells

were placed on centrifugation at 16,000 rpm for 30 min until a clear cell lysate was obtained.

His6-tag wild type E1 or doubly substituted E1 variants were purified by using a His6-tag Ni-NTA column. The column was equilibrated with 150 ml of sonication buffer and 50 ml of cell lysate was applied on the column. The column was then washed with 10 column volume (CV) of sonication buffer followed by 10 CV of binding buffer containing 50 mM KH_2PO_4 (pH 7.5), 0.3 M KCl, 5 mM $MgCl_2$, 2 mM ThDP and 50 mM imidazole. The bound proteins were eluted using elution buffer containing 50 mM KH_2PO_4 (pH 7.5), 0.3 M KCl, 5 mM $MgCl_2$, 2 mM ThDP and 200 mM imidazole. The fractions containing protein were dialyzed overnight in dialysis buffer containing 50 mM KH_2PO_4 (pH 7.5), 0.30 M KCl, 1 mM $MgCl_2$, 0.5 mM ThDP and 1 mM benzamidine HCl. Buffer exchange of the purified protein to 50 mM KH_2PO_4 (pH 7.5), 0.15 M KCl, 1 mM $MgCl_2$, 0.5 mM ThDP and 1 mM benzamidine HCl followed by protein concentration was done using a Millipore concentration unit. For the doubly substituted E1 variants, 10 % glycerol was added for protein storage. Purified proteins were stored in -80 °C and purity was determined by SDS-page.

2.2.3 E2•E3BP: Bacterial Strains, Plasmids, Overexpression, and Purification. Recombinant E2•E3BP core was overexpressed in *E. coli* cells containing the pACYC-T7-E2•E3BP vector and was purified as described previously[6]. A frozen cell stock was streaked on LB agar plates containing 35 µg/ml chloramphenicol and incubated at 37 °C overnight. A single colony was used to inoculate 10 ml of LB medium containing 35 µg/ml chloramphenicol grown overnight at 37 °C. The overnight culture was used to inoculate

700 ml of LB medium containing 35 µg/ml chloramphenicol and 0.3 mM lipoic acid. The culture was induced with 0.5 mM IPTG and incubated at 25 °C with shaking overnight. The cells were precipitated at 5,000 rpm at 4 °C, and stored at -20 °C. The cells were resuspended in 50 mM sodium phosphate, 10 mM Tris (pH 8.0) containing 0.1 M NaCl, 0.1 % Pluronics, one cOmplete ULTRA Roche® tablet and 0.3 mg/ml lysozyme and incubated on ice for 20 min. The cells were sonicated for 6 min (10 s pulsar on and 30 s pulsar off) using the Sonic Dismembrator Model 550 from Fisher Scientific. The lysate was centrifuged at 17,000 rpm at 4 °C for 30 min. To the clear lysate, PEG-8000 (50% w/v) was added dropwise while stirring on ice to 8% (v/v) and was incubated on ice for 15 min. The precipitated protein was removed by centrifugation at 17,000 rpm for 20 min and discarded. To the supernatant, an additional 8% volume of PEG was added and the precipitate was collected by centrifugation. To the 8-16% PEG precipitate, 15 ml of buffer A' (50 mM KH_2PO_4 (pH 7.2) supplemented with 0.5 mM EDTA, 0.2 M NH_4Cl, 1.0 mM β-mercaptoethanol and 0.1 % Pluronics was added to dissolve the pellet. DNase I (1,000 units), Nuclease (500 units) and 5 mM $MgCl_2$ was added, incubated on ice for 1 hour and clarified via centrifugation. The supernatant was applied on the Hiprep 26/60 Sephacryl-S-300 HR column equilibrated with buffer A'. Protein containing fractions were mixed with polyethylenimine (MW ~60,000) to a final level of 0.05 % and the precipitate formed was removed by centrifugation. E2•E3BP was pelleted by ultracentrifugation (Sorvall Discovery 90SE) of supernatant in a T-865 Fixed Angle Rotor at 35,000 rpm for 4 h and 4°C. Pellets were re-suspended in 500 µl of buffer A' containing 0.3 M additional $NH4Cl$ (total, 0.5 M) and left overnight (16 h). Resulting mixture was clarified by centrifugation and pellet was dissolved in 50 mM KH_2PO_4 (pH 7.2) supplemented with 0.4 M NH_4Cl, 0.5

M EDTA and 1.0 mM β-mercaptoethanol. The resulting purified protein was concentrated and stored at -80 °C and purity was confirmed by SDS-page.

2.2.4 C-terminally truncated E2•E3BP proteins: Bacterial Strains, Plasmids, Overexpression, and Purification. Construction of the plasmids for the following recombinant E2•E3BP-derived domains used in this study: L1, containing the outer lipoyl domain and linker (residues 1−98); the L2S didomain containing the inner lipoyl domain (L2), second hinge region, peripheral subunit-binding domain (S), and third hinge region (residues 128−330); the L1L2S tridomain, which comprises L1, L2, both hinge regions, and the subunit-binding domain S (residues 1−330); the L3S' didomain of E3BP (residues 1−230), all expressed from pET28b in *E. coli* BL21 (DE3) cells and purified using Ni Sepharose 6 Fast Flow column[59]. For each, an *E. coli* frozen stock was used to streak on LB agar plates containing 35 μg/ml kanamycin and incubated at 37 °C overnight. A single colony was used to inoculate 10 ml of LB medium containing 35 μg/ml kanamycin. The overnight culture was used to inoculate 700 ml of LB medium containing 35 μg/ml kanamycin and 0.3 mM lipoic acid. The culture was induced with 0.5 mM IPTG and was incubated at 30 °C with shaking overnight. The cells were collected at 4,500 rpm at 4 °C, and stored at -20 °C. The cells were resuspended in 50 ml of 20 mM KH_2PO_4 (pH 7.5) containing 0.3 M KCl, 1 mM benzamidine HCl, 1 mM PMSF, 0.6 mg/ml lysozyme and incubated on ice for 20 min. Dnase I (1,000 units), Nuclease (1,000 units) and 1 mM $MgCl_2$ were added and incubated on ice for 20 min. The cells were sonicated for 10 min (20 s pulsar on and 20 s pulsar off) using the Sonic Dismembrator Model 550 from Fisher Scientific. The lysate was clarified via centrifugation at 17,000 rpm at 4 °C for 30 min. The

supernatant was applied to a Ni Sepharose 6 Fast Flow Column and equilibrated with 20 mM KH_2PO_4 (pH 7.4) supplemented with 0.3 M KCl, 1.0 mM benzamidine HCl and 20 mM imidazole (binding buffer) followed by the same buffer except 50 mM imidazole (washing buffer). The enzyme was eluted with 20 mM KH_2PO_4 (pH 7.4) containing 0.3 M KCl, 1.0 mM benzamidine HCl and 300 mM imidazole. Fractions with enzyme were combined and dialyzed against 20 mM KH_2PO_4 (pH 7.4) containing 0.3 M NaCl and 1 mM benzamidine HCl. Buffer exchange was performed on the purified protein into 20 mM KH_2PO_4 (pH 7.4) with 0.15 M NaCl and 1.0 mM benzamidine HCl. Next, the enzyme was concentrated and stored at -80 °C and the purity was confirmed by SDS-page.

2.2.5 E3: Bacterial Strains, Plasmids, Overexpression, and Purification.

Recombinant E3 was overexpressed in *E. coli* cells and was purified as described earlier[60]. An *E. coli* frozen stock of E3 was streaked on LB agar plates containing 25 μg/ml kanamycin and 100 μg/ml ampicillin and was incubated at 37 °C overnight. A single colony was used to inoculate 10 ml of LB medium containing 25 μg/ml kanamycin and 100 μg/ml ampicillin. The overnight culture was used to inoculate 700 ml of LB medium containing 25 μg/ml kanamycin and 100 μg/ml ampicillin. The culture was induced with 0.5 mM IPTG and was incubated at 25 °C with shaking overnight. The cells were collected at 4,500 rpm at 4 °C, and stored at -20 °C. The cells were resuspended in 50 ml of 50 mM KH_2PO_4 (pH 7.5) containing 0.3 M KCl, 1 mM PMSF, 0.6 mg/ml lysozyme and incubated on ice for 20 min. DNase I (1,000 units), Nuclease (1,000 units) and 1 mM $MgCl_2$ were added and incubated on ice for 20 min. The cells were sonicated for 10 min (20 s pulsar on and 20 s pulsar off) and centrifugation at 16,000 rpm for 30 min. To the lysate, 0.8 %

streptomycin sulfate was added and incubated an additional 20 min on ice with stirring to digest the DNA, then clarified via centrifugation.   The clarified lysate was applied to a Ni Sepharose 6 Fast Flow Column and equilibrated with 50 mM KH_2PO_4 (pH 7.5) supplemented with 0.3 M KCl and 30 mM imidazole (binding buffer), followed by the same buffer except 50 mM imidazole (washing buffer). The enzyme was eluted with 50 mM KH_2PO_4 (pH 7.5) containing 0.3 M KCl and 300 mM imidazole.   Fractions with enzyme were combined and dialyzed against 50 mM KH_2PO_4 (pH 7.5) containing 0.3 M KCl, 1 mM benzamidine HCl and 25 μM FAD. Buffer exchange was performed on the purified protein into 50 mM KH_2PO_4 (pH 7.5) with 0.2 M KCl, 1.0 mM benzamidine HCl and 25 μM FAD. Next, the enzyme was concentrated and stored at -80 °C and the purity was confirmed by SDS-page.

2.2.6 PDK1-4: Bacterial Strains, Plasmids, Overexpression, and Purification. Recombinant rat PDK1, rat PDK2, human PDK3 and rat PDK4 were overexpressed and purified individually from *E. coli* BL21(DE3) cells transformed with pPDK expression vector using protocols reported in the literature[23,51,61,62]. According to the literature, the amino acid sequences of human PDK1 has 93% identity with rat PDK1, while human PDK2 has 96% identity with rat PDK2[15]. Human PDK3 shares 68% and 67% identity with human PDK1 and human PDK2, respectively[8].

The following protocol was used to purify all four of the PDKs where only the buffer system varied by PDK. An *E. coli* frozen stock of PDK1, PDK2, PDK3 or PDK4 was streaked on LB agar plates containing 45 μg/ml kanamycin and was incubated at 37 °C overnight. A single colony was used to inoculate 10 ml of LB medium containing 45

µg/ml kanamycin grown overnight at 37 ᵒC. The overnight culture was used to inoculate 700 ml of LB medium containing 45 µg/ml kanamycin. The culture was induced with 0.5 mM IPTG and was incubated at 25 ᵒC with shaking overnight. The cells were collected at 4,500 rpm at 4 °C, and stored at -20 °C. The cells were resuspended in 50 ml sonication buffer [PDK1/PDK2: 50 mM KH_2PO_4 (pH 7.5) containing 0.3 M KCl, 1 mM $MgCl_2$, 5 mM β-mercaptoethanol, 10 mM imidazole and 0.5% (w/v) Triton X-100 or for PDK3/PDK4: 50 ml of 20 mM Tris/HCl (pH 8.0) supplemented with 0.3M NaCl, 5.0 mM β-mercaptoethanol, 10 mM imidazole and 0.5% (w/v) Triton X-100]. To each, one cOmplete ULTRA Roche® tablet and 0.6 mg/ml lysozyme were added and incubated on ice for 20 min. Dnase I (1,000 units), Nuclease (1,000 units) and 1 mM $MgCl_2$ were added and incubated on ice for 20 min. The cells were sonicated for 10 min (20 s pulsar on and 20 s pulsar off) and centrifugation at 16,000 rpm for 30 min. To the lysate, 0.8 % streptomycin sulfate was added and incubated an additional 20 min on ice with stirring to digest the DNA, then clarified via centrifugation. The clarified lysate was applied to a Ni Sepharose 6 Fast Flow Column and equilibrated with 10-50 CV binding buffer [PDK1/PDK2: 50 mM KH_2PO_4 (pH 7.5) supplemented with 0.3 M KCl, 1mM β-mercaptoethanol, 30 mM imidazole, 0.05% Triton X-100 or PDK3/PDK4: 20 mM Tris/HCl (pH 8.0) supplemented with 0.3M NaCl, 15 mM imidazole]. For PDK3/PDK4, additional column wash was applied using the following washing buffer [20 mM Tris/HCl (pH 8.0) supplemented with 0.3M NaCl, 25 mM imidazole. The enzyme was eluted with 50 mM KH_2PO_4 (pH 7.5) containing 0.3 M KCl, 1.0 mM β-mercaptoethanol, 300 mM imidazole and 0.05% Triton X-100 for PDK1/PDK2 and 20 mM Tris/HCl (pH 8.0) supplemented with 0.3M NaCl, 100 mM imidazole for PDK3/PDK4. Fractions with

enzyme were combined and dialyzed against the following buffer for PDK1/PDK2: 50 mM KH_2PO_4 (pH 7.5) containing 0.3 M KCl, 1.0 mM DTT, 1.0 mM benzamidine HCl. Buffer exchange was used for PDK3/PDK4 into the following buffer: 20 mM Tris/HCl (pH 8.0) supplemented with 0.3M NaCl, 5.0 mM DTT, 0.5 mM EDTA and 1.0 mM benzamidine HCl plus 10 % (v/v) glycerol for storage. PDK1/PDK2 were further purified by gel filtration (HiPrep 16/60 Sephacryl S-100 column) using 50 mM KH_2PO_4 (pH 7.5) plus 0.2 M KCl as the running buffer and 50 mM KH_2PO_4 (pH 7.5) plus 0.4 M KCl, 10 mM β-mercaptoethanol, 1.0 mM benzamidine HCl and 50% (v/v) glycerol. Next, all PDK enzymes was concentrated and stored at -80 °C and the purity was confirmed by SDS-page.

2.2.7 Construction of Plasmid and Expression and Purification of the E2 Catalytic Domain. For expression of the E2 catalytic domain (C), DNA encoding residues 305-561 in wild-type human E2 comprising catalytic domain and linker region in front of it was synthesized by DNA2.0, Inc. (Menlo Park, CA). The E2CD gene was optimized for expression in *E. coli* cells and was inserted into pET-22b (+) through the BamHI and XhoI restriction sites. The TEV cleavage site was introduced in front of the XhoI site and the resulting plasmid was expressed in BL21 (DE3) cells. Cells were grown in LB medium supplemented with 50 μg/mL ampicillin and protein expression was induced by 0.50 mM isopropyl 1-thio-β-D-galactopyranoside (IPTG) overnight at 30 °C. Cells were resuspended in 50 mM KH_2PO_4 (pH 7.5) containing 0.30 M KCl, 1 mM DTT, 25 mM imidazole and protease inhibitor cocktail tablets (Roche Diagnostics, GmbH, Germany). Cells were treated with lysozyme (0.6 mg/mL) and then by 1,000 units of DNase1 (NEB) and 1,000 units of micrococcal nuclease (NEB) to remove nucleic acids. The protein was purified

using a Ni Sepharose 6 Fast Flow column (GE Healthcare) and 50 mM KH_2PO_4 (pH 7.5) containing 0.30 M KCl and 25 mM imidazole as binding buffer and 50 mM KH_2PO_4 (pH 7.5) containing 0.30 M KCl and 50 mM imidazole as washing buffer. Protein was eluted with 350 mM imidazole in binding buffer and was stored in 50 mM KH_2PO_4 (pH 7.5) containing 0.4 M NH4Cl, 0.5 mM EDTA, 1.0 mM DTT and 1.0 mM benzamidine HCl at -80 °C.

2.2.8 Enzyme Activity Measurements. Overall PDC activity was measured by reconstitution of E1 with recombinant E2•E3BP core and recombinant E3. The E1 component (1.0 μg) was preincubated in the cuvette with a mixture of E2•E3BP core and E3 at a mass ratio of 1:3:3 for 1 min at 37 °C in 50 mM KH_2PO_4 (pH 7.5) containing 2.0 mM $MgCl_2$, 0.20 mM ThDP, 4.0 mM DTT and 2.0 mM NAD^+. The reaction was initiated by the addition of 2.0 mM pyruvate and 0.20 mM CoA and the formation of NADH (H^+) was monitored at 340 nm at 37 °C[23].

2.2.9 Phosphorylation of E1 and its variants by PDK isozymes. The E1 and its E1-MS 2,3 (site 1 available), E1-MS 1,3 (site 2 available), and E1-MS 1,2 (site 3 available) variants were phosphorylated by four PDK isozymes in the presence of E2•E3BP core or the E2•E3BP-derived proteins (0.2-50 μM), or in their absence. A mass ratio of E1:PDK isozymes of 25:1 was used. Phosphorylation by PDK1 and by PDK2 was performed in 50 mM KH_2PO_4 (pH 7.5) containing 0.5 mM ThDP, 1.0 mM $MgCl_2$, 4.0 mM DTT and 0.1 mM EDTA at 30 °C[22]. For PDK3 and PDK4, the phosphorylation reaction was preceded by their activation in the presence of the source of the lipoyl domain for 1 h at 4 °C as

reported in the literature[51]. Phosphorylation by PDK3 and PDK4 was performed in 20 mM Tris-HCl (pH 7.4) containing 5.0 mM $MgCl_2$, 0.1 M KCl, and 2.0 mM DTT based on the previous report[51]. The phosphorylation by PDK4 was also performed in KH_2PO_4 (pH 7.5). The phosphorylation reaction was initiated by addition of 0.5 mM ATP (PDK1 and PDK4) or 2.0 mM ATP (PDK2, PDK3) or 0.1 mM ATP (PDK3). Aliquots (1 μg of E1) were withdrawn at the indicated times and added to a 1 mL cuvette containing all components for PDC assay. PDC was allowed to reconstitute for 1 min at 37 ^{o}C and the reaction was started by addition of pyruvate and CoA as above.

2.3 RESULTS AND DISCUSSION

2.3.1 New insight into the role of the E2•E3BP core and its derived domains on activation of four PDK isoforms as reflected by PDC inactivation kinetics.

To study the activation of the four PDK isoforms by E2•E3BP core and their derived domains, we relied on activity measurement (NADH production) by the reconstituted PDC, rather than on an assay of PDK activity by incorporation of ^{32}P from $[γ-^{32}P]ATP$ into E1, as reported in the earlier studies[23,51,61]. The new assay here developed responds to the effects of E1-phosphorylation on the assembly of the PDC, as reflected by the overall activity. Using the functional kinetic approach, we could assess the contribution of all lipoyl domain sources of the E2•E3BP core (L1, L2S, L1L2S, L3S') on activation of the four PDK isoforms. Earlier studies were mostly focused on the interaction of L2 with PDKs[7,52,63-66]. Our recent findings suggested that the L1L2S tridomain gives rise to stronger and more points of interaction with PDK1 and PDK2, than does the L2S

didomain[55]. Additionally, the L3S' also induced moderate interactions with both PDK1 and PDK2[55].

The activation of the PDK isoforms (as reflected by the % PDC activity remaining) by the E2•E3BP and its derived domains is shown in Figure 2.4 for PDK1, Figure 2.5 for PDK2, Figure 2.6 for PDK3, and in Figure 2.7 for PDK4. The values of k_{app} of PDC inactivation by PDK1-PDK4 in the absence and presence of the E2•E3BP derived lipoyl domains are presented in Table 2.1.
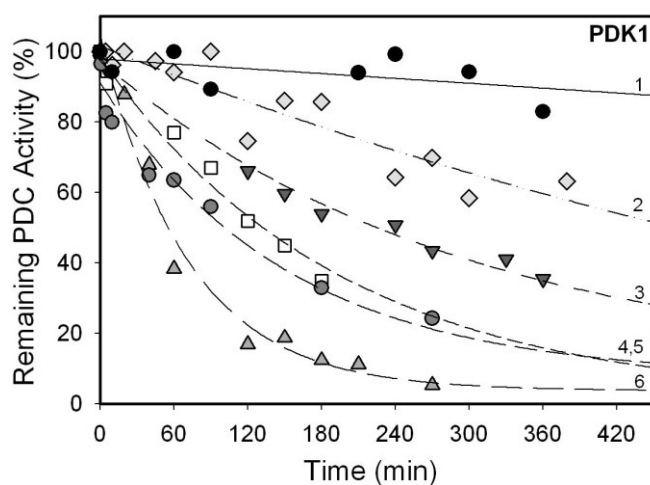
Figure 2.4 Time-dependence of PDC inactivation by PDK1. PDK1 (3.0 μg, 0.1 μM) in 50 mM KH$_2$PO$_4$ (pH 7.5) supplemented with 0.5 mM ThDP, 1.0 mM MgCl$_2$, 4.0 mM DTT and 0.1 mM EDTA was incubated with E1 (75 μg, 1.95 μM) in the presence of either L1L2S (3.0 μg, 0.3 μM) (line 6,▲); E2•E3BP (3.0 μg, 0.2 μM), (line 5,●); L2S (2.4 μg, 0.5 μM), (line 4,□); L1(3.0 μg, 1.0 μM) (line 3,▼); L3S' (1.0 μg, 0.5 μM) (line 2,◆) or with no lipoyl domain source (line 1,●). Phosphorylation was initiated by ATP (0.5 mM) at 23

ºC. Aliquots (1 µg E1) were withdrawn at different times and were mixed with E2•E3BP

and E3 at a mass ratio of E1: E2•E3BP: E3 of 1:3:3 to measure PDC activity.
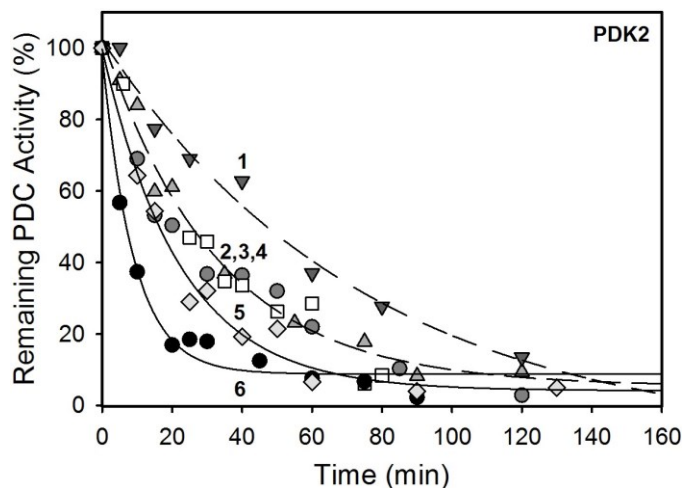
Figure 2.5 Time-dependence of PDC inactivation by PDK2. PDK2 (6.6 µg, 0.48 µM)

in 50 mM KH_2PO_4 (pH 7.5) supplemented with 0.5 mM ThDP, 1.0 mM $MgCl_2$, 4.0 mM

DTT, and 0.1 mM EDTA was incubated with E1 (80 µg, 3.5 µM) with no lipoyl domain

source (line 6,●); in the presence of either: L3S' (1.0 µg, 0.24 µM) (line 5,◆); E2· E3BP

(2.0 µg, 0.22 µM) (line 4, ●); L1L2S(1.2 µg, 0.22 µM), (line 3,▲); L2S (0.8 µg, 0.22

µM) (line 2,□) and L1 (0.4 µg, 0.22 µM), (line 1,▼). Phosphorylation was initiated by

ATP (2.0 mM) at 30ºC. Aliquots (1 µg E1) were withdrawn at different times and were

mixed with E2•E3BP and E3 at a mass ratio of E1: E2•E3BP: E3 of 1:3:3 to measure PDC

activity.
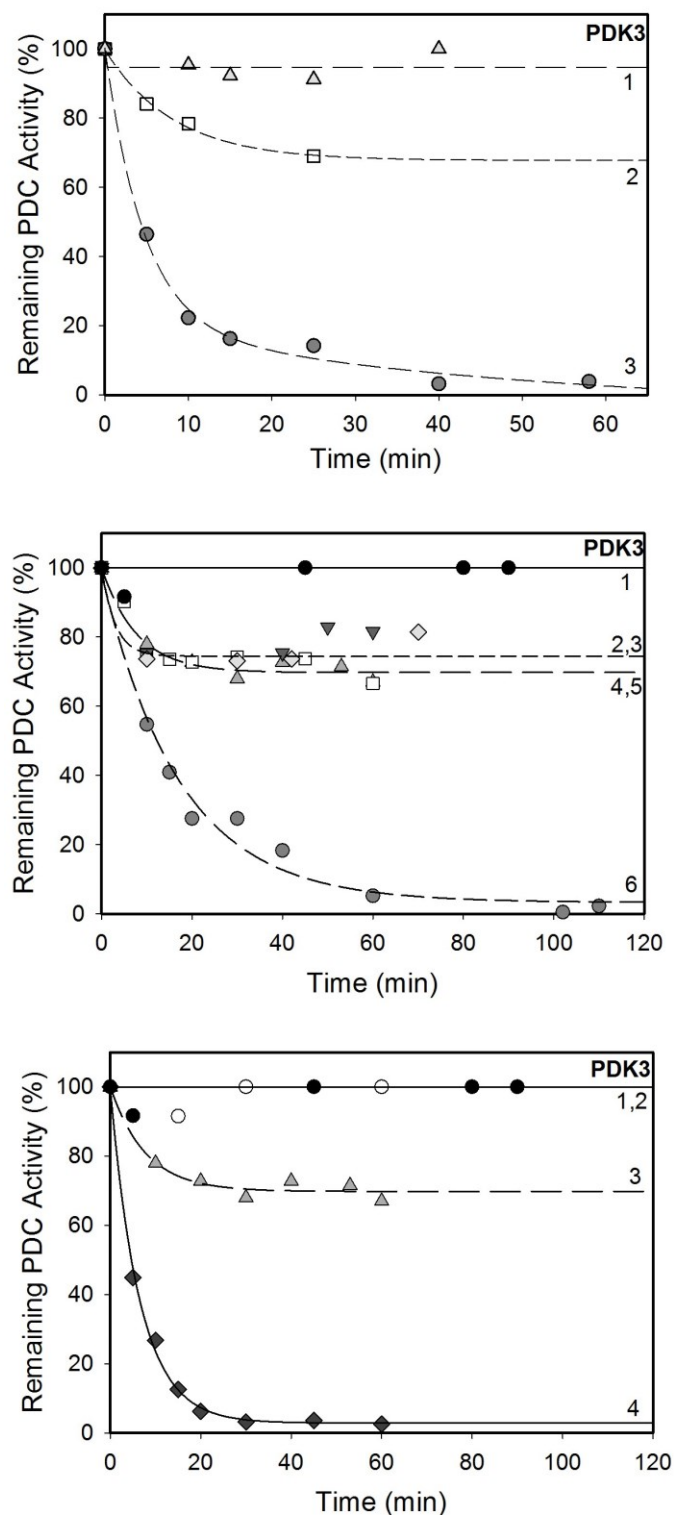
Figure 2.6 Time-dependence of PDC inactivation by PDK3. (**Top**) PDK3 (3.0 μg, 0.22 μM) in 20 mMTris·HCl (pH 7.4) supplemented with 0.1 M KCl, 5.0 mM MgCl$_2$ and 2.0

mM DTT was incubated with E1 (80µg, 3.5 µM) in the presence of either L2S (0.8µg, 0.22 µM) (line 1, ▲); L1L2S (1.2µg, 0.22 µM) (line 2, □) or E2•E3BP (2.0µg, 0.22 µM) (line 3, ●). Phosphorylation was initiated by ATP (2.0 mM) at 30 °C. (**Middle**) PDK3 (1.0 µg, 0.12 µM) in 20 mM Tris·HCl (pH 7.4) supplemented with 0.1 M KCl, 5.0 mM $MgCl_2$ and 2.0 mM DTT was first pre-incubated for 1 hour at 4 °C with either E2•E3BP (45µg, 7.55 µM), (line 6,●); L1L2S (10µg, 2.7 µM) (line 5,▲); L2S (5.0µg, 2.12 µM), (line 4,□); L1(50µg, 42 µM, (line 3,▼); L3S' (10µg, 4.0 µM) (line 2◆) or with no source of the lipoyl domain (line 1, ●). Phosphorylation was initiated by ATP (0.1 mM) at 30 °C. **(Bottom)** PDK3 (1.0µg, 0.12 µM) in 20 mM Tris-HCl (pH 7.4) supplemented with 0.1 M KCl, 5.0 mM $MgCl_2$ and 2.0 mM DTT was pre-incubated for 1 hour at 4 °C with either E2-Catalytic domain (1.0 µg, 0.33µM) plus L1L2S (1.0µg, 0.27µM) (line 4,◆); L1L2S (10 µg, 2.7 µM) (line 3,▲); E2-Catalytic domain (45 µg, 4.8 µM) (2,○) or with no lipoyl domain source (1,●). Phosphorylation reaction was initiated by ATP (0.1 mM) at 30 °C. For all, aliquots (1 µg E1) were withdrawn at different times and were mixed with E2•E3BP and E3 at a mass ratio of E1: E2•E3BP: E3 of 1:3:3 to measure PDC activity.
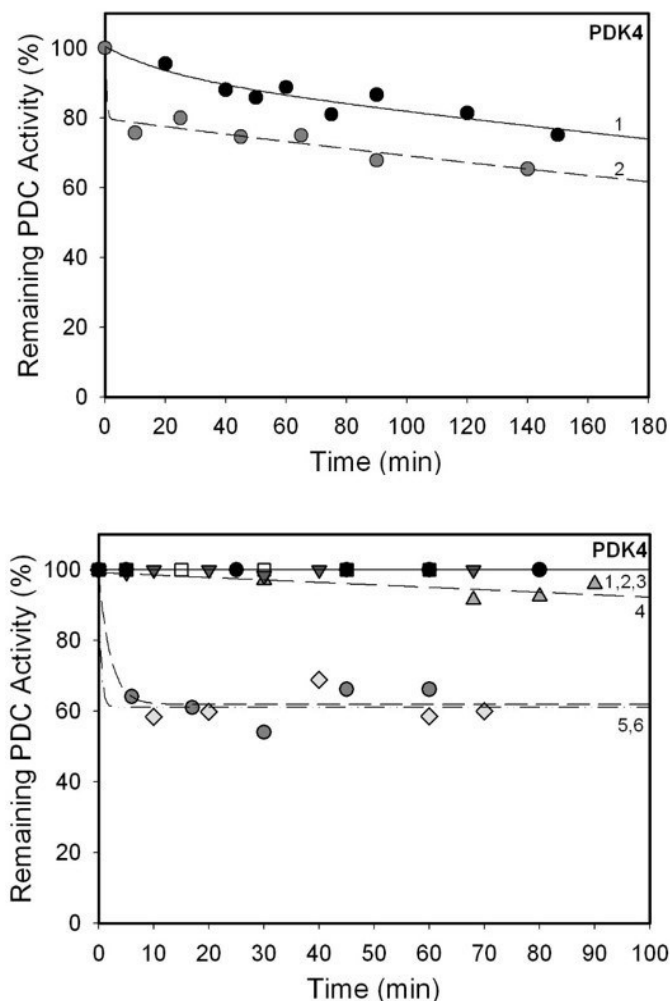
Figure 2.7 Time-dependence of PDC inactivation by PDK4. (Top) PDK4 (2.0 μg, 0.43μM) in 20 mM KH_2PO_4 (pH 7.5) supplemented with 2.0 mM $MgCl_2$, 0.2 mM EDTA and 2.0 mM DTT was pre-incubated for 1 h at 4 °C with E2•E3BP (120 μg, 40 μM) (line 2, ●) or in its absence (line 1,●). E1 (77 μg, 10 μM) was then added and the phosphorylation was initiated by ATP (0.5 mM) at 23 °C. **(Bottom)** PDK4 (2.0 μg, 0.22 μM) in 20 mM Tris·HCl (pH 7.4) supplemented with 0.1 M KCl, 5.0 mM $MgCl_2$, 2.0 mM DTT was pre-incubated for 1 h at 4 °C with either E2•E3BP (238 μg, 40 μM), (line 6, ●); L3S'(125 μg, 50 μM), (line 5,◆); L1L2S (37 μg, 10 μM), (line 4, ▲), L2S (12 μg, 5.0 μM (line 3, □), L1 (12 μg, 10 μM) (line 2,▼) or with no source of the lipoyl domain (line 1, ●)

Phosphorylation was initiated by ATP (0.5 mM) at 23 °C. For both, aliquots (1 µg E1) were withdrawn at different times and were mixed with E2•E3BP and E3 at a mass ratio of E1:E2·E3BP: E3 of 1:3:3 to measure PDC activity.

Table 2.1. PDC inactivation by PDK1-PDK4 with or without lipoyl domain source[a,b,c].

PDK isoforms	k_{app} of PDC inactivation with and without lipoyl domain source (min^{-1})							
	none	L1	L2S	L1L2S	C	C + L1L2S	L3S'	E2·E3BP
PDK1	n/a	0.003 (204)	0.005 (139)	0.014 (50)	0.003 (231)	0.007 (99)	0.001 (630)	0.007 (99)
PDK2	0.11 (6)	0.013 (53)	0.028 (25)	0.031 (22)	0.12 (6)	0.10 (7)	0.045 (15)	0.032 (22)
PDK3	n/a	0.004 (n/a)	0.006 (n/a)	0.012 (n/a)	n/a	0.15 (5)	0.003 (n/a)	0.058 (12)
PDK4	n/a	n/a	n/a	n/a	n/a	n/a	0.008 (n/a)	0.007 (n/a)

[a] The half time of PDC inactivation ($t_{1/2, min}$) is presented in the parenthesis. [b] Time course of the fraction of the remaining PDC activity was fit to a single exponential. [c] n/a, data not available due to no inactivation detected.
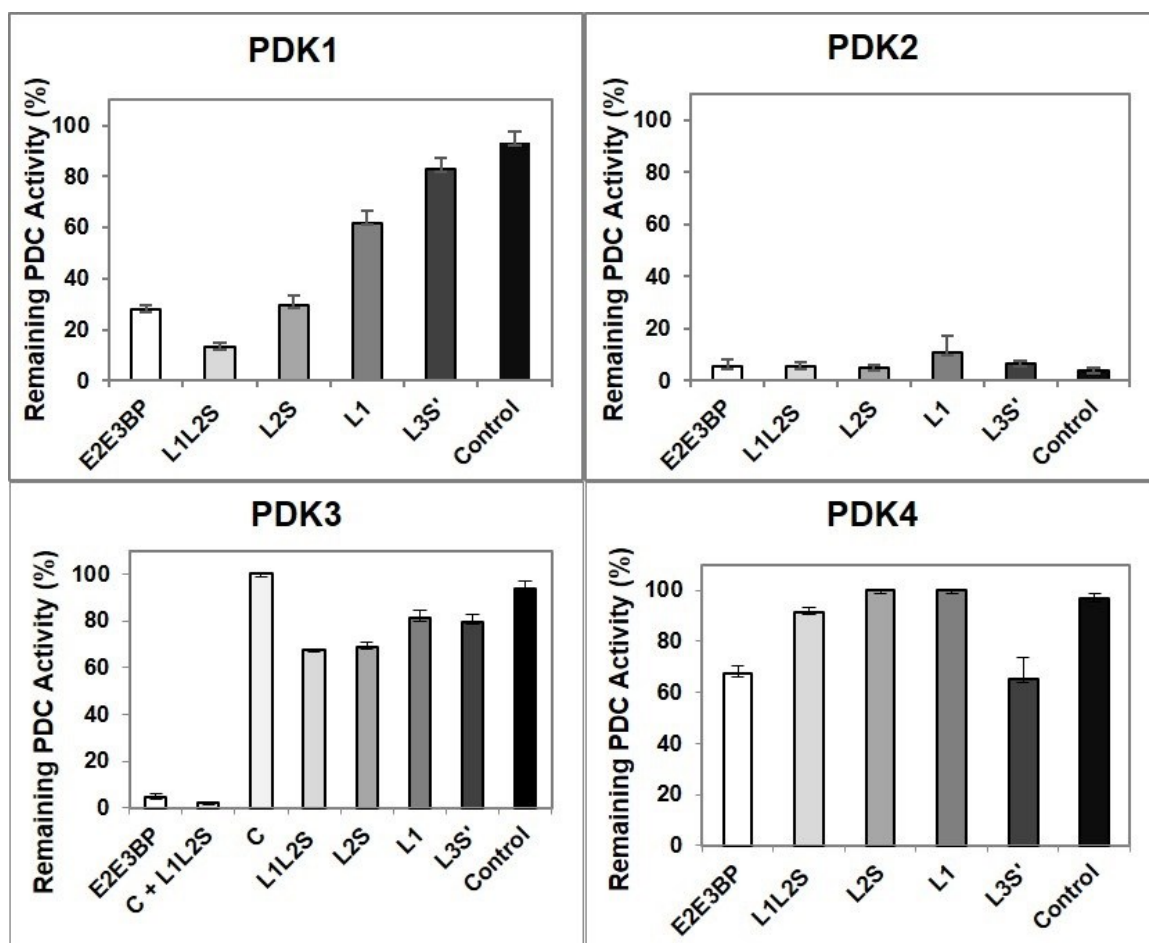
Figure 2.8 Comparison of the effect of the E2•E3BP core and its derived domains on PDC inactivation by PDK1-PDK4. Values on Y axis represent % of the remaining PDC activity. The E2•E3BP core and its C-terminally truncated proteins used for activation of PDK1- PDK4 are presented on the X axis. The time of E1 incubation with PDK1-PDK4 with or without lipoyl domain source was chosen as follows: 210 min for PDK1 (left panel, top); 90 min for PDK2 (right panel, top), and 60 min for PDK3 and PDK4 (left and right panels, bottom). Each experiment was done in triplicate and the standard error of mean (SEM) is shown.

The data summarized in Fig. 2.8 provide striking evidence that of all four PDK isoforms, PDK2 is the only isoform that was able to significantly reduce PDC activity (4.0 % remaining) even in the absence of E2•E3BP core or its derived domains (Figs. 2.5 and 2.8, Table 1). The extent of inactivation resulting from addition of E2•E3BP core or its derived domains, is reflected by the final PDC activity remaining: 5.7% (E2•E3BP core); 5.6% (L1L2S); 5.1 % (L2S); 11 % (L1) (Fig. 5). PDK2, apparently is also modestly activated by L3S' with 6.5% PDC activity remaining, comparable to 5.7% observed with E2•E3BP core. Given that PDK2 is the major isoform responsible for the regulation of PDC activity so far as its wide tissue distribution, high level of expression and its contribution to diabetes are concerned[8,49,61,67], this is an important observation.

Unlike PDK2, the other three PDKs required activation by E2•E3BP, in whose absence the PDC activity remaining was 93% for PDK1, 94% for PDK3 and 97% for PDK4 (see control experiments in Fig. 2.8 on the right hand side of each panel).

The PDK1 was activated by any source of the inner lipoyl domain (L2) (i.e., E2•E3BP, L1L2S or L2S; see Figs. 2.4 and 2.8). The activation of PDK1 by the L2 sources followed a specific pattern where L1L2S was most effective with 13% of PDC activity remaining. The overall pattern of activation was: L1L2S > E2•E3BP = L2S > L1 > L3S' that corresponds to PDC activities remaining of 13% (L1L2S), 28% (E2· E3BP), 29% (L2S), 62% (L1), and 83% (L3S') in Fig. 2.8.

The PDK3 isoform proved to be more difficult to activate, requiring also a long pre-incubation time with E2•E3BP, or with the lipoyl domain source before the E1 phosphorylation reaction is started, leading to some inconsistences in the literature[51,53,54]. As shown in Fig. 2.6, about 5% of the PDC activity remained when PDK3 was activated

by E2•E3BP (k_{app} of inactivation = 0.058 min^{-1}) as compared with 94 % activity remaining in the absence of PDK3 activation (not presented). Our data correlate well with the 17-fold and 15-fold enhancement of PDK3 activity by E2 and E2•E3BP when the incorporation of ^{32}P from [γ-^{32}P]ATP into E1 was analyzed[51]. Much less PDK3 activation was achieved by other lipoyl domain sources according to PDC activity remaining: L1L2S (68%), L2S (95%), using the molar ratio for lipoyl domain source to PDK3 of 1:1 (Fig. 2.6, top). Surprisingly, no further PDK3 activation was observed on increasing the amount of the lipoyl domain source even at much higher molar ratios of lipoyl domain source to PDK3: L1L2S, (23:1), L2S (18:1), L3S' (33:1), and L1 (350:1). Even under these conditions, 76.5% PDC activity remained with no additional PDC inactivation (Fig. 2.6, middle). These results suggest that PDK3 may require the catalytic domain from either E2 (**C**) or E3BP (**C'**) for activation, perhaps in combination with the lipoyl domain source. To test this hypothesis, we showed that while the independently expressed E2-catalytic domain (**C**) was not effective in activating PDK3 by itself, in combination with L1L2S, only 2% of PDC activity remained after 20 min of incubation with a k_{app} of inactivation of 0.15 min^{-1} (Fig. 2.6, bottom). In comparison with L1L2S by itself only 68% of the PDC activity remained, indicating that combination of E2-catalytic domain and L1L2S is needed for more effective activation of PDK3. This suggests a remarkable example of synergistic catalysis by individual domains. When tested with PDK1, the C domain plus L1L2S gave similar results as with E2•E3BP core, and therefore did not have such a dramatic effect on PDK1 as it did with PDK3 (Figure 2.9).
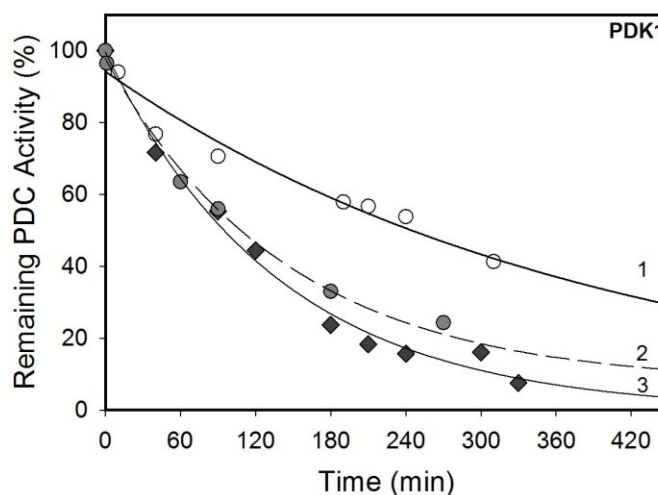
Figure 2.9 Time-dependence of PDC inactivation by PDK1 with E2-Catalytic domain.

PDK1 (1.2 μg, 0.1 μM) in 50 mM KH$_2$PO$_4$ (pH 7.5) supplemented with 0.5 mM ThDP, 1.0

mM MgCl$_2$, 4.0 mM DTT and 0.1 mM EDTA was incubated with E1 (30 μg, 1.95 μM) in

the presence of either E2-Catalytic domain (1.2 μg, 0.4 μM) plus L1L2S (1.2 μg, 0.32 μM)

(line 3,◆); E2•E3BP (3.0 μg, 0.2 μM), (line 2,●); or E2-Catalytic domain (1.2 μg, 0.4 μM)

(line 1,○). Phosphorylation was initiated by ATP (0.5 mM) at 23 ℃. Aliquots (1 μg E1)

were withdrawn at different times and were mixed with E2•E3BP and E3 at a mass ratio

of E1: E2•E3BP: E3 of 1:3:3 to measure PDC activity.

Data for PDK4 (Figs. 2.7 and 2.8, Table 2.1) indicate that PDK4 was the least

effective of the four PDK isoforms, irrespective of the lipoyl domain source, even with

prior pre-incubation. Modest reduction of the PDC activity observed when E2•E3BP

(67%) or L3S' (65%) were present, while L1L2S (92%), L2S (100%), L1 (100%) were not

effective despite their good binding constants to PDK4 presented for the first time

(Appendix B). Our results suggesting that PDK4 has the lowest activation by the E2•E3BP

core among all four PDKs is in accord with reports from other groups. Despite the highest

PDK4 activity among all four PDKs toward ^{32}P incorporation into E1, only a modest PDC inactivation was detected with no E2•E3BP core present (Fig. 2.7), reflecting the unique biochemical properties of PDK4. Earlier, the unique PDK4 structure with a favored open conformation of the active center has been reported[62,68]. It is plausible that PDK4 may require factors other than E2•E3BP core for activation to reach its full catalytic potential.

2.3.2 Site-specificity of PDK isoenzymes using single phosphorylation site E1 variants. As there are three phosphorylation sites in E1α (the E1 is an $\alpha_2\beta_2$ heterotetramer), it was important to analyze with the newly developed assay the specificities of the four PDKs toward the three phosphorylation sites of E1. It was previously reported that all four PDKs phosphorylate *site 1* and *site 2*, however, with different rates on the basis of incorporation of ^{32}P from [γ-^{32}P]ATP into E1: for *site 1*, PDK2 > PDK4≈PDK1 > PDK3; for *site 2*, PDK3 > PDK4 > PDK2 > PDK1. *Site 3* was phosphorylated by PDK1 only[23,24,65]. In this paper the specificity of the four PDKs toward the three phosphorylation sites was assessed by measuring the overall complex activity. The PDC was reconstituted with E1 variants containing double substitutions at phosphorylation sites with only one site available for phosphorylation: E1-MS 2,3 (MS, mutated *sites 2* and *3*, *site* 1 is available); E1-MS 1,3 (*site 2* is available); E1-MS 1,2 (*site 3* is available) to test which of the three sites contributes the most to the inactivation of E1 by phosphorylation for each PDK.

With PDK1 the highest rate of PDC inactivation was toward the E1-MS 2,3 variant (*site* 1 available) (Figure 2.10 top, left and Table 2.2). The remaining PDC activity was less than 10% after 50 min of incubation and k_{app} = 0.054 min^{-1} could be calculated for PDC inactivation. This rate was even higher than that for the wild-type E1 (k_{app} =0.018

min[-1]). With the other two variants E1-MS 1,3 (*site 2* available) and E1-MS 1,2 (*site 3* available) no greater than 20% PDC inhibition resulted even after >250 min of their treatment by PDK1, and did not allow calculation of rate constants for PDC inactivation in Table 2.2. The results in Table 2.2 are in agreement with the literature[23,24].
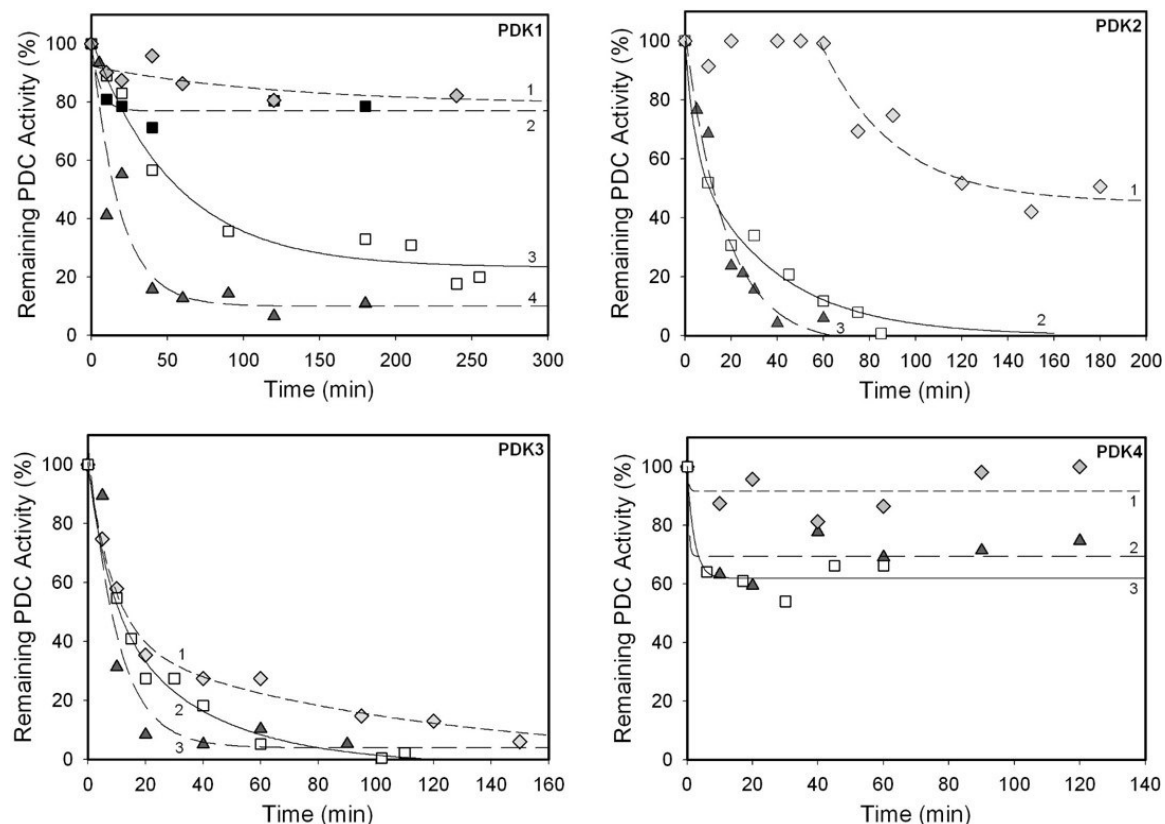
Figure 2.10. Time-dependence of PDC inactivation by PDK1-PDK4 using single phosphorylation site (doubly-substituted) E1 variants. Top, left: The E1 (□) or E1-MS 2,3 (▲) or E1-MS 1,3 (◆) or E1-MS 1,2 (■), all at concentration of 5.0 μM (38.5 μg), were incubated with PDK1 (0.3 μM, 1.54 μg) activated by L1L2S (0.8 μM, 1.54 μg) in 50 mM KH$_2$PO$_4$ (pH 7.5). **Top, right:** The E1 (□) or E1-MS 2,3 (▲) or E1-MS 1,3 (◆) or E1-MS 1,2 (■), all at 3.5 μM (81 μg) were incubated with PDK2 (0.48 μM, 6.6 μg) in 50 mM KH$_2$PO$_4$ (pH 7.5). **Bottom, left:** PDK3 (0.12 μM, 1.0 μg) was first activated by E2•E3BP

(7.55 µM, 45 µg) in 20 mM Tris·HCl (pH 7.4). The E1 (□) or E1-MS 2,3 (▲) or E1-MS 1,3 (◆) or E1-MS 1,2 (■), all at concentration of 1.95 µM, (3.0 µg) was then added to start phosphorylation. **Bottom, right:** PDK4 (0.22 µM, 2.0 µg) was first activated by E2•E3BP (40 µM, 238 µg) in 20 mM Tris·HCl (pH 7.4). The E1 (□) or E1-MS 2,3 (▲) or E1-MS 1,3 (◆) or E1-MS 1,2 (■), all at concentration of 3.5 µM, (54 µg) was then added to start the phosphorylation. Time course of the fraction of the remaining activity was fit to a single exponential.

Table 2.2. Kinetic parameters for E1 and its doubly substituted (single phosphorylation site) variants inactivated by PDK1- PDK3.

k_{app} (min^{-1})	E1	E1-MS2,3	E1-MS1,3	E1-MS1,2
PDK1[a]	0.018 ±0.003	0.054±0.025	n/a[b]	n/a[b]
PDK2[a]	0.057±0.011	0.061±0.006	n/a[c]	n/a
PDK3[a]	0.058±0.016	0.099±0.032	0.062±0.01	n/a

[a] PDK1 and PDK2 were activated by L1L2S; PDK3 was activated by E2•E3BP core.

[b] n/a, not available. No greater than 20% of E1-MS1,3 and E1-MS1,2 inhibition by PDK1 was detected.

[c] About 100% activity remained after 60 min treatment by PDK2.

[a,b,c] The experimental conditions are presented on Fig. 4. Time course of the fraction of the remaining activity was fit to single exponential according to eq. $f = f1 \times (1- e^{-kt})$.

With PDK2, *site 1* clearly contributed to PDC inactivation (Fig. 2.10 top, right). After only 20 min, PDK2 was able to inactivate E1-MS 2,3 to less than 20% of PDC activity remaining with k_{app} of 0.061 min^{-1}, comparable to the k_{app} of 0.057 min^{-1} for the wild-type E1 (Table 2.2). For the E1-MS 1,3 variant, however, nearly 100% of the PDC activity remained during the first 60 min of incubation with PDK2, and only after 120 min was PDK2 able to reduce PDC activity to ~50%. According to reported data, the PDK2 displayed the highest activity for *site 1* followed by PDK4 and PDK1[24]. Earlier, PDK3 was reported to have the lowest activity toward *site 1*, even when activated by the E2•E3BP core[23,24], but was able to inactivate E1-MS 2,3 and E1-MS 1,3, or even wild-type E1 at rather similar high rates (0.099 min^{-1}, 0.062 min^{-1} and 0.058 min^{-1}, respectively). Again, *site 1* is mostly responsible for the PDC inactivation by PDK3, similarly to PDK1 and PDK2 (Fig. 2.10 bottom, left and Table 2.2). However, the highest activity exhibited toward *site 2* makes PDK3 unique and differentiates it among the four PDKs. Although PDK4 could only partially inactivate PDC reconstituted with wild-type E1 (about 65 % of the PDC activity remaining), its site-specificity was also examined. Most of the PDC activity lost was due to phosphorylation of site 1 as E1-MS 2,3 gave similar results to wild-type E1, where PDC activity remained at 70% or 65%, respectively, after 120 min (Fig. 2.10, bottom, right). On PDC reconstitution with E1-MS 1,3, the activity remained unchanged at 90-95% after 120 min. Again, the lack of significant PDC inactivation by PDK4 is consistent, irrespective of the site selected.

The following could be concluded: (i) Most of the PDC activity lost was due to phosphorylation at *site 1* on E1 when treated by PDK1, PDK2, PDK3 and less so by PDK4. (ii) A high PDK3 activity toward *site 1* and *site 2* was detected indicating that E2•E3BP

core is needed for its activation that was confirmed by experiments with independently expressed E2 catalytic (**C**) domain.

From these studies on PDK 1-4 activation by the E2•E3BP core and its derived domains, it has become evident that each of the four PDK isoforms has its own preferences for activation by PDC, which are not limited by binding to the L2 or L3 domains only[69]. The PDK1 was the only isoform that exhibits different activation by E2•E3BP derived domains (based on % of the PDC activity remaining) with L1L2S (k_{app} = 0.014 min^{-1}) > E2•E3BP core (0.007 min^{-1}) ≈ L2S (0.005 min^{-1}) > L1 (0.003 min^{-1}) > L3S' (0.001 min^{-1}) (Table 2.2). However, the k_{app} of PDC inactivation by PDK1 was still slow in comparison with PDK2. The order of PDK1 activation indicates best activation by the L1L2S tridomain; inclusion of L1S adds significantly to activation by L2S.

The activation of PDK2 by E2•E3BP core and its derived domains was more evident from the calculated k_{app} of PDC inactivation: it was the fastest rate among the four PDK isoforms even without activation (k_{app} ~ 0.11 min^{-1}), that was not improved further by E2•E3BP derived domains with E2•E3BP core (k_{app} = 0.032 min^{-1}) ≈ L1L2S (k_{app} = 0.031 min^{-1}) ≈ L2S (0.028 min^{-1}) > L1 (k_{app}=0.013 min^{-1}). Additionally, the PDK2 was significantly activated by L3S' as well (k_{app} =0.045 min^{-1}), indicating that most of the PDK2 activation was achieved by L2S or L3S'. It should also be emphasized that PDK2 could actually bind L3S' according to fluorescence titration studies.

PDK3 required E2•E3BP core for its activation (k_{app} = 0.058 min^{-1}), with essentially no activation by E2•E3BP derived domains. The E2 catalytic domain with L1L2S tridomain provided the highest rate of PDC inactivation among all E2•E3BP-derived

domains (k_{app}= 0.15 min^{-1}), in what appears to be a case of synergistic catalysis by two domains.

PDK4 was only weakly activated by L3S' (k_{app} =0.008 min^{-1}) and by E2•E3BP core (k_{app} = 0.007 min^{-1}), but in both cases the rate of PDC inactivation was slow.

Further information was gathered from studying the single phosphorylation site E1 proteins. The loss of PDC activity with PDK1-3 was shown to be mostly due to phosphorylation of *site 1* with the following relative reactivities: PDK3 (k_{app}=0.099 min^{-1}) > PDK2 (k_{app}=0.061 min^{-1}) ≈ PDK1 (k_{app}=0.054 min^{-1}). With PDK3, the rate constant of PDC inactivation at phosphorylation *site 1* (k_{app}=0.099 min^{-1}) and *site 2* (k_{app}=0.062 min^{-1}) were nearly the same, unusual in this regard. For PDK4, the results raise a question: is this kinase really specific to this target PDC?

From these studies it has also become evident that there is no strong correlation between the ability of the E2•E3BP-derived domains to activate PDK and their binding affinities for the PDK isoforms[69]. Among the four PDK isoforms, PDK1 revealed the weakest binding of E2•E3BP-derived domains; its ability to bind any source of the lipoyl domain correlated well with low rates of PDC inactivation detected. The PDK1 isoform prefers binding to L1, rather than to L2; binding to L2 was very weak with K_d= 17 μM. Also, no apparent binding to L3S' was detected for PDK1. In contrast, both PDK2 and PDK4 revealed binding to L3S' with K_d = 2.07 μM and 5.02 μM, respectively, providing an explanation why they could be activated by L3S'. It appears that PDK2 and PDK3 interact similarly with the lipoyl domain source, with both L1 and L2S contributing significantly to binding, a finding not correlated with their ability to activate the kinases. As mentioned above, PDK2 is active even in the absence of the E2•E3BP core or its derived

domain, while only the E2•E3BP core could activate PDK3. This disagreement between binding and activation abilities of E2•E3BP derived domains was even more pronounced with PDK4, where with good binding constants to the lipoyl domain source, they could not achieve activation of PDK4.

2.4 CONCLUSIONS

We can draw the following general conclusions of importance relevant to PDK isozyme-specific drug design.

1. No strong correlation could be observed between the ability of E2•E3BP core and its derived domains to activate the PDK isoforms and the binding constants for the corresponding complexes formed between a PDK and an E2•E3BP-derived domain.

2. The approach to inhibit interaction of PDK isoforms and E2•E3BP core as a route to intervention in diseases is not promising for PDK2 (no activation is needed, only modest additional activation/inhibition results from the presence of E2•E3BP-derived domains), or PDK4 (no significant activation results from E2•E3BP core or from any of the E2•E3BP-derived domains). On the other hand, the approach is plausible and promising for PDK1 and PDK3.

3. PDK3 alone among the four isoforms is subject to activation by a combination of L1L2S and the E2 catalytic domain, providing a novel hitherto unexplored target for drug design.

CHAPTER 3

Validation of the Interaction 'Hot Spots' on the E2 Component with the Kinases of the Human Pyruvate Dehydrogenase Complex

3.1 INTRODUCTION

Previous studies on PDK activation suggested that binding to the E2•E3BP core improved PDK activity. For instance, PDK2 was activated upon binding to E2[51], or to the L2S didomain, but not to the isolated L2[52] whereas PDK3 was activated equally on binding to either E2 or isolated L2[10,51,53,54]. In order to explain the mechanism of activation for the PDKs, crystal structures of PDK2-L2 (Figure 3.1) and PDK3-L2 (Figure 3.2) were solved. While crystal structures of PDK3 and PDK2 with L2[54,66,70], and of PDK4[62] and PDK1[71] are published by themselves, the premise of all earlier work is that interactions between PDC and the kinases are limited to the inner E2 lipoyl domain (L2).

From these crystal structures, the interaction surface between PDK2-L2 and PDK3-L2 were determined resulting in the identification of some important residues on both the PDKs and L2. First, the lipoyl-binding pocket on the PDKs as well as the lipoyl-lysine residue on L2 were determined to be critical for PDK activity (Figure 3.3)[54]. Additionally, it was determined that the C-terminal tail of one PDK subunit binds to L2 in complex with the other PDK subunit forming cross-tail interactions. Furthermore, hydrophobic interactions as well as electrostatic interactions, specifically an acidic cluster, were identified at the interface of the PDKs with L2.
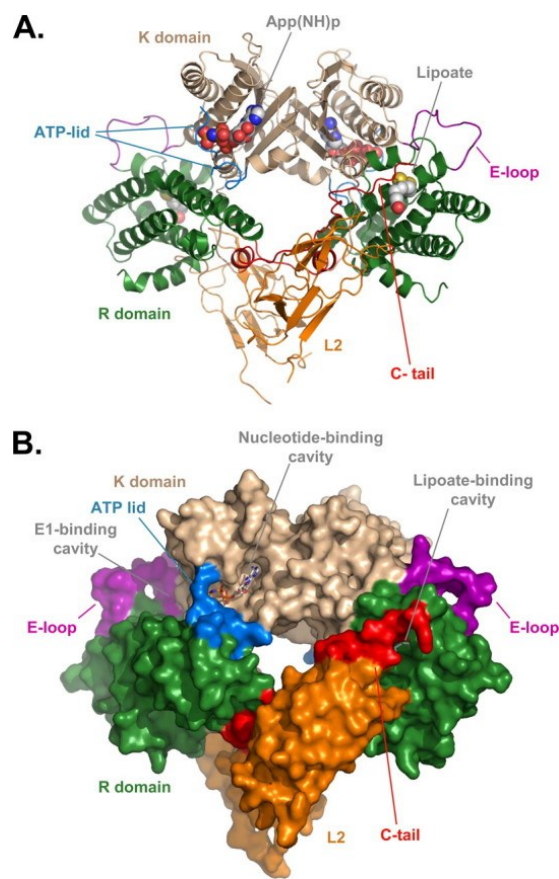
Figure 3.1 Three-dimensional structure of human PDK2-L2 complex as presented in Green et al[66].
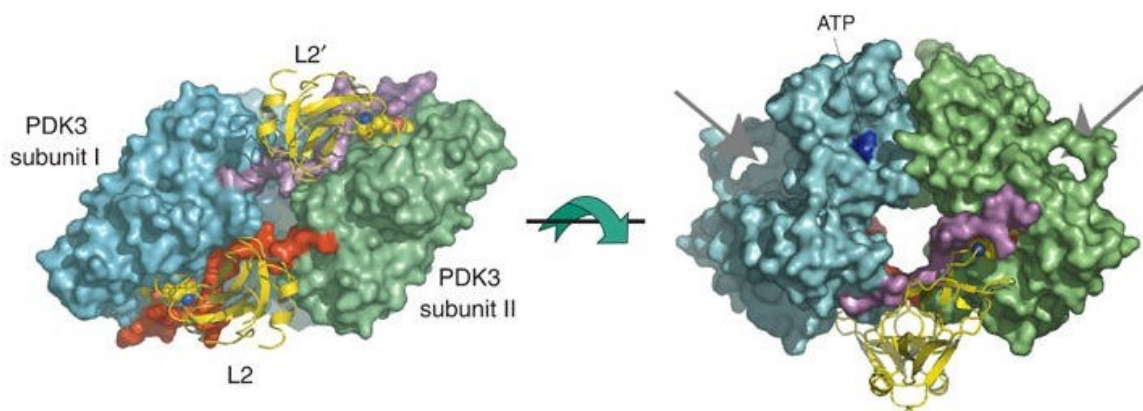
Figure 3.2 Three-dimensional structure of human PDK3-L2 complex as presented in Kato et al[54].
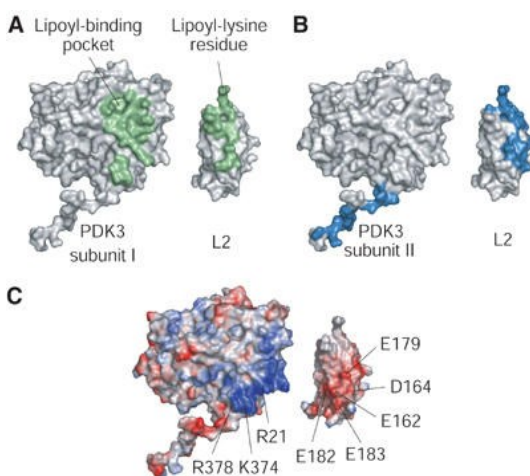
Figure 3.3 Interaction surfaces between PDK3-L2[54] with the binding interface in green (a), cross-tail binding interface in navy (b), and the electrostatic/ hydrophobic interactions (c) with positively charged residues in blue and negatively charged residues in red.

Recently, the Jordan group successfully defined the interaction loci between PDK1 and PDK2 with the E2•E3BP core by two complementary methods, HD-exchange mass spectrometry (HDX-MS) and multinuclear nuclear magnetic resonance (NMR) spectroscopy[55]. The studies described here interrogate the sites on E2•E3BP identified to interact with PDK1 or PDK2 (Glu35, Val198, Glu153, Glu209) in addition to the lipoyl-lysine sites found on L1 (Lys 46) and L2 (Lys 173). Based on the x-ray data mentioned above, Glu153 and Glu209 are located near the acidic cluster (electrostatic interactions with PDKs) whereas Glu35 is located near the lipoyl-lysine site on L1 (electrostatic interaction for stabilization) and Val198 located near a hydrophobic patch (hydrophobic interaction with PDKs) all possibly critical for E2-PDK binding[10,48,54,66]. Additionally, studies on alanine substituted lipoyl-lysine site K173 on L2 have shown its important role in L2-PDK2 and L2-PDK3 interaction[10,48]. Therefore, E1 phosphorylation by PDK1,

PDK2 or PDK3 in the presence of the constructed L1L2S mutants based on the above residues were tested to identify the resulting effects on overall PDC activity. The overall impact is that once it is confirmed whether the 'hot spots' interrogated indeed are important for the interaction of E2•E3BP with the PDKs, against which rational drug design could be undertaken (See Appendix C. for list of known inhibitors).

3.2 MATERIALS AND METHODS

3.2.1 Materials. Ni-NTA agarose used for protein purification was purchased from GE Healthcare Life Sciences. Thiamin diphosphate (ThDP), dithiothreitol (DTT), isopropyl-β-D-thiogalactopyranoside (IPTG), NAD^+ and coenzyme A (CoA) were purchased from Affymetrix USB. Sodium pyruvate was purchased from Sigma Aldrich.

3.2.2 Purification of E1. A coexpression vector for PDHc-E1 (pET-28b-PDHA1/PHDHB) harboring coding sequences of both human E1α and human E1β subunits was constructed as described previously[56]. The PDHc-E1 was overexpressed in E. coli BL21 cells and purified using Ni-NTA-agarose chromatography. See Chapter 2 (section 2.2.2) for details.

3.2.3 Purification of PDK1, PDK2 and PDK3. Recombinant rat PDK1 and PDK2 were used for the studies. The sequences of mammalian PDK isozymes are highly conserved for each of the four isoforms (>94% identical between human and rat)[5]. The PDKs were overexpressed and purified to 90−95% purity according to a literature protocol with some modifications[19,61]. See Chapter 2 (section 2.2.6) for details.

3.2.4 Site-directed mutagenesis. Several mutants of the L1L2S tridomain were made based on the 'hot-spots' identified by NMR and HDX-MS: Glu35 (L1) – Glu35Ala and Glu35Lys; Glu153 (L2) – Glu153Ala, Glu153Lys and Glu153Gln; Val198 (L2) – Val198Ala; and Glu209 (L2) – Glu209Ala, Glu209Lys and Glu209Gln. Site-directed mutagenesis was carried out by polymerase chain reaction (PCR). The following mutagenic primers (antisense) were used:

5'-CTGCAATTAGGTCACCTGCATTGATTTTGTCCCCCTC-3' for E35A,

5'-GAGGGGGACAAAATCAATAAAGGTGACCT AATTGCAGAGG-3' for E35K,

5'-GGCACAGTTCAGAGATGGGCAAAAAAGTGGGTGAG AAG-3' for E153A,

5'-GGCACAGTTCAGAGATGGAAAAAAAAGTGGGTGAGAAG-3' for E153K,

5'-GGCACAGTTCAGAGATGGCAAAAAAAGTGGGTGAGAAG-3' for E153Q,

5'-C CTGAAGGCACAAGAGATGCCCCTCTAGGAACCCCACTC-3' for V198A,

5'-ACCCCACTCTGTATCATTGTAGCAAAAGAGGCAGATATATCAGC-3' for E209A,

5'-ACCCCACTCTGTATCATTGTAAAAAAAGAGGCAGATATATCAGC-3' for E209K,

 and 5'ACCCCACTCTGTATCATTGTACAAAAAGAGGCAGATATATCAGC-3' for E209Q (all from IDT technologies, Inc.).

The doubly-substituted L1L2S variants were as follows: L1L2S E35A/K173A, L1L2S E35K/K173A, L1L2S K46A/E209A and L1L2S K46A/E209K. L1L2S K46A or L1L2S K173A cDNA was used for site-directed mutagenesis carried out by PCR using the above primers for E35A, E35K, E209A or E209K. All were cloned into a pET-28a vector

(Novagen) through the XhoI and NdeI restriction sites. The nucleotide sequence of each mutant L1L2S cDNA was verified by DNA sequencing.

3.2.5 Purification of L1L2S and L1L2S variants. Human L1L2S tridomain, which comprises L1, L2, both hinge regions, and the subunit-binding domain (S, residues 1−330), and the L1L2S variants were expressed from pET28b vector in *E. coli* BL21 (DE3) cells and purified on Ni Sepharose 6 Fast Flow column[19,20,59,72]. Two singly substituted variants of L1L2S were used in this study: L1L2S-ML1 with the Lys46Ala substitution in the outer L1 domain with inner L2 domain available for modification) and L1L2S-ML2 (Lys173Ala substitution in the inner L2 domain with outer L1 domain available for modification). All L1L2S variants followed the same purification method as described for the C-terminally truncated E2•E3BP proteins. See Chapter 2 (section 2.2.4) for more details.

3.2.6 Overall Activity/ Inactivation of E1 Assay. E1 is being phosphorylated by PDK1, PDK2, or PDK3 in the presence or absence of each L1L2S variants as the only E2 source (with the exception of PDK3, which requires E2 catalytic domain in addition to L1L2S) to test whether or not the substitution affects PDK-E2•E3BP binding and resulting PDK activity/ overall PDC activity. The inactivation of E1 by phosphorylation was carried out as described previously with the following modifications[23]: (a) Phosphorylation buffer used: 50 mM potassium phosphate, pH 7.5, 0.5 mM ThDP, 1.0 mM MgCl$_2$, 4.0 mM DTT, 0.1 mM EDTA. (b) 0.5 mM ATP was used with PDK1, 2.0 mM ATP was used with PDK2, and 0.1 mM was used with PDK3 to initiate the phosphorylation reaction. (c) 0.24 – 0.6 μM L1L2S or L1L2S variant was used based on the particular PDK[51]. (d) The amount of

E1 used was based on S0.5 values for each site[24]. (e) The amount of PDK1 or PDK2 used was based on the mass ratio of 25:1 E1:PDK. For all assays, aliquots were withdrawn at different incubation times and the activity of the overall PDC reaction was measured upon assembly with E2•E3BP and E3 for 1 min at 37 °C.

3.3 RESULTS AND DISCUSSION

3.3.1 New insight into the interaction loci between PDK1, PDK2 or PDK3 with singly substituted L1L2S tridomain variants and the effects on activation of the PDKs as reflected by PDC inactivation kinetics.

In order to investigate the amino acid residues on E2•E3BP core identified to interact with PDKs, we relied on activity measurement (NADH production) by the assembled PDC, rather than on an assay of PDK activity by incorporation of ^{32}P from [γ-^{32}P]ATP into E1, as reported in the earlier studies[22,51,61]. The new assay developed here responds to the effects of E1-phosphorylation on the assembly of the PDC, as reflected by the overall activity. To investigate the significance of the amino acid residues identified by the Jordan group[55] (E35, V198, E153, E209) as well as the lipoyl-lysine attachment sites on L1 (K46) and L2 (K173), we carried out alanine, glutamine, and lysine site-directed mutagenesis. Using the functional kinetic approach, we could assess the effect of single substitutions on L1L2S tridomain listed above on the activation of PDK1-3. Previous studies were focused on the interaction of L2 with PDK2 and PDK3[10,48,54,66]. Our studies show that single substitutions made on L1 had an impact on PDK1-3 activity, as did the substitutions on L2, including both lipoyl-lysine sites. Additionally, we have shown that all three PDKs have unique interaction patterns with the L1L2S tridomain.
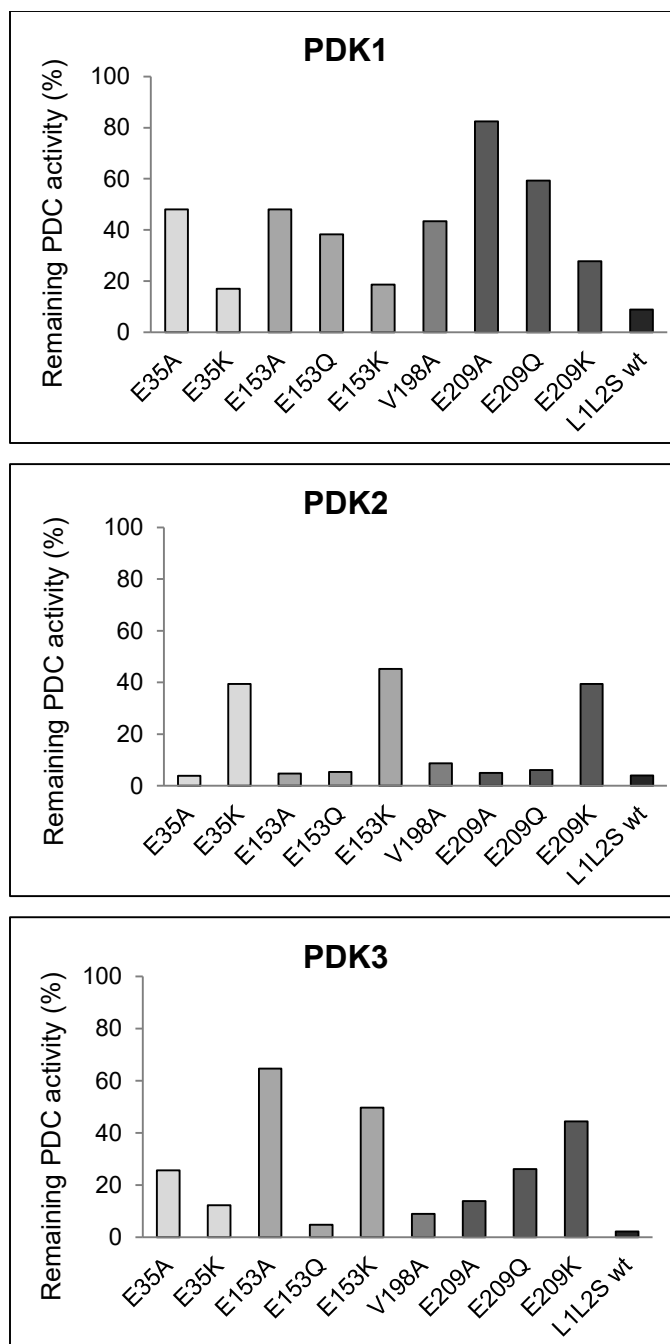
Figure 3.4. Effects of singly substituted tridomain L1L2S variants on PDK1-3 activation. The L1L2S variants used to test its effects on PDK1-3 activation are presented on the X axis. The time of E1 incubation with PDK1-3 was chosen as follows: 180 minutes for PDK1 (top); 30 minutes for PDK2 (middle); 30 minutes for PDK3 incubated with E2p core in addition to L1L2S variants (bottom).

Table 3.1. PDK1-3 activation by singly substituted tridomain L1L2S variants. For each PDK, $t_{1/2}$ was determined based on remaining PDC activity (%) and time.

		$t_{1/2}$ (min)	
L1L2S	**PDK1**	**PDK2**	**PDK3**[a]
unaltered	53.3	4.5	3.0
E35A	157.5	5.1	14.9
E35K	63.0	28.5	3.8
E153A	216.6	2.5	47.5
E153Q	102.0	4.6	3.3
E153K	69.3	24.2	29.7
V198A	165.4	6.3	5.7
E209A	n/a	2.6	10.6
E209Q	231.0	6.6	13.4
E209K	72.7	23.6	25.6
K46A	n/a	17.2	n/a
K173A	n/a	87.5	n/a

[a] PDK3 was activated by E2p core and L1L2S variants

PDK1. The effect of the singly substituted L1L2S variants on PDK1 activation, reflected by % PDC activity remaining, is summarized in Figure 3.4 (Top) and Table 3.1. Beginning with site E35 located on L1 of L1L2S, E35A had a $t_{1/2}$ of ~ 158 minutes resulting in a 3-fold difference in comparison to wild-type L1L2S (Table 3.1, Figure 3.5 Left). Although the E35A variant does hinder PDK1 activity, it should be noted that the overall PDC activity is eventually reduced to 20% after ~350 minutes (Figure 3.5 Right). The E35K variant had less of an effect on PDK1 with a $t_{1/2}$ of 63 minutes versus wild type L1L2S with $t_{1/2}$ of 53 minutes.
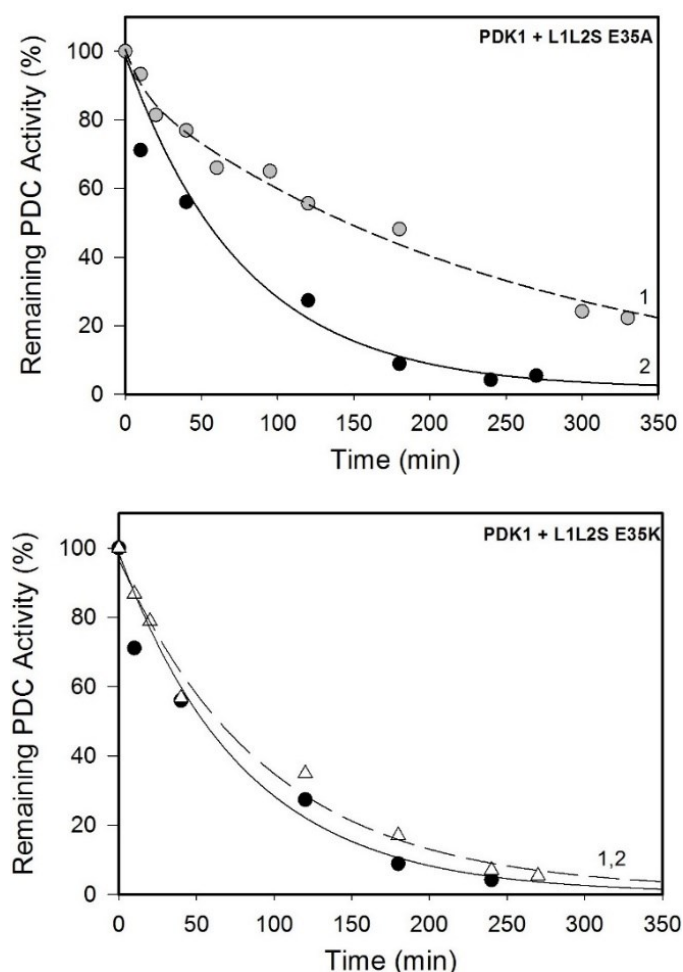
Figure 3.5. Time dependence of the PDC inactivation by PDK1 in the presence of site E35 L1L2S variants. PDK1 (0.6 μg, 0.12 μM) was incubated with E1 (15 μg, 1.95 μM) in the presence of either L1L2S (0.6 μg, 0.32 μM), (2, ●) or **(top)** L1L2S E35A (0.6 μg, 0.32 μM), (1, ○) or **(bottom)** L1L2S E35K (0.6 μg, 0.32 μM), (1, △). Phosphorylation reaction was initiated by ATP (0.5 mM) at 23 °C. Phosphorylation reaction mixture was in 50 mM KH_2PO_4 (pH 7.5) supplemented with 0.5 mM ThDP, 1.0 mM $MgCl_2$, 4.0 mM DTT, 0.1 mM EDTA. Aliquots (1 μg E1) of phosphorylation reaction were withdrawn at different times and were mixed with E2•E3BP and E3 at a mass ratio of E1:E2•E3BP:E3 of 1:3:3 in 1 mL of the PDC reaction assay. After 1 min of incubation at 37 °C, the reaction was initiated by addition of CoA and pyruvate.

Figure 3.6. Time dependence of the PDC inactivation by PDK1 in the presence of site E153 L1L2S variants. PDK1 (0.6 μg, 0.12 μM) was incubated with E1 (15 μg, 1.95 μM) in the presence of either L1L2S (0.6 μg, 0.32 μM), (2, ●) or **(top)** L1L2S E153A (0.6 μg, 0.32 μM), (1, ○), **(middle)** L1L2S E153Q (0.6 μg, 0.32 μM), (1, ▼) or **(bottom)** L1L2S

E153K (0.6 μg, 0.32 μM), (1, △). Phosphorylation reaction was initiated by ATP (0.5 mM) at 23 °C. Phosphorylation reaction mixture was in 50 mM KH_2PO_4 (pH 7.5) supplemented with 0.5 mM ThDP, 1.0 mM $MgCl_2$, 4.0 mM DTT, 0.1 mM EDTA. Aliquots (1 μg E1) of phosphorylation reaction were withdrawn at different times and were mixed with E2•E3BP and E3 at a mass ratio of E1:E2•E3BP:E3 of 1:3:3 in 1 mL of the PDC reaction assay. After 1 min of incubation at 37 °C, the reaction was initiated by addition of CoA and pyruvate.

Of the substitutions tested at site E153 located on L2, the alanine substitution seemed to have the largest effect on PDK1 activity with the glutamine and lysine substitutions having minimal to no effect. The E153A variant had a $t_{1/2}$ value of 216 min, or approximately a 4-fold difference in comparison with wild type L1L2S (Table 3.1, Figure 3.6). Additionally, when PDK1 was tested with the E153A variant, the remaining PDC activity never falls below 40% activity. On the other hand, both the E153Q and E153K variants had similar $t_{1/2}$ values at ~70 min, which was almost identical to wild type L1L2S at 53 minutes.

The alanine substitution at site V198 (L2) had similar results to the other alanine variants, with a $t_{1/2}$ of 165 min, a 3-fold difference versus wild type L1L2S, with PDC activity remaining at 40% (Table 3.1, Figure 3.7).

The substitutions at site E209 had the largest effect on PDK1 activity in comparison to the other variants. First, the E209A variant had the most significant effect on PDK1, where PDC activity remained at 80% activity even after 300 minutes (Figure 3.8). Next,

the E209Q variant also perturbed PDK1 activity with a $t_{1/2}$ value of 230 minutes corresponding to a 4.3-fold difference in activity versus wild type L1L2S (Table 3.1).

Figure 3.7. Time dependence of the PDC inactivation by PDK1 in the presence of site V198 L1L2S variant. PDK1 (0.6 µg, 0.12 µM) was incubated with E1 (15 µg, 1.95 µM) in the presence of either L1L2S (0.6 µg, 0.32 µM), (2, ●) or **(above)** L1L2S V198A (0.6 µg, 0.32 µM), (1, ◎). Phosphorylation reaction was initiated by ATP (0.5 mM) at 23 °C. Phosphorylation reaction mixture was in 50 mM KH_2PO_4 (pH 7.5) supplemented with 0.5 mM ThDP, 1.0 mM $MgCl_2$, 4.0 mM DTT, 0.1 mM EDTA. Aliquots (1 µg E1) of phosphorylation reaction were withdrawn at different times and were mixed with E2•E3BP and E3 at a mass ratio of E1:E2•E3BP:E3 of 1:3:3 in 1 mL of the PDC reaction assay. After 1 min of incubation at 37 °C, the reaction was initiated by addition of CoA and pyruvate.

Figure 3.8. Time dependence of the PDC inactivation by PDK1 in the presence of site E209 L1L2S variants. PDK1 (0.6 μg, 0.12 μM) was incubated with E1 (15 μg, 1.95 μM) in the presence of either L1L2S (0.6 μg, 0.32 μM), (2, ●) or **(top)** L1L2S E209A (0.6 μg,

0.32 μM), (1, ◎), **(middle)** L1L2S E209Q (0.6 μg, 0.32 μM), (1, ▼) or **(bottom)** L1L2S E209K (0.6 μg, 0.32 μM), (1, △). Phosphorylation reaction was initiated by ATP (0.5 mM) at 23 °C. Phosphorylation reaction mixture was in 50 mM KH_2PO_4 (pH 7.5) supplemented with 0.5 mM ThDP, 1.0 mM $MgCl_2$, 4.0 mM DTT, 0.1 mM EDTA. Aliquots (1 μg E1) of phosphorylation reaction were withdrawn at different times and were mixed with E2•E3BP and E3 at a mass ratio of E1:E2•E3BP:E3 of 1:3:3 in 1 mL of the PDC reaction assay. After 1 min of incubation at 37 °C, the reaction was initiated by addition of CoA and pyruvate.

Additionally, it should be noted that the remaining PDC activity remains at ~35% activity even after 300 minutes. It is the only site in which the glutamine substitution had such a large effect on PDK1. Furthermore, while the lysine substitution at E209 had little effect on PDK1 with a $t_{1/2}$ of 73 minutes, it still represented the largest effect among all lysine substitutions with a ~1.5-fold difference versus wild type L1L2S.

Overall, a pattern did emerge where all of the alanine substitutions made on L1L2S had the largest effect on PDK1 (Figure 3.4, top). Following the alanine substitutions, the lysine substitutions were tested since it was hypothesized that changing the residue to the opposite charge could have an even larger effect on PDK1 activity. To our surprise, the lysine substitutions did not affect PDK1 activity; in fact, the activity remained very close to the wild type L1L2S. It is possible that the size of the residue side chain plays a larger role than charge for PDK1 interaction.

PDK2. The effect of the singly substituted L1L2S variants on PDK2 activation was studied and the results are summarized in Figure 3.4 (Middle) and Table 3.1. Substitutions made at site E35 located on L1 of L1L2S were tested where E35K had a much larger effect on PDK2 than E35A. First, the E35A variant behaved very similar to wild type L1L2S with a $t_{1/2}$ value of ~5 min (Table 3.1, Figure 3.9). On the other hand, the E35K variant had a 6-fold difference in rate ($t_{1/2} = 28.5$ min) in comparison to wild type L1L2S.
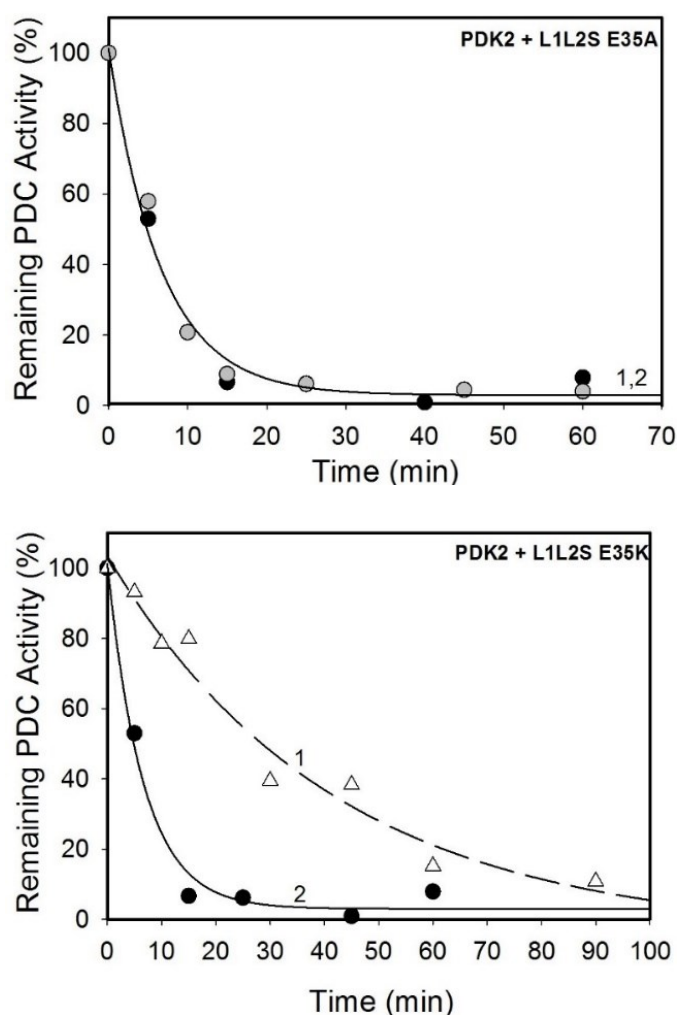
Figure 3.9. Time dependence of the PDC inactivation by PDK2 in the presence of site E35 L1L2S variants. PDK2 (2.2 μg, 0.48 μM) was incubated with E1 (27 μg, 3.5 μM) in

the presence of either L1L2S (0.45 μg, 0.24 μM), (2, ●) or **(top)** L1L2S E35A (0.45 μg, 0.24 μM), (1, ◐) or **(bottom)** L1L2S E35K (0.45 μg, 0.24 μM), (1, △). Phosphorylation reaction was initiated by ATP (2.0 mM) at 30 °C. Phosphorylation reaction mixture was in 50 mM KH_2PO_4 (pH 7.5) supplemented with 0.5 mM ThDP, 1.0 mM $MgCl_2$, 4.0 mM DTT, 0.1 mM EDTA. Aliquots (1 μg E1) of phosphorylation reaction were withdrawn at different times and were mixed with E2•E3BP and E3 at a mass ratio of E1:E2•E3BP:E3 of 1:3:3 in 1 mL of the PDC reaction assay. After 1 min of incubation at 37 °C, the reaction was initiated by addition of CoA and pyruvate.

Site E153 also had similar results with E153A and E153Q having little to no effect on PDK2 versus the E153K substitution. The E153A variant had a $t_{1/2}$ value of ~2.5 min and the E153Q a $t_{1/2}$ of ~5 min, both of which were the same or better than wild type L1L2S (Table 3.1). Again, the lysine substitution at site E153 produced the largest effect on PDK2 with a 5.4-fold difference in rate versus wild type L1L2S (Figure 3.10).
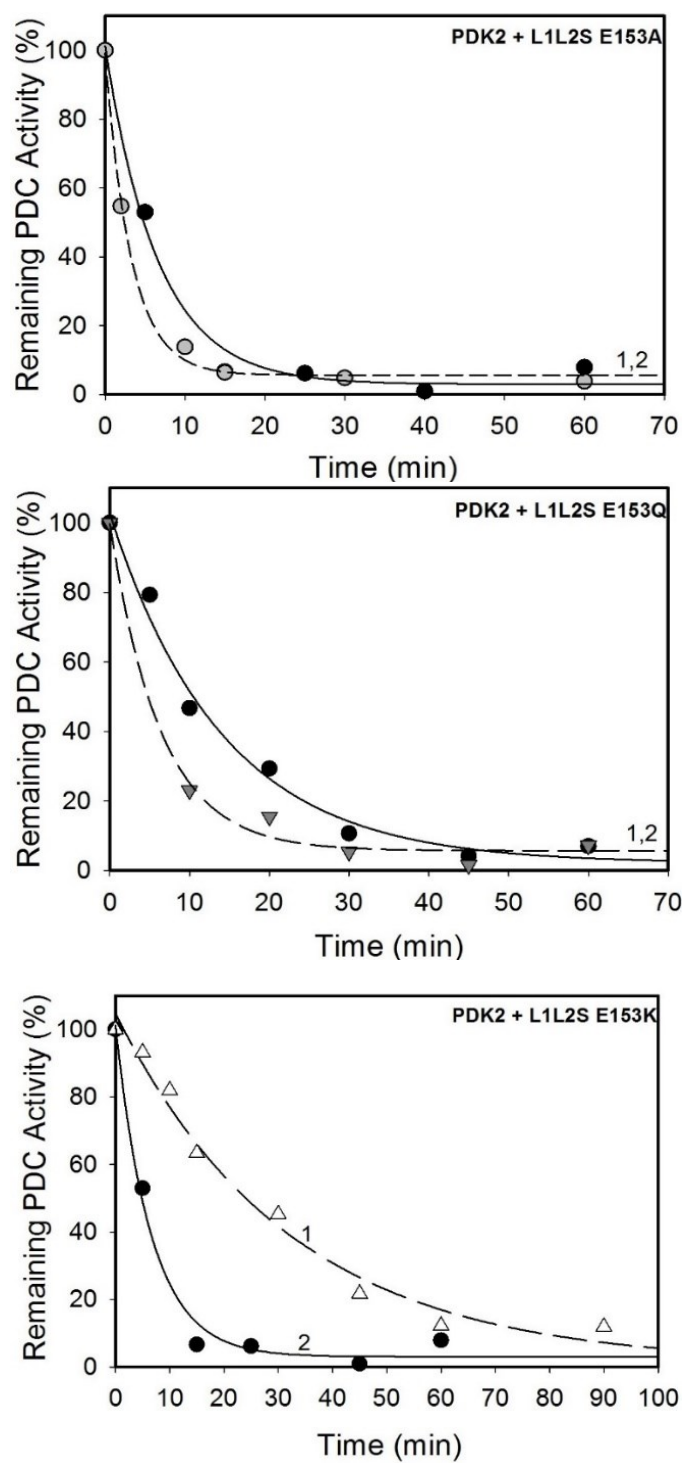
Figure 3.10. Time dependence of the PDC inactivation by PDK2 in the presence of site E153 L1L2S variants. PDK2 (2.2 μg, 0.48 μM) was incubated with E1 (27 μg, 3.5 μM) in the presence of either L1L2S (0.45 μg, 0.24 μM), (2, ●) or **(top)** L1L2S E153A

(0.45 μg, 0.24 μM), (1, ◐), **(middle)** L1L2S E153Q (0.45 μg, 0.24 μM), (1, ▼) or **(bottom)**

L1L2S E153K (0.45 μg, 0.24 μM), (1, △). Phosphorylation reaction was initiated by ATP

(2.0 mM) at 30 °C. Phosphorylation reaction mixture was in 50 mM KH_2PO_4 (pH 7.5)

supplemented with 0.5 mM ThDP, 1.0 mM $MgCl_2$, 4.0 mM DTT, 0.1 mM EDTA. Aliquots

(1 μg E1) of phosphorylation reaction were withdrawn at different times and were mixed

with E2•E3BP and E3 at a mass ratio of E1:E2•E3BP:E3 of 1:3:3 in 1 mL of the PDC

reaction assay. After 1 min of incubation at 37 °C, the reaction was initiated by addition

of CoA and pyruvate.

Unlike PDK1, the alanine substitution at site V198 had no effect on PDK2 with a

$t_{1/2}$ of ~6 minutes (Table 3.1, Figure 3.11). These results reiterate the emerging pattern

with PDK2, where the alanine substitutions simply do not effect PDK2 activity at these
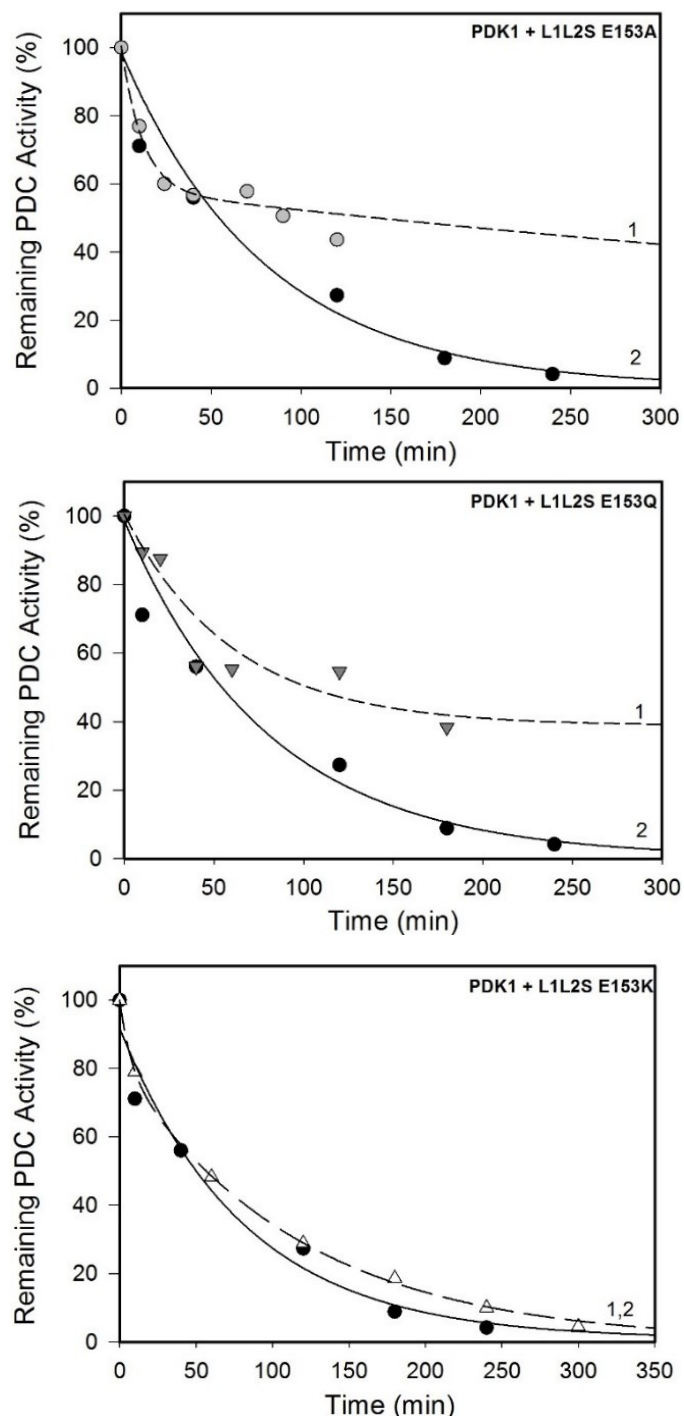
residue sites.
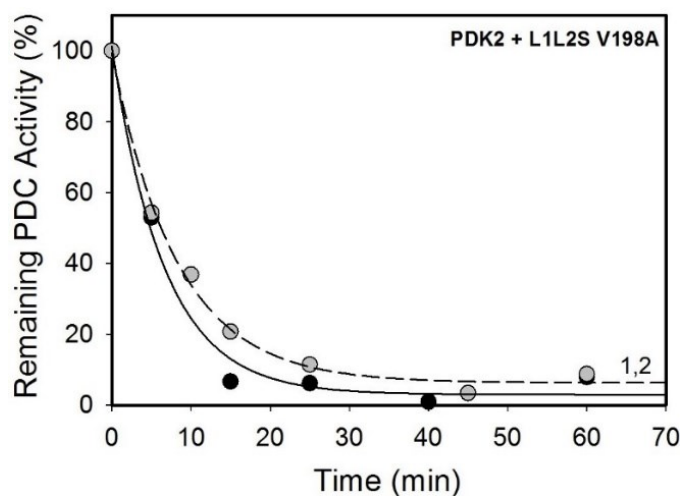
Figure 3.11. Time dependence of the PDC inactivation by PDK2 in the presence of

site V198 L1L2S variant. PDK2 (2.2 μg, 0.48 μM) was incubated with E1 (27 μg, 3.5

μM) in the presence of either L1L2S (0.45 μg, 0.24 μM), (2, ●) or **(above)** L1L2S V198A

(0.45 μg, 0.24 μM), (1, ○). Phosphorylation reaction was initiated by ATP (2.0 mM) at 30 °C. Phosphorylation reaction mixture was in 50 mM KH_2PO_4 (pH 7.5) supplemented with 0.5 mM ThDP, 1.0 mM $MgCl_2$, 4.0 mM DTT, 0.1 mM EDTA. Aliquots (1 μg E1) of phosphorylation reaction were withdrawn at different times and were mixed with E2•E3BP and E3 at a mass ratio of E1:E2•E3BP:E3 of 1:3:3 in 1 mL of the PDC reaction assay. After 1 min of incubation at 37 °C, the reaction was initiated by addition of CoA and pyruvate.

Finally, substitutions at site E209 gave very similar results to those seen with site E153. The alanine and glutamine substitutions again had no effect on PDK2. In fact, the E209A variant was slightly faster than wild type L1L2S with a $t_{1/2}$ value of 2.6 min (Table 3.1). The E209Q variant was almost identical to wild type L1L2S at $t_{1/2}$ of 6.6 min. Once more the lysine substitution at site E209 gave the largest effect on PDK2 with approximately 5-fold difference in rate when compared to wild type L1L2S (Figure 3.12).
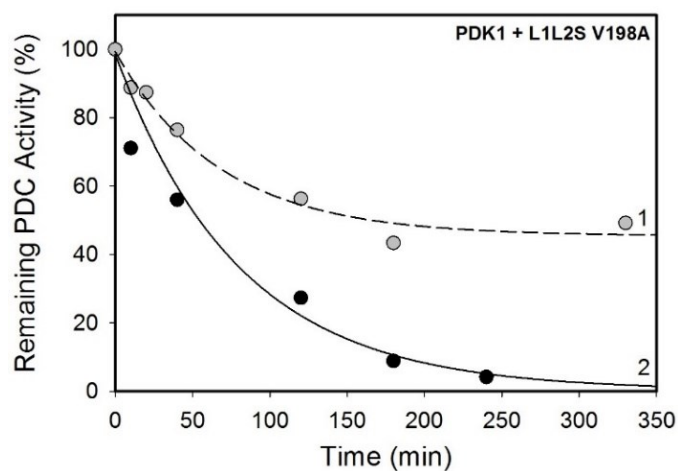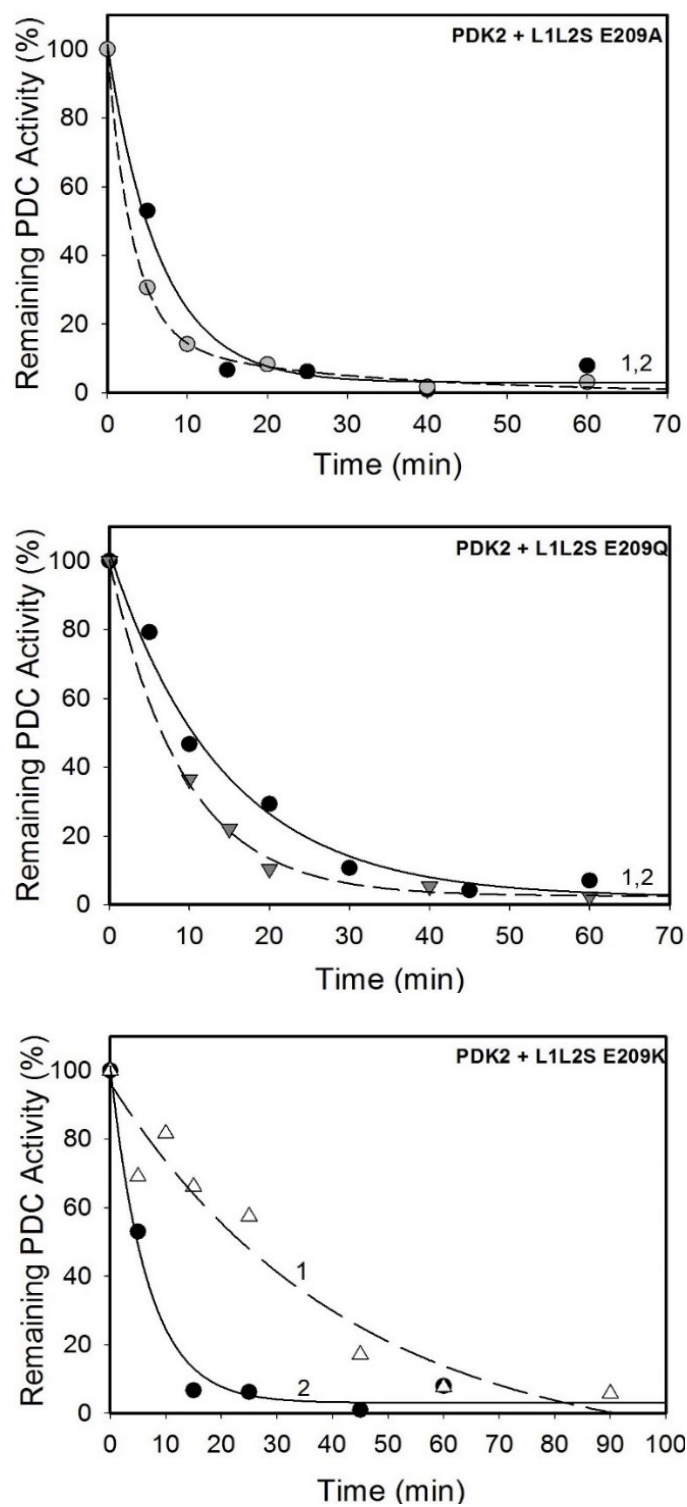
Figure 3.12. Time dependence of the PDC inactivation by PDK2 in the presence of site E209 L1L2S variants. PDK2 (2.2 μg, 0.48 μM) was incubated with E1 (27 μg, 3.5

μM) in the presence of either L1L2S (0.45 μg, 0.24 μM), (2, ●) or **(top)** L1L2S E209A (0.45 μg, 0.24 μM), (1, ◕), **(middle)** L1L2S E209Q (0.45 μg, 0.24 μM), (1, ▼) or **(bottom)** L1L2S E209K (0.45 μg, 0.24 μM), (1, △). Phosphorylation reaction was initiated by ATP (2.0 mM) at 30 °C. Phosphorylation reaction mixture was in 50 mM KH_2PO_4 (pH 7.5) supplemented with 0.5 mM ThDP, 1.0 mM $MgCl_2$, 4.0 mM DTT, 0.1 mM EDTA. Aliquots (1 μg E1) of phosphorylation reaction were withdrawn at different times and were mixed with E2•E3BP and E3 at a mass ratio of E1:E2•E3BP:E3 of 1:3:3 in 1 mL of the PDC reaction assay. After 1 min of incubation at 37 °C, the reaction was initiated by addition of CoA and pyruvate.
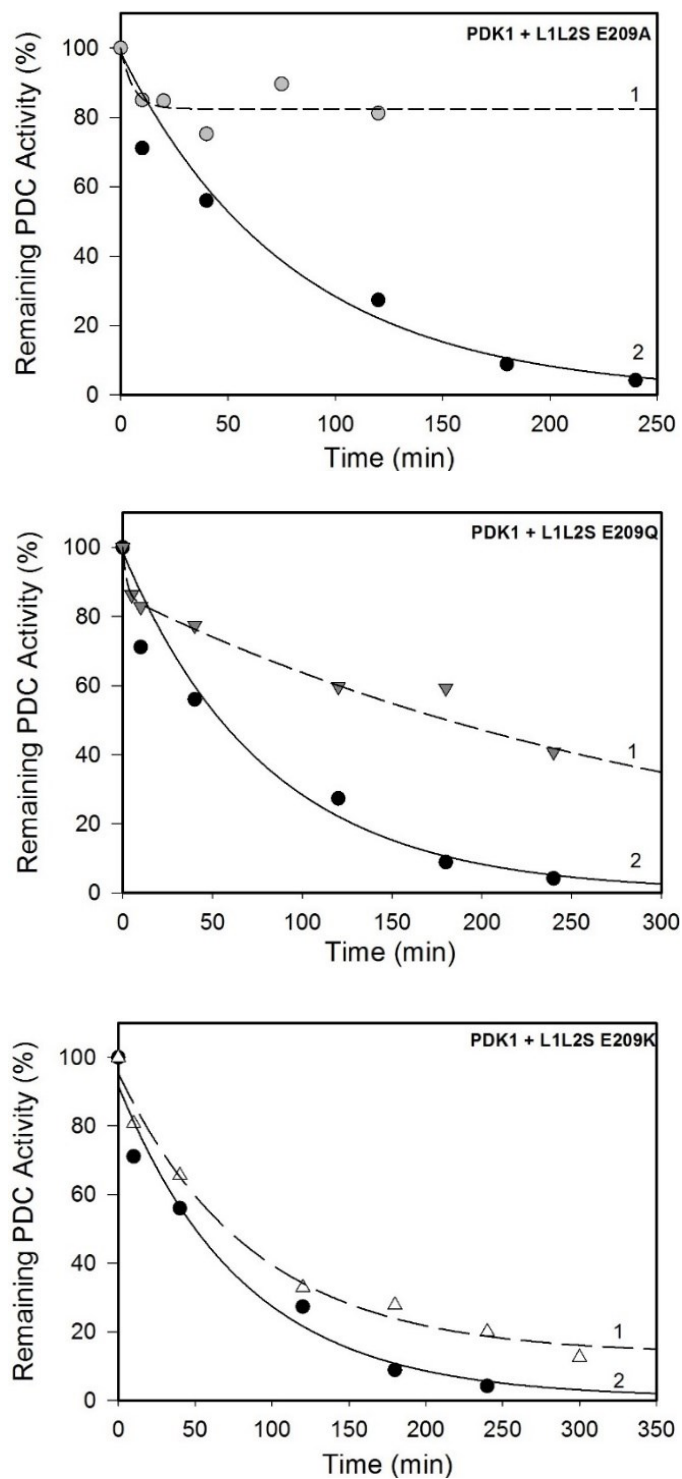
Testing of all the singly substituted L1L2S variants with PDK2 revealed a completely opposite perturbation pattern in comparison to the effects observed with PDK1. In the case of PDK2, it is obvious that with sites E35, E153 and E209 the lysine substitutions produced the largest effect on PDK2 activity (Figure 3.4, middle).

PDK3. Finally, overall PDC activity of phosphorylated E1 by PDK3 in the presence of all the single L1L2S substitutions along with the E2p core domain, which was shown to provide the best PDK3 activation, were tested (Figure 3.4 (Bottom), Table 3.1). First, site E35 on L1 of L1L2S was studied with PDK3, where the E35A variant had a greater effect on PDK3 activity with a 5-fold difference in rate when compared to wild type L1L2S with E2p core (Table 3.1, Figure 3.13). In contrast, the E35K variant had no effect on PDK3 activity with a $t_{1/2}$ value of 3.8 min versus wild type L1L2S plus E2p core at 3.0 min.
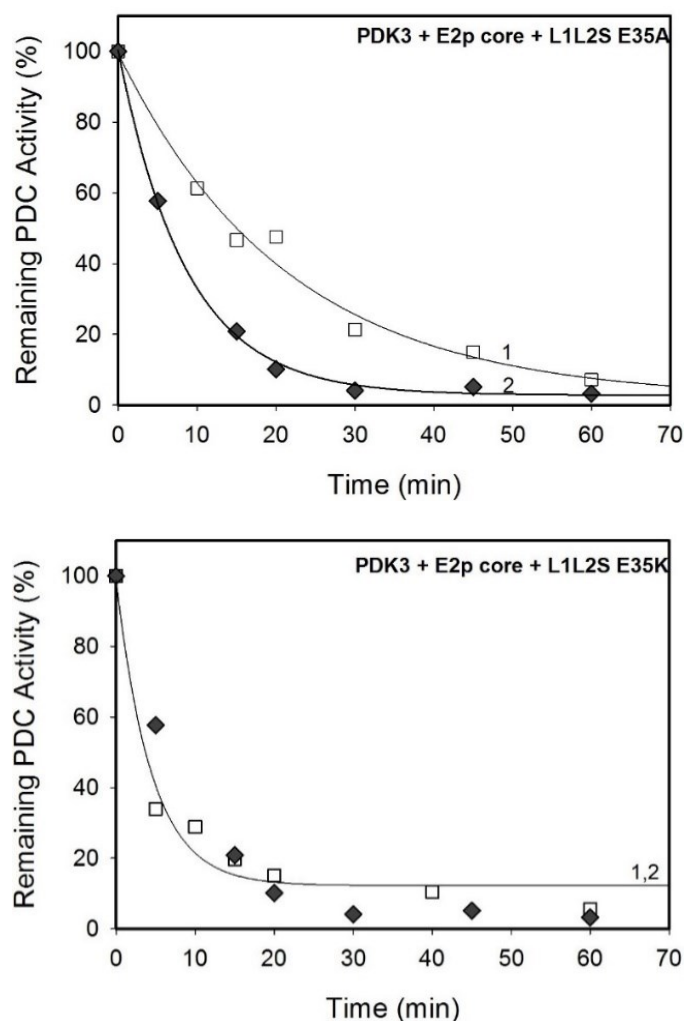
Figure 3.13. Time dependence of the PDC inactivation by PDK3 in the presence of E2p core and site E35 L1L2S variants. PDK3 (0.6 µg, 0.12 µM) was incubated with E2p core (0.6 µg, 0.40 µM) and either L1L2S (0.6 µg, 0.32 µM), (2, ◆) or **(top)** L1L2S E35A (0.6 µg, 0.32 µM), (1, ☐) or **(bottom)** L1L2S E35K (0.6 µg, 0.32 µM), (1, ☐) for 1 hour at 4 °C. E1 (15 µg, 1.95 µM) was then added and phosphorylation reaction was initiated by ATP (0.1 mM) at 30 °C. Phosphorylation reaction mixture was in 20 mM Tris/HCl (pH 7.4) supplemented with 5.0 mM $MgCl_2$, 0.1 M KCl, 2.0 mM DTT. Aliquots (1 µg E1) of phosphorylation reaction were withdrawn at different times and were mixed with E2•E3BP

and E3 at a mass ratio of E1:E2•E3BP:E3 of 1:3:3 in 1 mL of the PDC reaction assay. After

1 min of incubation at 37 °C, the reaction was initiated by addition of CoA and pyruvate.

Of all the substitutions tested, the alanine substitution at site E153 had the largest

effect on PDK3 activity. With a $t_{1/2}$ value of 47.5 min, the difference in rate was 15.6-fold

versus wild type L1L2S with E2p core (Table 3.1, Figure 3.14). The lysine substitution at

site E153 had a similar effect on PDK3 with a 10-fold difference in rate ($t_{1/2}$ of ~30 min).

The glutamine substitution, however, had no effect on PDK3 with a $t_{1/2}$ of 3.3 min.
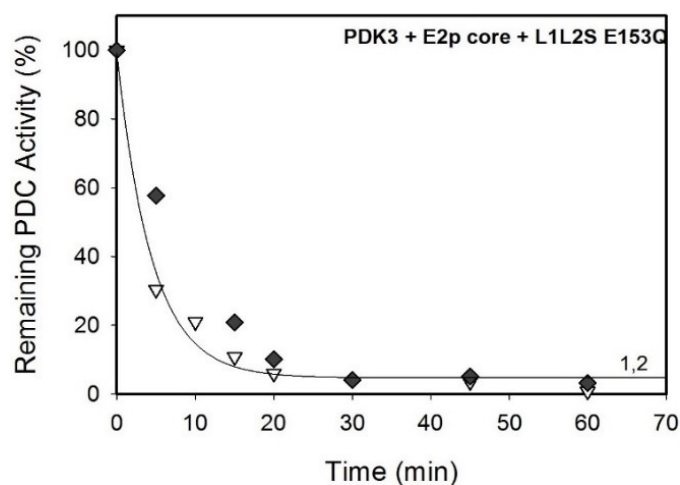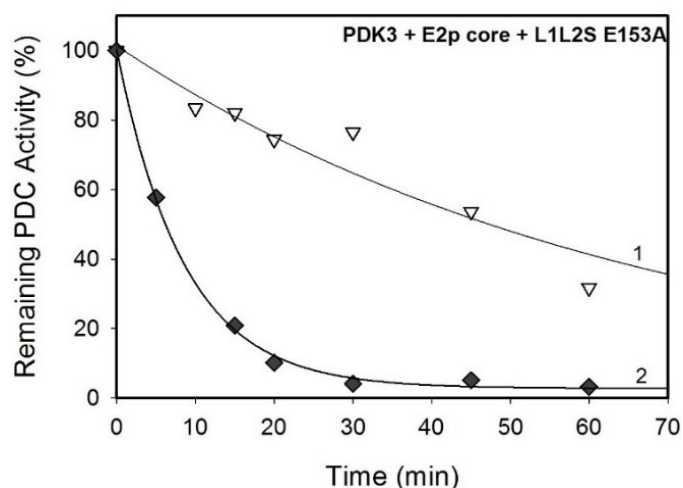
Figure 3.14. Time dependence of the PDC inactivation by PDK3 in the presence of E2p core and site E153 L1L2S variants. PDK3 (0.6 µg, 0.12 µM) was incubated with E2p core (0.6 µg, 0.40 µM) and either L1L2S (0.6 µg, 0.32 µM), (2, ◆) or **(top)** L1L2S E153A (0.6 µg, 0.32 µM), (1, ▽), **(middle)** L1L2S E153Q (0.6 µg, 0.32 µM), (1, ▽) or **(bottom)** L1L2S E153K (0.6 µg, 0.32 µM), (1, ▽) for 1 hour at 4 °C. E1 (15 µg, 1.95 µM) was then added and phosphorylation reaction was initiated by ATP (0.1 mM) at 30 °C. Phosphorylation reaction mixture was in 20 mM Tris/HCl (pH 7.4) supplemented with 5.0 mM MgCl$_2$, 0.1 M KCl, 2.0 mM DTT. Aliquots (1 µg E1) of phosphorylation reaction were withdrawn at different times and were mixed with E2•E3BP and E3 at a mass ratio of E1:E2•E3BP:E3 of 1:3:3 in 1 mL of the PDC reaction assay. After 1 min of incubation at 37 °C, the reaction was initiated by addition of CoA and pyruvate.

Next, the V198A variant was tested with little to no effect on PDK3 activity. The t$_{1/2}$ value of 5.7 min provided a 2-fold reduction in rate when compared with wild type L1L2S plus E2p core (Figure 3.15). It is possible that site V198 does not play a large role in PDK3 activation/ interaction.

Figure 3.15. Time dependence of the PDC inactivation by PDK3 in the presence of E2p core and site V198 L1L2S variant. PDK3 (0.6 μg, 0.12 μM) was incubated with E2p core (0.6 μg, 0.40 μM) and either L1L2S (0.6 μg, 0.32 μM), (2, ◆) or **(above)** L1L2S V198A (0.6 μg, 0.32 μM), (1, ◉) for 1 hour at 4 °C. E1 (15 μg, 1.95 μM) was then added and phosphorylation reaction was initiated by ATP (0.1 mM) at 30 °C. Phosphorylation reaction mixture was in 20 mM Tris/HCl (pH 7.4) supplemented with 5.0 mM $MgCl_2$, 0.1 M KCl, 2.0 mM DTT. Aliquots (1 μg E1) of phosphorylation reaction were withdrawn at different times and were mixed with E2•E3BP and E3 at a mass ratio of E1:E2•E3BP:E3 of 1:3:3 in 1 mL of the PDC reaction assay. After 1 min of incubation at 37 °C, the reaction was initiated by addition of CoA and pyruvate.

Figure 3.16. Time dependence of the PDC inactivation by PDK3 in the presence of E2p core and site E209 L1L2S variants. PDK3 (0.6 μg, 0.12 μM) was incubated with

E2p core (0.6 μg, 0.40 μM) and either L1L2S (0.6 μg, 0.32 μM), (2, ◆) or **(top)** L1L2S E209A (0.6 μg, 0.32 μM), (1, ▢), **(middle)** L1L2S E209Q (0.6 μg, 0.32 μM), (1, ▢) or **(bottom)** L1L2S E209K (0.6 μg, 0.32 μM), (1, ▢) for 1 hour at 4 °C. E1 (15 μg, 1.95 μM) was then added and phosphorylation reaction was initiated by ATP (0.1 mM) at 30 °C. Phosphorylation reaction mixture was in 20 mM Tris/HCl (pH 7.4) supplemented with 5.0 mM $MgCl_2$, 0.1 M KCl, 2.0 mM DTT. Aliquots (1 μg E1) of phosphorylation reaction were withdrawn at different times and were mixed with E2•E3BP and E3 at a mass ratio of E1:E2•E3BP:E3 of 1:3:3 in 1 mL of the PDC reaction assay. After 1 min of incubation at 37 °C, the reaction was initiated by addition of CoA and pyruvate.

Lastly, site E209 was substituted with alanine, lysine and glutamine all of which had some effect on PDK3 activity. The E209A variant had the smallest, but significant, effect with a 3.5-fold reduction in rate ($t_{1/2}$ of 10.6 min) versus wild type (Figure 3.16). Similar to the alanine substitution, the E209Q variant gave a 4.5-fold difference in rate, or $t_{1/2}$ of 13.4 min, in comparison to wild type. Of the three substitutions, the E209K variant had the largest effect on PDK3 activity with a $t_{1/2}$ of 25.6 min resulting in an 8.5-fold reduction in rate.

After studying all of the singly substituted L1L2S variants, it is clear that substitutions made at site E153 had the largest effect on PDK3 activity (Figure 3.4, bottom). Based on the results with E153A and E153K, the charge of the residue side chain seems to play an important role in PDK3-L1L2S interaction. Additionally, all three

substitutions made at site E209 also had a significant effect on PDK3 activity (E209K > E209Q > E209A).

3.3.2 New insight into the interaction loci between PDK1, PDK2 or PDK3 with doubly substituted L1L2S variants and the effects on activation of the PDKs as reflected by PDC inactivation kinetics.

In addition to the activity studies, further fluorescence studies were done to test whether PDK1-3 binding would be effected by the substitutions on L1L2S with the greatest effect on PDK activity. First, the L1L2S-ML1 and L1L2S-ML2 used in florescence were studied with PDK1-3 to test the effects on PDK activity (in ML1 the lysine site of lipoylation in L1 (K46) is substituted to alanine, while in ML2, the lysine site of lipoylation in L2 (K173) is substituted to alanine). Out of all the substitutions studied, the L1L2S variants, K46A and K173A, had the greatest effect on PDK activity with the most striking results found on PDK1 and PDK3.

PDK1. In the case of PDK1, remaining PDC activity remains at 94.6% and 76.3% for L1L2S K46A and L1L2S K173A, respectively, after 5 hours (Figure 3.17). Out of all the substitutions studied, the lipoyl-lysine substitutions had the largest effect on PDK1 by essentially shutting down PDK1 activity. Furthermore, the following doubly substituted L1L2S variants were studied: L1L2S E35A/K173A, L1L2S E35K/K173A, L1L2S K46A/E209A and L1L2S K46A/E209K (Figure 3.18). The remaining PDC activity for all of the double substitutions remained very close to the single lipoyl-lysine substitutions. The remaining PDC activities were as follows: 95.9% for L1L2S E35A/K173A, 90.6% for

L1L2S E35K/K173A, 85.7% for L1L2S K46A/E209A and 88.2% for L1L2S K46A/E209K all over a period of 5 hours.
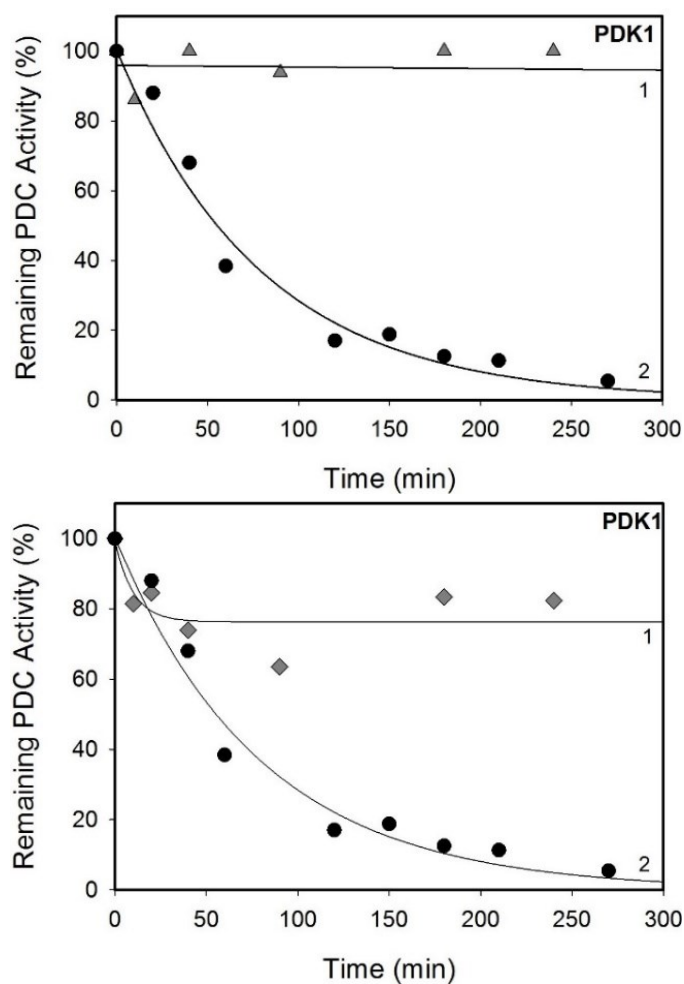
Figure 3.17. Time dependence of the PDC inactivation by PDK1 in the presence of L1L2S K46A or K173A. (Top) Time dependence of the PDC inactivation by PDK1 in the presence of L1L2S K46A. PDK1 (0.6 µg, 0.12 µM) was incubated with E1 (15 µg, 1.95 µM) in the presence of either L1L2S K46A (0.6 µg, 0.32 µM), (1, ▲) or L1L2S (0.6 µg, 0.32 µM), (2, ●). **(Bottom)** Time dependence of the PDC inactivation by PDK1 in the presence of L1L2S K173A. PDK1 (0.6 µg, 0.12 µM) was incubated with E1 (15 µg, 1.95 µM) in the presence of either L1L2S K173A (0.6 µg, 0.32 µM), (1, ◆) or L1L2S (0.6 µg,

0.32 µM), (2, ●). **(Both)** Phosphorylation reaction was initiated by ATP (0.5 mM) at 23

°C. Phosphorylation reaction mixture was in 50 mM KH_2PO_4 (pH 7.5) supplemented with

0.5 mM ThDP, 1.0 mM $MgCl_2$, 4.0 mM DTT, 0.1 mM EDTA. Aliquots (1 µg E1) of

phosphorylation reaction were withdrawn at different times and were mixed with E2•E3BP

and E3 at a mass ratio of E1:E2•E3BP:E3 of 1:3:3 in 1 mL of the PDC reaction assay.

After 1 min of incubation at 37 °C, the reaction was initiated by addition of CoA and

pyruvate.

Figure 3.18. Time dependence of the PDC inactivation by PDK1 in the presence of doubly-substituted L1L2S variants. PDK1 (0.6 µg, 0.12 µM) was incubated with E1 (15

µg, 1.95 µM) in the presence of either L1L2S (0.6 µg, 0.32 µM), (2, ●) or **(top, left)** L1L2S E35A/K173A (0.6 µg, 0.32 µM), (1, ◈), **(top, right)** L1L2S K46A/E209A (0.6 µg, 0.32 µM), (1, ▲), **(bottom, left)** L1L2S E35K/K173A (0.6 µg, 0.32 µM), (1, ◇), or **(bottom, right)** L1L2S K46A/E209K (0.6 µg, 0.32 µM), (1, △). Phosphorylation reaction was initiated by ATP (0.5 mM) at 23 °C. Phosphorylation reaction mixture was in 50 mM KH_2PO_4 (pH 7.5) supplemented with 0.5 mM ThDP, 1.0 mM $MgCl_2$, 4.0 mM DTT, 0.1 mM EDTA. Aliquots (1 µg E1) of phosphorylation reaction were withdrawn at different times and were mixed with E2•E3BP and E3 at a mass ratio of E1:E2•E3BP:E3 of 1:3:3 in 1 mL of the PDC reaction assay. After 1 min of incubation at 37 °C, the reaction was initiated by addition of CoA and pyruvate.

PDK3. PDK3 displayed similar results to those exhibited by PDK1 with the single lipoyl-lysine substitutions, L1L2S K46A and L1L2S K173A, with E2p core. For both L1L2S K46A and L1L2S K173A the activity remained at ~90.0% after 60 minutes in comparison to the wild type L1L2S with E2p core, which reached <20% PDC activity after 15 minutes (Figure 3.19). The L1L2S doubly substituted variants listed above were studied and all had similar effects on PDK3. The PDC activities remaining were as follows: 90.0% for L1L2S E35A/K173A, 87.0% for L1L2S E35K/K173A, 83.0% for L1L2S K46A/E209A and 86.4% for L1L2S K46A/E209K, all over a period of 60 minutes (Figure 3.20).
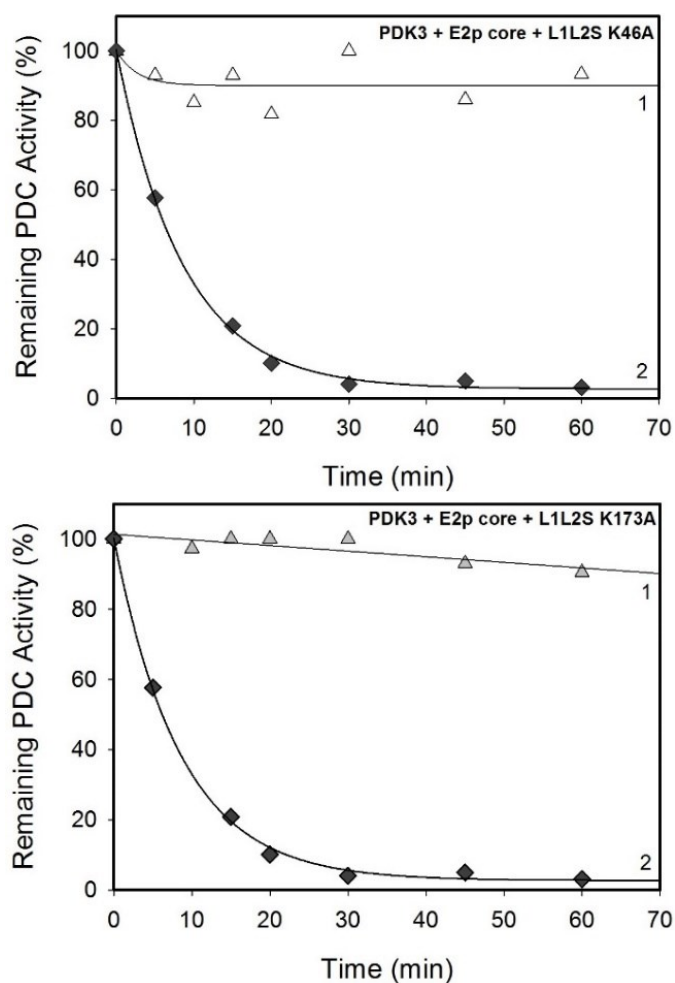
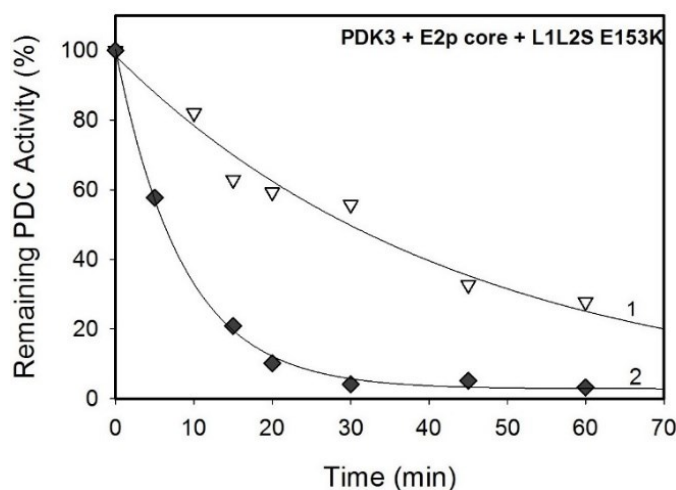**Figure 3.19. Time dependence of the PDC inactivation by PDK3 in the presence of E2p core and L1L2S K46A or K173A. (Top)** Time dependence of the PDC inactivation by PDK3 in the presence of E2p core and L1L2S K46A. PDK3 (0.6 μg, 0.13 μM) was incubated with E2p core (0.6 μg, 0.40 μM) and either L1L2S K46A (0.6 μg, 0.32 μM), (1, △) or L1L2S (0.6 μg, 0.32 μM), (2, ◆) for 1 hour at 4 °C. **(Bottom)** Time dependence of the PDC inactivation by PDK3 in the presence of E2p core and L1L2S K173A. PDK3 (0.6 μg, 0.13 μM) was incubated with E2p core (0.6 μg, 0.40 μM) and either L1L2S K173A (0.6 μg, 0.32 μM), (1, △) or L1L2S (0.6 μg, 0.32 μM), (2, ◆) for 1 hour at 4 °C. **(Both)** E1 (15 μg, 1.95 μM) was then added and phosphorylation reaction was initiated by ATP (0.1 mM) at 30 °C. Phosphorylation reaction mixture was in 20 mM Tris/HCl (pH 7.4)

supplemented with 5.0 mM MgCl$_2$, 0.1 M KCl, 2.0 mM DTT. Aliquots (1 μg E1) of phosphorylation reaction were withdrawn at different times and were mixed with E2•E3BP and E3 at a mass ratio of E1:E2•E3BP:E3 of 1:3:3 in 1 mL of the PDC reaction assay. After 1 min of incubation at 37 °C, the reaction was initiated by addition of CoA and pyruvate.
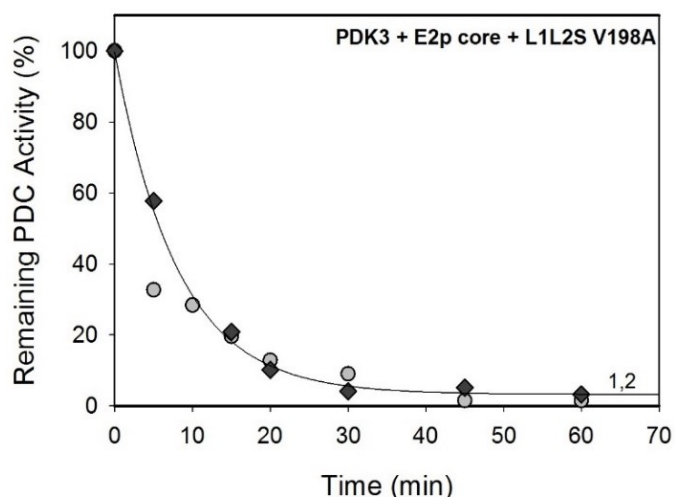

Figure 3.20. Time dependence of the PDC inactivation by PDK3 in the presence of E2p core and the doubly-substituted L1L2S variants. PDK3 (0.6 μg, 0.12 μM) was incubated with E2p core (0.6 μg, 0.40 μM) and either L1L2S (0.6 μg, 0.32 μM), (2, ◆) or **(top, left)** L1L2S E35A/K173A (0.6 μg, 0.32 μM), (1, △), **(top, right)** L1L2S

K46A/E209A (0.6 μg, 0.32 μM), (1, △), **(bottom, left)** L1L2S E35K/K173A (0.6 μg, 0.32 μM), (1, △), or **(bottom, right)** L1L2S K46A/E209K (0.6 μg, 0.32 μM), (1, △) for 1 hour at 4 °C. E1 (15 μg, 1.95 μM) was then added and phosphorylation reaction was initiated by ATP (0.1 mM) at 30 °C. Phosphorylation reaction mixture was in 20 mM Tris/HCl (pH 7.4) supplemented with 5.0 mM MgCl$_2$, 0.1 M KCl, 2.0 mM DTT. Aliquots (1 μg E1) of phosphorylation reaction were withdrawn at different times and were mixed with E2•E3BP and E3 at a mass ratio of E1:E2•E3BP:E3 of 1:3:3 in 1 mL of the PDC reaction assay. After 1 min of incubation at 37 °C, the reaction was initiated by addition of CoA and pyruvate.
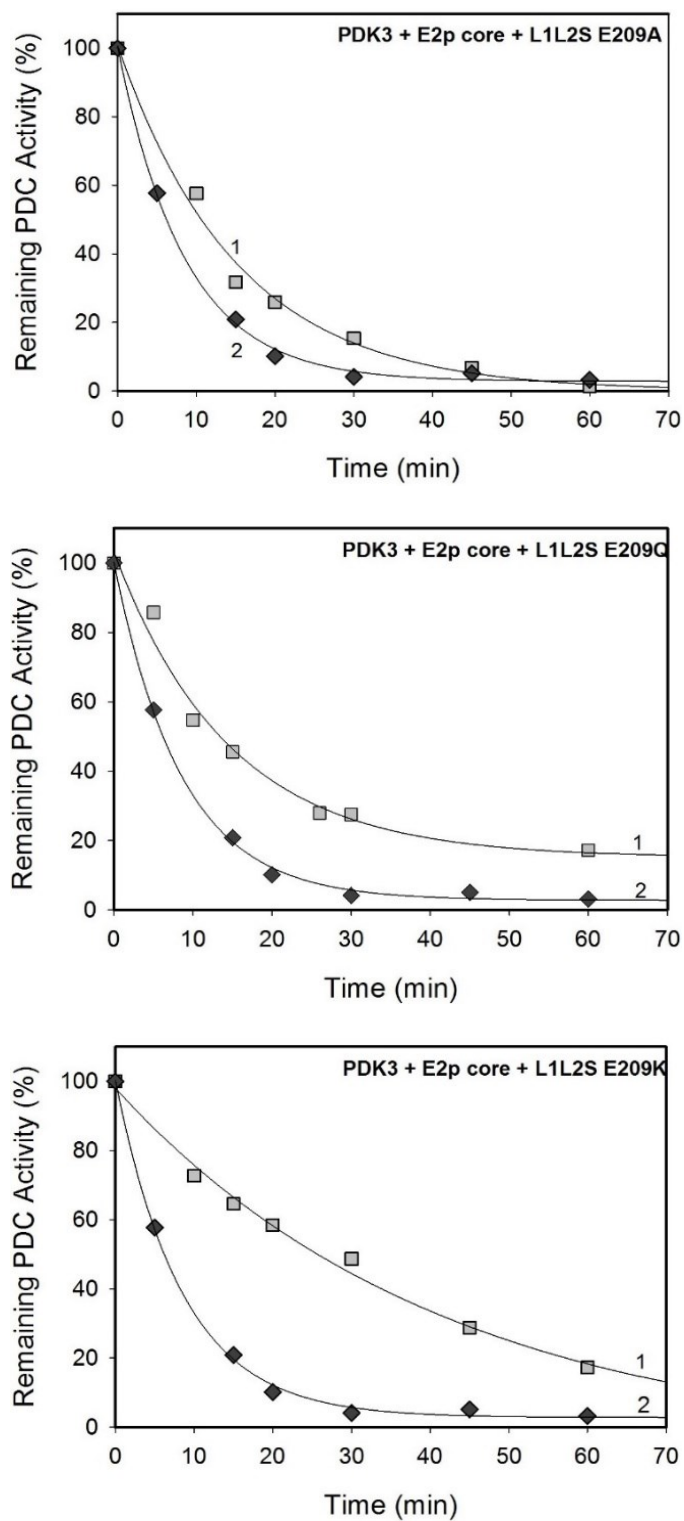
PDK2. The activity of PDK2 was slightly affected by substitutions made at the lipoyl-lysine sites, however the effect was not as apparent as with PDK1 or PDK3 (Figure 3.21). The L1L2S K46A had a smaller effect on PDK2 with 24.8% remaining PDC activity after 90 minutes versus the wild type L1L2S with ~3.00% remaining PDC activity. The L1L2S K173A, on the other hand, had a larger effect on PDK2 with PDC activity remaining at 49.0% after the same 90 minutes. The double substitutions were studied and all had similar effects on PDK2. The $t_{1/2}$ values were as follows: 25.7 min. for L1L2S E35A/K173A, 16.9 min. for L1L2S E35K/K173A, 31.5 min. for L1L2S K46A/E209A and 27.7 min. for L1L2S K46A/E209K versus 4.56 min. for wild type L1L2S (Figure 3.22).
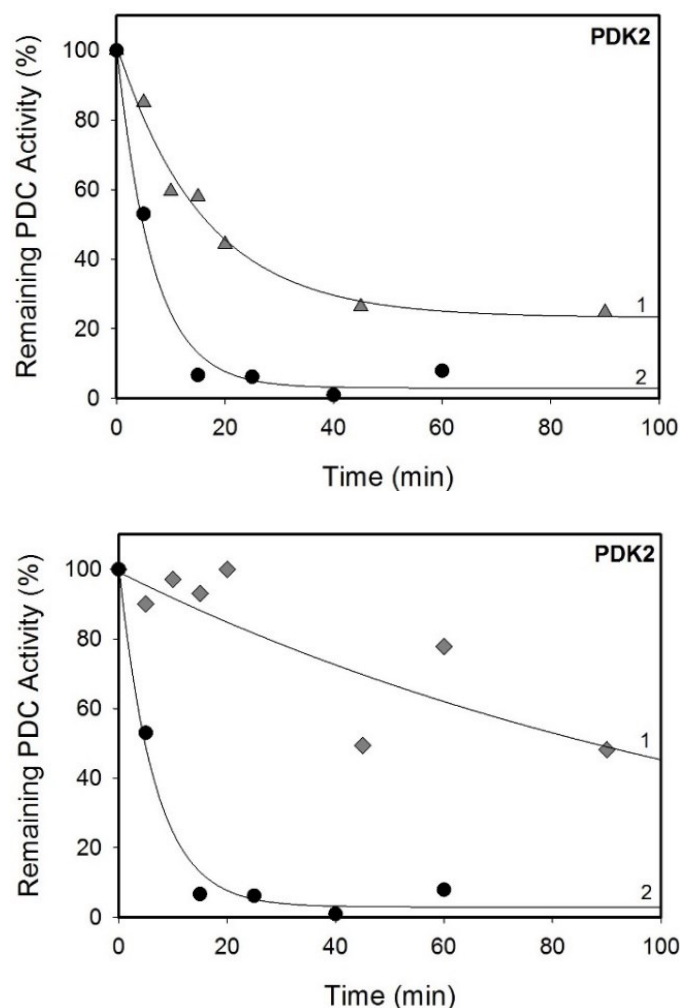
Figure 3.21. Time dependence of the PDC inactivation by PDK2 in the presence of L1L2S K46A or K173A. (Top) Time dependence of the PDC inactivation by PDK2 in the presence of L1L2S K46A. PDK2 (2.2 µg, 0.48 µM) was incubated with E1 (27 µg, 3.5 µM) in the presence of either L1L2S K46A (0.45 µg, 0.24 µM), (1, ▲) or L1L2S (0.45 µg, 0.24 µM), (2, ●). **(Bottom)** Time dependence of the PDC inactivation by PDK2 in the presence of L1L2S K173A. PDK2 (2.2 µg, 0.48 µM) was incubated with E1 (27 µg, 3.5 µM) in the presence of either L1L2S K173A (0.45 µg, 0.24 µM), (1, ◆) or L1L2S (0.45 µg, 0.24 µM), (2, ●). **(Both)** Phosphorylation reaction was initiated by ATP (2.0 mM) at 30 °C. Phosphorylation reaction mixture was in 50 mM KH_2PO_4 (pH 7.5) supplemented

with 0.5 mM ThDP, 1.0 mM MgCl$_2$, 4.0 mM DTT, 0.1 mM EDTA. Aliquots (1 µg E1) of phosphorylation reaction were withdrawn at different times and were mixed with E2•E3BP and E3 at a mass ratio of E1:E2•E3BP:E3 of 1:3:3 in 1 mL of the PDC reaction assay. After 1 min of incubation at 37 °C, the reaction was initiated by addition of CoA and pyruvate.

Figure 3.22. Time dependence of the PDC inactivation by PDK2 in the presence of the doubly-substituted L1L2S variants. PDK2 (2.2 µg, 0.48 µM) was incubated with E1 (27 µg, 3.5 µM) in the presence of either L1L2S (0.45 µg, 0.24 µM), (2, ●) or **(top, left)** L1L2S E35A/K173A (0.45 µg, 0.24 µM), (1, ◇), **(top, right)** L1L2S K46A/E209A (0.45 µg, 0.24

μM), (1, ▲), **(bottom, left)** L1L2S E35K/K173A (0.45 μg, 0.24 μM), (1, ◇), or **(bottom, right)** L1L2S K46A/E209K (0.45 μg, 0.24 μM), (1, △). Phosphorylation reaction was initiated by ATP (2.0 mM) at 30 °C. Phosphorylation reaction mixture was in 50 mM KH$_2$PO$_4$ (pH 7.5) supplemented with 0.5 mM ThDP, 1.0 mM MgCl$_2$, 4.0 mM DTT, 0.1 mM EDTA. Aliquots (1 μg E1) of phosphorylation reaction were withdrawn at different times and were mixed with E2•E3BP and E3 at a mass ratio of E1:E2•E3BP:E3 of 1:3:3 in 1 mL of the PDC reaction assay. After 1 min of incubation at 37 °C, the reaction was initiated by addition of CoA and pyruvate.
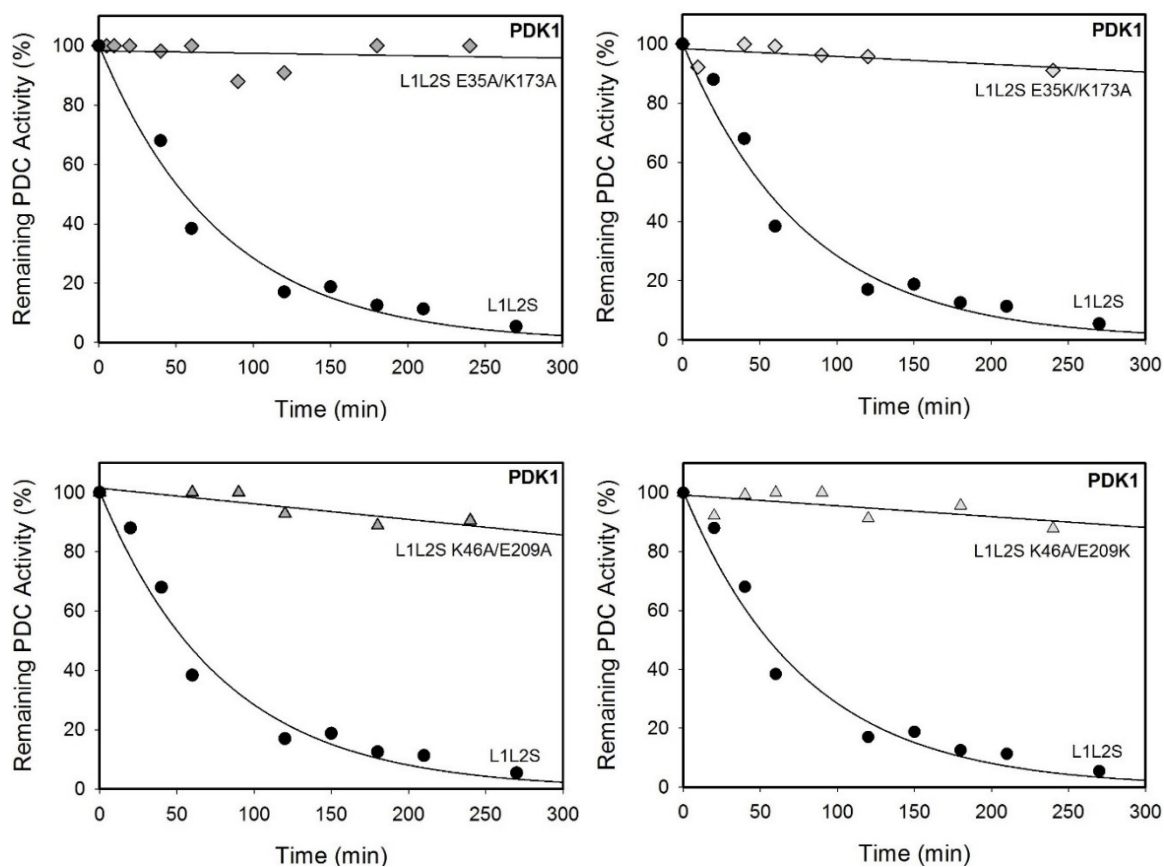
Table 3.2. Kinetic parameters for L1L2S and its singly substituted variants inactivated by PDK1-PDK3.

L1L2S	(a) PDK1		(b) PDK2		(c) PDK3[a]	
	k_{app} (min^{-1})	Ratio k_{app} (%)	k_{app} (min^{-1})	Ratio k_{app} (%)	k_{app} (min^{-1})	Ratio k_{app} (%)
unaltered	0.013 ± 0.0007	100	0.152 ± 0.02	100	0.240 ± 0.005	100
E35A	0.004 ± 0.0001	30.8	0.147 ± 0.019	96.7	0.047 ± 0.008	19.6
E35K	0.011 ± 0.0005	84.6	0.024 ± 0.007	15.8	0.22 ± 0.05	91.7
E153A	0.0032 ± 0.001	24.6	0.307 ± 0.02	202	0.015 ± 0.002	6.25
E153Q	0.0063 ± 0.0009	48.5	0.157 ± 0.018	103	0.230 ± 0.033	95.8
E153K	0.010 ± 0.0002	76.9	0.0312 ± 0.006	20.5	0.023 ± 0.002	9.60
V198A	0.0044 ± 0.0002	33.8	0.121 ± 0.009	79.6	0.124 ± 0.010	52.0
E209A	0.0017 ± 0.0002	13.1	0.316 ± 0.028	208	0.066 ± 0.004	27.5
E209Q	0.003 ± 0.0002	23.1	0.1095 ± 0.006	72.0	0.069 ± 0.012	28.8
E209K	0.0115 ± 0.0019	88.5	0.023 ± 0.010	15.1	0.024 ± 0.005	10.0
K46A	n/a	n/a[b]	0.063 ± 0.009	41.4	0.0099 ± 0.002	4.13
K173A	n/a	n/a[c]	0.008 ± 0.002	5.3	0.0032 ± 0.0002	1.33

[a] PDK3 was activated by E2p core and L1L2S variants

[b,c] n/a, not available. About 80-90% activity remained after 300 min treatment with PDK

Through our studies on the effects of singly substituted L1L2S variants on PDK1-3 activation, it has become evident that PDK activation by the E2•E3BP core are unique extending beyond the interaction with L2 domain. Beginning with PDK1, substitutions made at site E209 on L2 of L1L2S perturbed PDK1 activity the most. Specifically, when comparing the rate of PDK1 activation by L1L2S E209A (k_{app} = 0.002 min^{-1}) versus unaltered L1L2S (k_{app} = 0.013 min^{-1}), the rate of activation was only 13% (Table 3.2 a). The E209Q variant had similar results with a k_{app} of 0.003 min^{-1}, or 23% rate of activation, both of which effected PDK1 activity the most of all the variants. The E209K variant, however, had no effect on PDK1 activity as the rate of activation was 88.5% (k_{app} = 0.012 min^{-1}). Based on the results above, we can conclude that the charge on the residue side chain does not play an important role. It is clear that site E209 is important for PDK1 activation/ interaction perhaps forming hydrogen bonds. To date, there are no crystal structures for PDK1-L2 interaction only that of PDK1[71], therefore, these results provide unique insight into PDK1 interaction with E2•E3BP.

A similar pattern emerged with the substitutions at site E153 (Table 3.2 a). First, the alanine substitution, E153A, again had the largest effect on PDK1 activation with a k_{app} of only 0.0032 min^{-1}, or 24.6% activation in comparison with wild type. The glutamine substitution, although not as large of an effect, had a k_{app} of ~0.006 min^{-1} (48.5%) while the lysine substitution had little to no effect on PDK1 with ~77% activation. Although the effect on PDK1 activity is not as large as with site E209, the studies with the E153 variants revealed another residue involved in PDK1 activation. As with E209, site E153 is not involved in acid/base catalysis, but rather may contribute to hydrogen bonding.

Next, at site E35, we tested both alanine and lysine substitutions (Table 3.2 a). This is the first example of a residue on L1 of L1L2S being tested for PDK interaction/ activation. The E35A variant lead to significant changes, with only 31% activation in comparison with unaltered L1L2S. However, the E35K variant did not affect PDK1 activity as much with 85% activation. In keeping with the pattern for PDK1, again the alanine substitution had the larger effect, while the lysine substitution displayed little to no effect on PDK1. Therefore, as before with the other residues, site E35 does not seem to participate in any electrostatic interactions.

For site V198 only the alanine substitution was tested with similar results as the other alanine substitutions made at the other sites. The V198A variant had a k_{app} of 0.0044 min^{-1} (or ~ 34% activation), making it an important residue for PDK1 interaction/ activation. In the case of site V198, it is possible that it plays a role in hydrophobic interactions with PDK1.

In the presence of PDK2, a different pattern emerged when tested with all of the L1L2S variants (Table 3.2 b). Unlike PDK1, the alanine and glutamine variants had little to no effect on PDK2 activity with a rate of ~72-100% activation versus unaltered L1L2S (k_{app} = 0.152 min^{-1}). The only substitution on L1L2S that had any effect on PDK2 activation were the glutamate to lysine substitutions. First, when compared with unaltered L1L2S, the E35K variant only provided 16% rate of activation. Previously, only the PDK2-L2 interaction has been studied[48,66] and therefore these results provide significant insight to PDK2-L1L2S interaction. It is clear that site E35 located on L1 plays an important role in PDK2 interaction/activation, specifically it may provide electrostatic interactions with PDK2 due to its proximity to the 'DKA' site of L1.

Next, the E153K variant was studied providing further insight into PDK2 activation with only 20% rate of activation versus the unaltered L1L2S (Table 3.2 b). Based on the available PDK2-L2 crystal structure, site E153 is located near the identified acidic cluster on L2[48,66]. Furthermore, it was shown that the glutamate to lysine substitution provided a large effect on PDK2 suggesting that site E153 may be involved in electrostatic interactions with PDK2 (Figure 3.23).
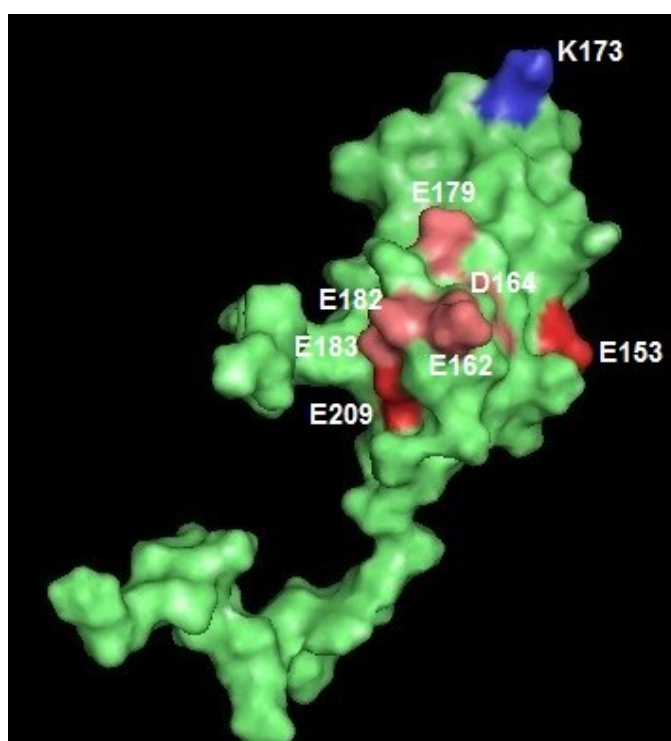
Figure 3.23 Space filling representation of L2 based on Popov et al.[48]. Previously identified acidic cluster known to interact with PDK2 or PDK3 are in salmon, and the lipoyl lysine site of L2 (inner lipoyl domain) is in blue. Our identified residues, E153 and E209, are shown in red. The graphics were generated using PyMOL, version 1.8.4.0.

Similar to the results above, the lysine substitution on site E209 had the largest effect on PDK2 activity. For the E209K variant only 15% rate of activation was observed versus unaltered L1L2S (Table 3.2 b). Again, this suggests that site E209 may be involved in electrostatic interactions with PDK2 especially since site E209 is located near the acidic cluster previously identified[48,66] (Figure 3.23).

Lastly, PDK3 was tested with the singly substituted L1L2S variants providing yet a third different activation pattern (Table 3.2 c). The most significant impact on PDK3 activity was observed when site E153 on L2 was substituted with alanine with a rate of 6.25% of the unaltered L1L2S or lysine with a rate of 9.60%. Based on these results, site E153 is an important residue for PDK3 interaction/activation and may be responsible for H-bonding with the C-terminal tail on PDK3 as seen in the crystal structure of PDK3-L2[54]. The other E153 variant, E153Q, did not affect PDK3 activity as it had a rate of 96% which could be due to the fact that glutamine may still provide some H-bonding whereas lysine and alanine substitutions would completely perturb any H-bonding. Following site E153, all the substitutions on site E209 provided strong effects on PDK3 activity as follows: E209K had a rate of 10%, E209A with 28% and E209Q with 30%. This suggests that the negative charge on the E209 side chain plays an important role in PDK3 interaction, which would be disrupted by the substitutions tested. Furthermore, both site E153 and E209 are located near the acidic cluster previously identified to interact with PDK3 via electrostatic interactions[10,54].

As for the inner lipoyl domain, L1, the E35A variant had a rate of 20%, however, the E35K variant did not affect PDK3 activation with a rate of 92%. It is possible the size

of the side chain of E35 participates in hydrophobic interactions with PDK3 rather than electrostatic interactions due to charge.

The studies with the lipoyl-lysine residue substitutions and the doubly substituted L1L2S variants provided some more insight into PDK-L1L2S interaction. <u>Remarkably, for PDK1 and PDK3, alanine substitution of either lipoyl-lysine residues, L1L2S K46A or L1L2S K173A, completely shuts down PDK activity keeping overall PDC activity at around 90-100% (Figures 3.17 and 3.19).</u> This suggests that both lipoyl-lysine residues are imperative for PDK1 or PDK3 activation. This is the first time it has been shown that both lipoyl-lysine sites on L1 and L2 interact with PDK1 or PDK3 indicating that both the inner and outer lipoyl domains are important for PDK1 or PDK3 activation.

PDK2, on the other hand, did not demonstrate such a large dependence on both lipoyl-lysine sites as did PDK1 and PDK3 (Figure 3.21). The L1L2S K46A and L1L2S K173A variants had a $t_{1/2}$ of ~20 minutes, and more importantly reach ~20% remaining PDC activity in 90 minutes (Table 3.1). When comparted with the unaltered L1L2S, the K46A variant had a rate of activation of 41% clearly indicating that although the rate is perturbed, PDK2 can still reduce PDC activity (Table 3b). From these studies it is obvious that each PDK is unique in the way it interacts with L1L2S providing specific targets to suppress PDK activity.

3.4 CONCLUSIONS

Evidence from the overall PDC activity experiments conducted with PDK1-3 and the L1L2S variants suggests that the residues previously identified by the Jordan group[55] as well as the lipoyl lysine residues do in fact play an important role in PDK- E2•E3BP core interaction. Importantly, each of the PDKs studied interact with the identified residues in a different fashion, which can be exploited for PDK-specific drug design.

For PDK1, the largest effect on PDK activation was seen by all alanine substitutions while the lysine substitutions had surprisingly little effect on PDK1 activity. Glutamine substitutions behaved similarly to the alanine variants. Additionally, site E209 seemed to be the most important residue identified as any substitution at this site had the largest effect overall. These results suggest that charge does not play an important role in PDK1-E2•E3BP core interaction; these are the first results verifying PDK1-E2•E3BP core interactions as the only x-ray structure available is of PDK1 alone.

PDK2 studies yielded completely different results, where only the lysine substitutions had any impact on PDK activation. These results suggest that the charge of the amino acid side chain is important for PDK2- E2•E3BP core interaction. Furthermore, the lysine substitution at site E35 located on L1, one of the lysine substitution effecting PDK activation, was not identified previously as the crystal structure was of PDK2 bound to only L2.

Unlike PDK1 and PDK2, the pattern that emerged with PDK3 was specific to certain residues rather than a blanket pattern based on substitution. For instance, alanine and lysine substitutions on site E153 displayed one of the largest effects on PDK3

activation as well as all substitutions on site E209. Both sites are located near a previously identified acidic cluster[54], and therefore it is possible that they are involved in extensive hydrogen-bonding with PDK3.

The lipoyl-lysine residues play a major role in PDK activation, where the lipoyl lysine residues of the E2•E3BP core with bound reduced dihydrolipoamide projects into a hydrophobic pocket within PDKs forming an anchoring scaffold. In the case of both PDK1 and PDK3, alanine substitution at either lipoyl-lysine residue effectively shuts down PDK activity suggesting that both sites on the inner and outer lipoyl domains are imperative to PDK activation. PDK2, on the other hand, can still be activated by L1L2S variants with either lipoyl-lysine residue substituted for alanine. For the first time, these results indicate that for PDK1 and PDK3 activation, a synergistic dependence occurs where *both* lipoyl-lysine sites are essential for interaction whereas PDK2 activation does not have such a dependence. Again, we have shown the importance of studying the entire E2•E3BP core and its effects on PDK activation in order to provide a whole picture necessary for specific drug design.

CHAPTER 4

Chiral carboligation catalyzed by the E1 component of the 2-oxoglutarate dehydrogenase complex

4.1 INTRODUCTION

Carboligation, or C-C bond formation, is known to be catalyzed by some ThDP-dependent enzymes including transketolases, glyoxylate carboligase, 1-deoxy-D-xylulose-5-phosphate synthase, and benzaldehyde lyase.[73-77] For nearly all other ThDP-dependent 2-oxoacid decarboxylases, carboligation (C-C bond formation) is a known side reaction. Previously, the synthetic program in the Jordan group began with various active site variants in both yeast pyruvate decarboxylase (YPDC) from *Saccharomyces cerevisiae* and the E1 component of *Escherichia coli* pyruvate dehydrogenase complex (E1p) capable of catalyzing such reactions[78-80].

Recently, the Jordan group has explored the E1 component of the *Escherichia coli* 2-oxoglutarate dehydrogenase complex (OGDHc) in the synthesis of chiral carboligation products with multiple functional groups[81]. With varying substrates and acceptors, it was demonstrated that E1oec can in fact accept substrates in addition to its natural substrate, 2-oxoglutarate, as well as different aldehyde acceptors in the carboligation reaction. Other recent examples of E1o-catalyzed carboligation reaction include studies reported by Müller et al. where 2-oxoglutarate was used as the sole substrate with several aliphatic and aromatic aldehyde acceptors[73,82].

The general mechanism common to all ThDP-dependent decarboxylation is as follows: E1o catalyzes the initial formation of a pre-decarboxylation covalent ThDP-bound intermediate by reaction at the C2 thiazolium atom of the enzyme-bound ThDP with the substrate's keto carbon. Decarboxylation of this intermediate leads to a strongly nucleophilic enamine, which, in the absence of the other components of the complex (the E2o-E3 sub-complex), may react with electrophilic compounds leading to the formation of acetoin-like or acetolactate-like ligated products (Scheme 4.1).

Scheme 4.1 E1o catalyzed reaction mechanism of the carboligase product.
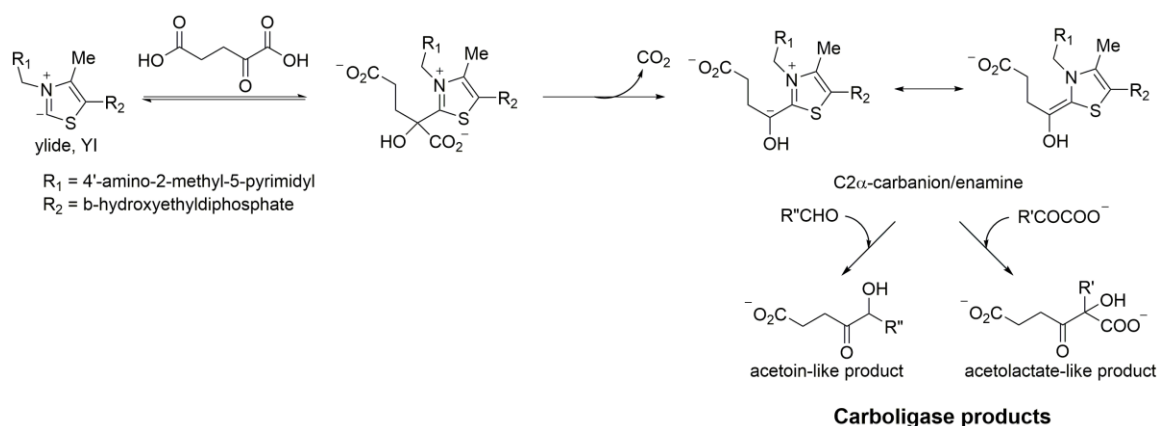
The carboligase products with a chiral α-hydroxyketone are valuable building blocks for organic synthesis. In these studies, we aim to expand on the list of possible substrates and acceptors with various functional groups, as well as gain further kinetic information on these alternative substrates and acceptors (Figure 4.1). The products were confirmed by CD spectroscopy and ^{1}H nuclear magnetic resonance (NMR). This work reinforces the use of E1o as a chiral synthetic tool demonstrated by the fact that (a) the enzyme accepts the 2-oxoacid, 2-oxoadipate, as well as the carboxylic acids, 2-

ketohexanoic acid and 2-oxo-5-hexenoic acid, as substrates and (b) that the straight chain aldehydes, butyraldehyde and propanal, can also serve as aldehyde acceptors in addition to glyoxylate.
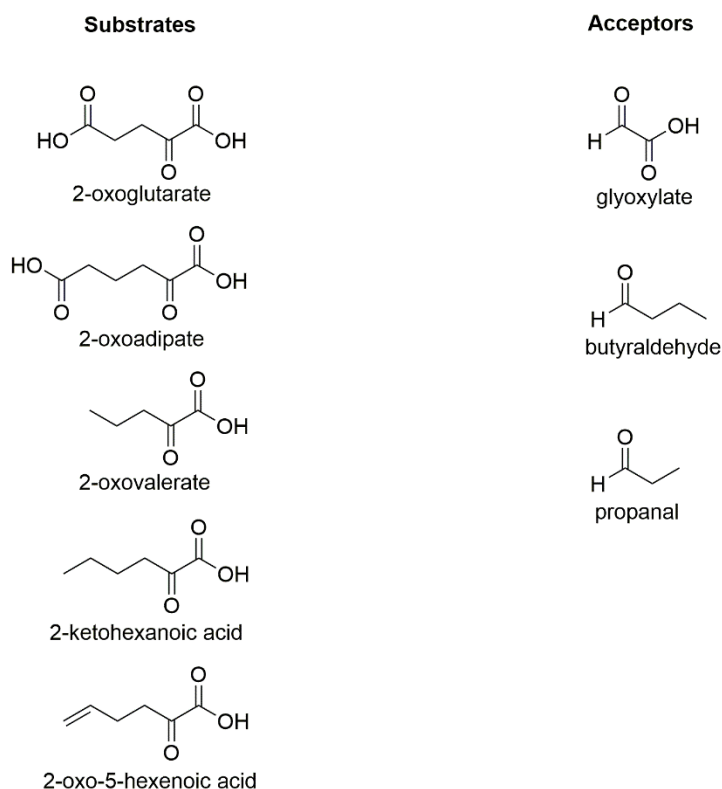
Figure 4.1 Substrates and acceptors for carboligase reaction.

4.2 MATERIALS and METHODS

4.2.1 Materials. Ni-NTA agarose used for protein purification was purchased from GE Healthcare Life Sciences. Thiamin diphosphate (ThDP), dithiothreitol (DTT), isopropyl-β-D-thiogalactopyranoside (IPTG), NAD^+, coenzyme A (CoA), Micrococcal Nuclease, and DNase I, Lyophilized were purchased from Affymetrix USB. *E. coli* strain JW0715 containing the plasmid pCA24N encoding the OGDHc-E1 (E1o) component [ASKA clone (-)] was obtained from National Bio Resource Project (NIG, Japan). Sodium pyruvate, 2,6-

dichlorophenolindophenol (DCPIP), 2-oxoglutarate (2-OG), 2-oxovalerate (2-OV), 2-oxoadipate (2-OA), and glyoxylic acid were purchased from Sigma Aldrich. Butyraldehyde and propanal were purchased from Acros Organics (part of Thermo Fisher Scientific). 2-Ketohexanoic acid (2-OH) was purchased from Santa Cruz Biotechnology. 4-Pentenal was purchased from Thermo Fisher Scientific Chemicals.

4.2.2 Wild type E1o-ec and E1o-ec H298D: Bacterial Strains, Plasmids, Overexpression, and Purification.

Bacterial Strains, Plasmids and Overexpression[83]. Recombinant wild type E1o-ec was obtained from *E. coli* strain JW0715 containing the plasmid pCA24N encoding the OGDHc-E1 (E1o) component. An *E. coli* AG1 frozen stock harboring the E1o plasmid was streaked on LB agar plates containing chloramphenicol (100 μg/mL) and incubated at 37 °C overnight. A single colony was used to inoculate 5 tubes with 10 ml LB containing chloramphenicol (100 μg/mL). The overnight culture, ~ 14 ml for a 20:1 dilution, was then used to inoculate 6 x 700 ml of LB medium containing chloramphenicol (100 μg/mL), 1.0 mM thiamin hydrochloride, and 2.0 mM $MgCl_2$. Cells were grown for about 2-2.5 hours at 37 °C to OD_{600} = 0.60-0.70, then 0.50 mM IPTG was added and cells were grown overnight at 30 °C with shaking. The cells were collected at 4400 g at 4 °C and washed with 20 mM KH_2PO_4 (pH 7.0) containing 0.15 M NaCl. Cell pellets were stored at -20 °C until purification.

Cell Disruption and Purification. All subsequent steps were carried out at 4 °C. The cells were resuspended in 40-50 ml sonication buffer: 20 mM KH_2PO_4 (pH 7.4) containing 0.3 M NaCl, 5.0 mM $MgCl_2$, 2.0 mM ThDP, 1.0 mM benzamidine HCl, 25 mM imidazole,

and 1.0 mM PMSF (1.0 mM). Lysozyme was added to a final concentration of 0.60 mg/ml, and cells were incubated for 20 min on ice. Nuclease and DNase were added at 1,000 units each and cells were incubated for 20 min on ice. The cells were sonicated for 10 min (20 s pulsar "on" and 20 s pulsar "off") using the Sonic Dismembrator Model 550 (Fisher Scientific). The lysate was centrifuged at 30,000 g at 4 °C for 30 min.

His$_6$-tag wild type E1o or E1o variant were purified by using a Ni Sepharose 6 Fast Flow Column (GE Healthcare). The column was equilibrated with 150 ml of sonication buffer and 50 ml of cell lysate was applied on the column. The column was then washed with 10 column volume (CV) of binding buffer containing 20 mM KH_2PO_4 (pH 7.5), 0.3 M KCl, 5 mM $MgCl_2$, 2 mM ThDP and 25 mM imidazole followed by 10 CV of washing buffer containing 20 mM KH_2PO_4 (pH 7.5), 0.3 M KCl, 5 mM $MgCl_2$, 2 mM ThDP and 50 mM imidazole. The bound proteins were eluted using elution buffer containing 20 mM KH_2PO_4 (pH 7.5), 0.3 M KCl, 5 mM $MgCl_2$, 2 mM ThDP and 200 mM imidazole. Fractions with enzyme were combined, dialyzed against 20 mM KH_2PO_4 (pH 7.5), 0.30 M KCl, 2.0 mM $MgCl_2$, 0.5 mM ThDP and 1.0 mM benzamidine HCl. Next, the protein was precipitated by PEG-8000 (50% w/v) adding 0 – 16% PEG dropwise (~4 ml per 25 ml protein) on ice with stirring for 10-15 minutes. The protein was collected by centrifugation at 17,640 g for 20 minutes at 4 °C. The resulting protein pellet was dissolved in ~0.5 ml of 50 mM KH_2PO_4 (pH 7.5) containing 0.4 M ammonium chloride, 1.0 mM $MgCl_2$, 0.2 mM ThDP, and 1.0 mM benzamidine HCl. The purity was confirmed by SDS-PAGE. Wild type E1o and E1o variants were stored at -80 °C.

4.2.3 Construction of Plasmid, Expression, and Purification of human E1o reported elsewhere[84].

4.2.4 CD Spectroscopy for Product Accumulation.

CD spectra were recorded on a Chirascan CD Spectrometer (Applied Photophysics, Leatherhead, U.K.) in 2.4 ml volume with 1 cm path length cell at 30 °C in the near-UV (270 – 400 nm) wavelength region. E1oec (1.0 mg/ml) in 50 mM KH_2PO_4 (pH 7.5) containing 0.15 M NaCl, 0.1 mM ThDP, and 0.5 mM $MgCl_2$ was incubated with 5.0 mM 2-OA in the presence of the acceptor 15 mM glyoxylic acid and CD spectra was acquired at various times to detect product accumulation. E1oh (1.0 mg/ml, 4.4 μM) in 50 mM KH_2PO_4 (pH 7.5) containing 0.15 M NaCl, 0.2 mM ThDP, and 1.0 mM $MgCl_2$ was incubated with 2.0 mM 2-OG in the presence of the acceptor 1.0 mM glyoxylic acid and CD spectra was acquired at various times to detect product accumulation.

4.2.5 Steady State Kinetics of E1o-ec activity.

Time dependent product formation was monitored continuously at 278 nm in the kinetics mode by CD. A typical reaction mixture in a 2.4 ml cuvette contained 50 mM KH_2PO_4 (pH 7.5), 0.15 M NaCl, 0.2 mM ThDP, and 1.0 mM $MgCl_2$, and varying concentrations of glyoxylic acid and fixed concentration of 2-OG or varying concentrations of 2-OA and fixed concentration of glyoxylic acid. The reaction was started by the addition of 20 μg of E1o-ec and was monitored for 500 s at 30 °C. A similar reaction mixture was used with varying concentrations of 2-OG and fixed concentration of glyoxylic acid with E1o-h. The reaction was started with 10 μg E1o-h and was monitored for 500 s at 37 °C. Steady state

velocities calculated from the linear region of the progress curves were fit to a hyperbolic Michaelis-Menten plot (Equation 4.1).

4.2.6 E1o-ec specific activity assay with DCPIP.

The E1-specific activity of wild type E1oec and E1oec H298D were measured by monitoring the reduction of DCPIP at 600 nm using a Varian DMS 300 spectrophotometer. The assay medium (1 ml) contained in 50 mM KH_2PO_4 (pH 7.5), 0.5 mM $MgCl_2$, 0.2 mM ThDP, 0.1 mM DCPIP and 2.0 mM 2-OG or 20.0 mM 2-OV at 30 °C. The reaction was initiated by adding the enzyme (20 μg). One unit of activity is defined as the amount of DCPIP reduced (μmol/min/mg of E1o). For K_m measurement, similar conditions were used in the presence of substrates [2-OH (2.0 – 20 mM) or 2-oxo-5-hexenoic acid (2.0 – 20 mM)]. The observed slope was plotted against [substrate] and the resulting progress curves were fit to a hyperbolic Michaelis-Menten plot and K_m values were calculated by using Equation 4.1.

$$v = (V_m * x^n) / (x^n + K_m^n) \hspace{3cm} \textbf{Equation 4.1}$$

Where V_m is the maximum slope observed, x is the ligand concentration, n is the Hill coefficient ($K_m = S_{0.5}$ if $n \neq 1$) and K_m is the Michaelis constant for the varied substrate.

4.2.7 Carboligation reaction on an analytical scale.

20 mM butyraldehyde and 30 mM 2-oxoglutarate were incubated with 0.7 mg/ml E1o-ec in 1.2 mL of reaction buffer (50 mM KH_2PO_4 (pH 7.5) supplemented with 0.2 M NH_4Cl, 0.5 mM ThDP, 2.0 mM $MgCl_2$ and 5% DMSO). The reaction mixture was incubated for 20-24 hours at room temperature and 400 rpm using an orbital shaking platform on a

magnetic stirrer. After reaction was completed, circular dichroism (CD) spectroscopy was performed at 270-450 nm range for product detection. For NMR analysis, the complete reaction mixture was extracted as follows: (1) 25 μl of 50% formic acid to bring the pH down to ~3, (2) spin the sample down at 3,000 rpm for 5 minutes to pellet any protein precipitation and transfer to new tube, (3) add 3 x 300 μl $CDCl_3$ (plus 18 mg Na_2SO_4 if strong emulsion forms) and spin down sample at 3,000 rpm for 3 minutes. CD spectroscopy was again performed on the remaining water layer to estimate the amount of product extracted.

4.3 RESULTS AND DISCUSSION

The studies reported here are an extension of the previously reported studies done by the Jordan group adding to the repertory of E1o-ec in chiral synthesis. In addition to the use of 2-oxoacids as substrates, structurally similar carboxylic acids were also tested for the first time (Figure 4.1). First, kinetic studies were conducted to verify whether or not the substrates from Figure 4.1 are accepted by E1o. Upon verification that they were in fact accepted substrates, overnight carboligation reaction products were confirmed via CD spectroscopy and ^{1}H NMR (Figure 4.2). CD spectroscopy provides valuable information regarding stereochemistry of the resulting carboligation products. Specifically, the (*R*) enantiomer displays a negative CD peak while the (*S*) enantiomer a positive one all around 278-285 nm similar to the CD spectrum of acetoin enantiomers.
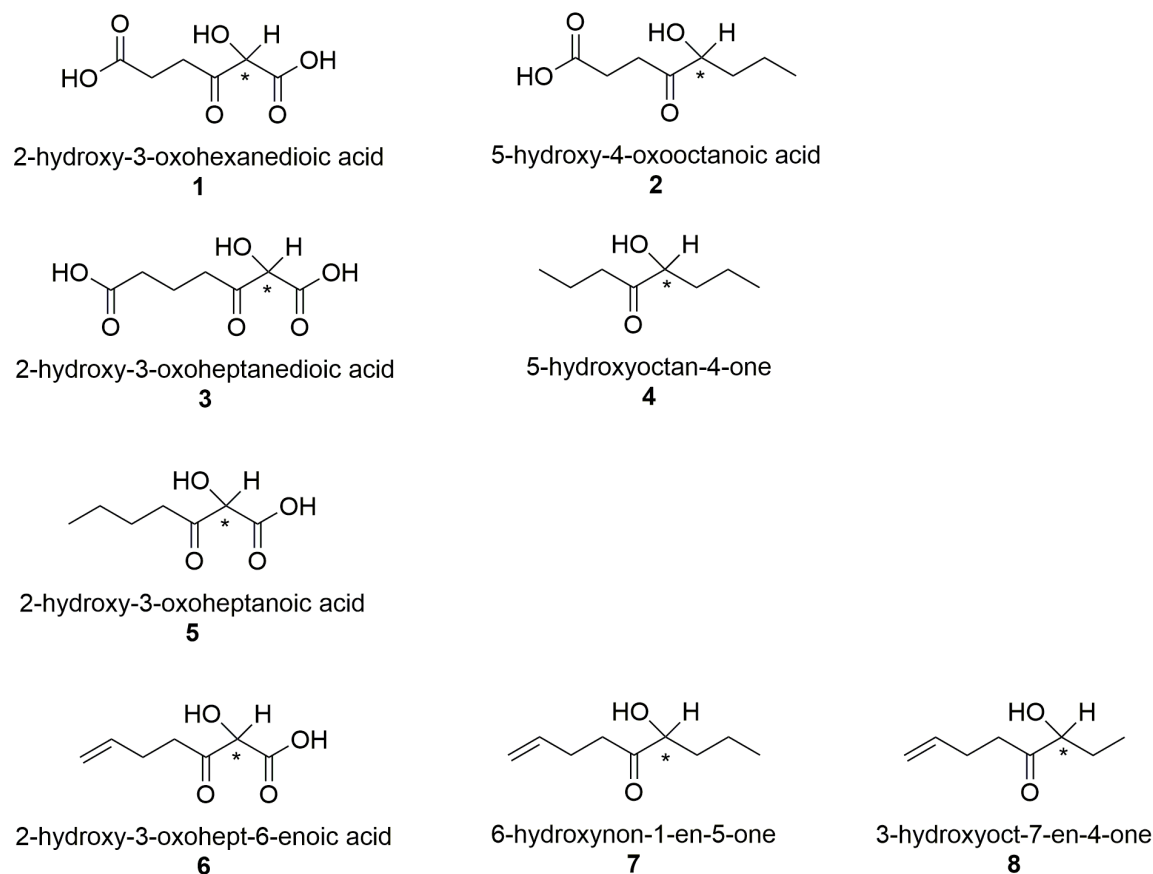
Figure 4.2. Structure and nomenclature of the chiral products produced from the E1o catalyzed reaction.

4.3.1 Steady-state kinetics of E1o-ec by CD spectroscopy or E1o specific activity assay with DCPIP.

First, kinetic studies were conducted to verify if the following substrates are accepted by E1o-ec in addition to gathering kinetic data for the acceptor, glyoxylate. Through the use of either CD spectroscopy, for product accumulation studies or kinetic mode studies, or the E1o specific activity assay with DCPIP, various kinetic parameters were obtained (Table 4.1).

Table 4.1. E1o specific activity and kinetic parameters for various substrates and acceptor.

Substrate or Acceptor	DCPIP Activity (μmol min^{-1}· mg^{-1})	Kinetic Parameters		
		k_{cat} (s^{-1})	K_m (mM)	k_{cat}/K_m (s^{-1}mM^{-1})
2-oxoglutarate[a]	0.620 ± 0.03	2.15 ± 0.10	2.61×10^{-3}	824
Glyoxylate	n/a[c]	0.521	5.71 ± 0.64	0.09
2-oxovalerate[a,b]	0.357 ± 0.018	1.24 ± 0.06	7.02 ± 0.02	0.18
2-oxoadipate	n/a[c]	0.030	12.3 ± 1.8	0.0024
2-ketohexanoic acid	0.020	0.110	4.32 ± 0.50	0.0225
2-oxo-5-hexenoic acid	0.0417	0.146	8.01	0.0183

[a] as determined by Shim et al.[83]

[b] DCPIP assay conducted with E1o-ec H298D

[c] n/a, not applicable. Kinetic parameters from CD Spectroscopy data.

Beginning with the E1o-ec natural substrate, 2-oxoglutarate, and glyoxylate as the acceptor, the K_m value was determined for glyoxylate using a fixed concentration of 2-oxoglutarate (Figure 4.3). The kinetic mode on the CD spectrometer was used to monitor product formation at 278 nm, with a negative slope indicating the accumulation of a (-) peak. As shown previously, the negative peak at 278 nm indicated the formation of the (*R*)-enantiomer[81].
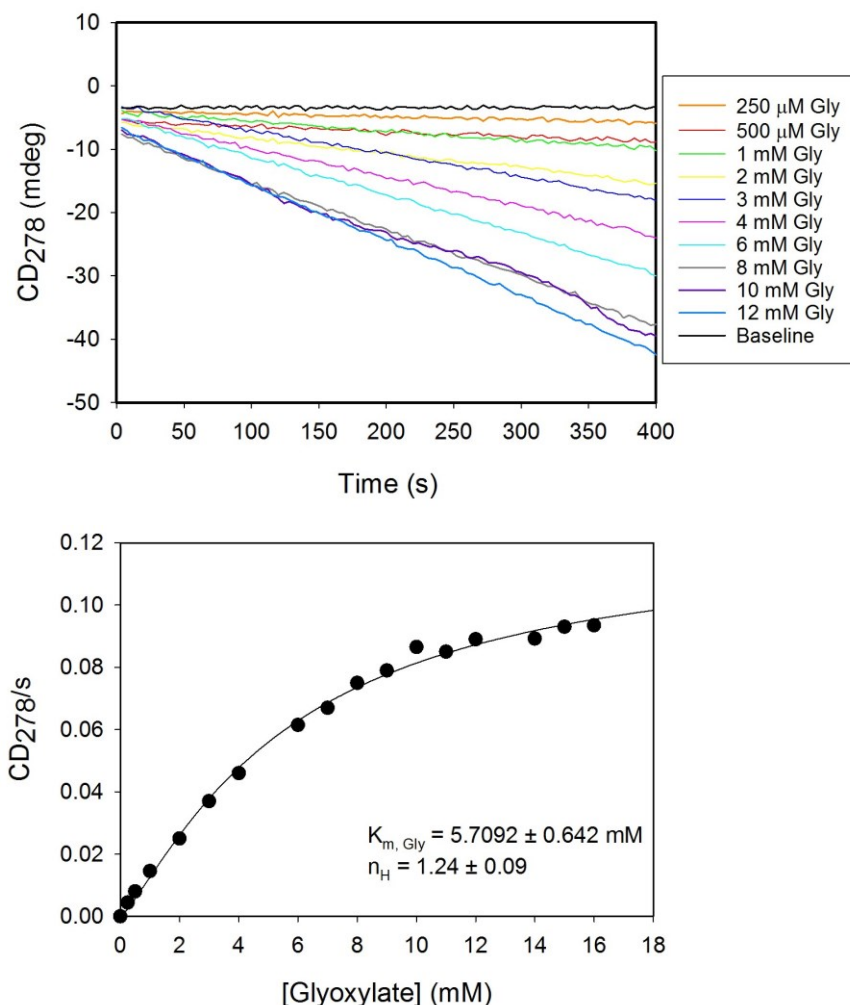
Figure 4.3. Steady-state kinetics for E1oec with 2-OG and glyoxylate using kinetic mode on CD spectrometer (top) and resulting Michaelis-Menten plot (bottom).

Similar experiments were conducted with the substrate 2-oxoadipate, which demonstrated for the first time that E1o-ec does in fact accept 2-oxoadipate as a substrate. First, a wavelength scan was conducted using CD spectroscopy were the carboligation product peak at (+) 278 nm accumulated over time (Figure 4.4, top). The positive peak does indicate that the resulting carboligation product is the (*S*)-enantiomer. Upon confirmation that E1oec does in fact accept 2-oxoadipate as a substrate, steady state kinetic data were collected using CD spectroscopy (Figure 4.4, middle and bottom).
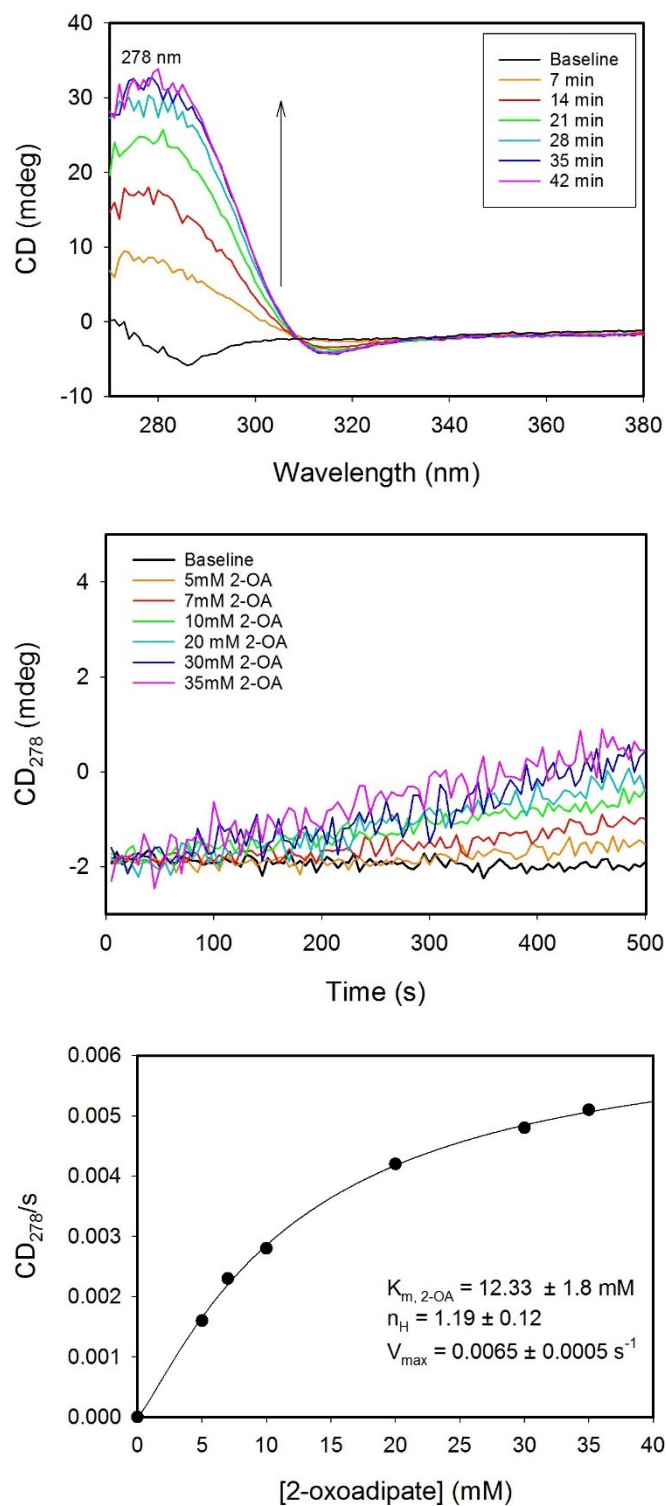
Figure 4.4. Product detection and kinetics for E1o-ec catalyzed reaction of 2-OA with

glyoxylate. (Top) Near-UV CD wavelength scan acquired at the indicated times to detect

accumulation of (*S*)-chiral carboligation product produced by E1o-ec (1.0 mg/ml) from 2-oxoadipate (5 mM) and glyoxylate (15 mM) at 30 °C in 50 mM KH_2PO_4 (pH 7.5) containing 0.15 M NaCl, 1.0 $MgCl_2$ and 0.1 mM ThDP. (Middle) Steady-state progress curves of the reaction with E1o-ec (80 µg) at the indicated concentrations of 2-oxoadipate (2-OA) in the presence of 30 mM glyoxylate in 50 mM KH_2PO_4 (pH 7.5) containing 0.15 M NaCl, 1.0 $MgCl_2$ and 0.1 mM ThDP. (Bottom) Dependence of the ellipticity at 278 nm on the concentration of 2-oxoadipate. The data were fit using the Hill equation.

In the case of the carboxylic acid substrates, the E1o specific activity assay with DCPIP was used where DCPIP acts as the acceptor similar to the carboligation reactions. The two substrates tested were 2-ketohexanoic acid (Figure 4.5), containing a saturated side chain, and 2-oxo-5-hexenoic acid (Figure 4.6), containing a terminal alkene functional group. Both carboxylic acids tested were shown to be accepted by E1o-ec as substrates demonstrating once again the versatility of E1o for carboligation reactions.
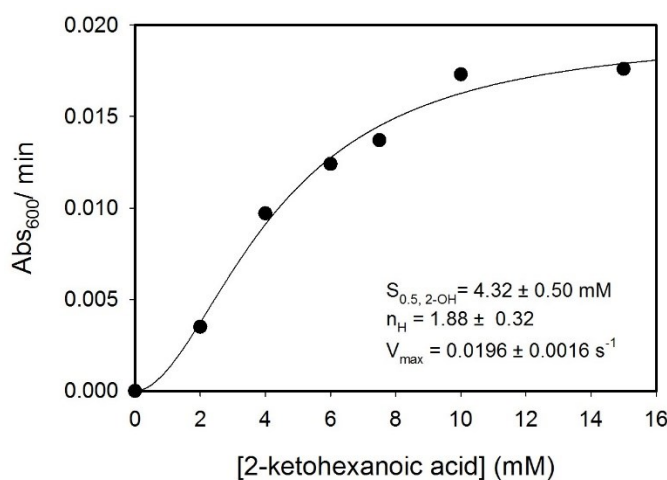
Figure 4.5. E1o-ec specific activity assay with 2-ketohexanoic acid.
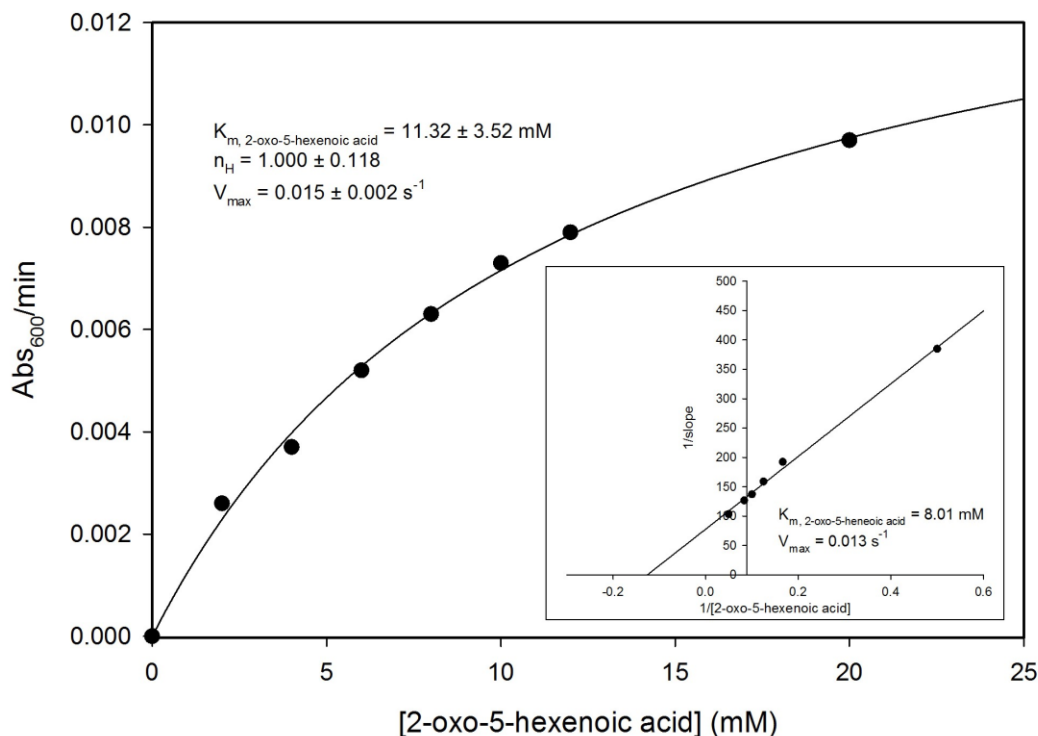
Figure 4.6. E1o-ec specific activity assay with 2-oxo-5-hexenoic acid.

4.3.2 Carboligation reaction on an analytical scale with E1o-ec or E1o-ec H298D.

Once the 2-oxo acid and carboxylic acid substrates were confirmed to be accepted as substrates by E1o, glyoxylate and the straight chain aldehydes were introduced as acceptors to test E1o-catalyzed chiral carboligation reactions. Similar to the analytical scale production and work up implemented by Müller et al.[82] with some modifications, the chiral carboligation product was confirmed by CD spectroscopy and NMR spectroscopy. First, the carboligation product peak was detected by CD spectroscopy followed by pH adjustment to ~3, conditions under which product extraction into chloroform could be performed. The ^{1}H NMR spectrum of the resulting extracted product was then recorded. As all the carboligation products have in common the CH-OH functional group, they all exhibit a ^{1}H NMR resonance with a proton chemical shift near 4-5 ppm (Figure 4.2).

First, the 2-oxo acids, 2-oxoglutarate and 2-oxovalerate, were tested with the straight chain acceptor, butyraldehyde (Figures 4.7 and 4.8). As determined previously[83], the E1o-ec variant, H298D, was shown to accept 2-oxovalerate as a substrate and therefore was used in these studies. In both cases, the (*R*)-enantiomer was produced as apparent by the negative CD peak at 279 nm with 2-oxoglutarate (Figure 4.7) and 2-oxovalerate (Figure 4.8).
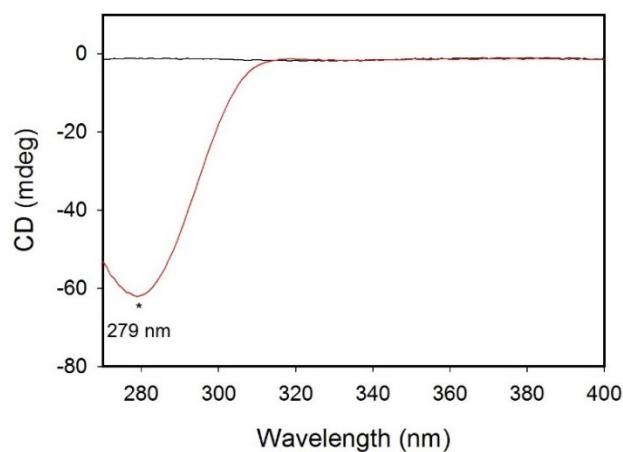
Figure 4.7. E1o-ec catalyzed carboligation reaction of 2-OG with butyraldehyde. A 1 mm path length cuvette was used, therefore actual ellipticity is 10x of that shown.
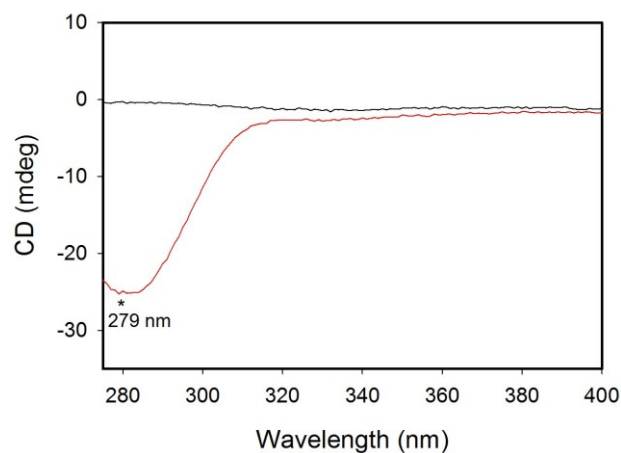
Figure 4.8. E1o-ec H298D catalyzed carboligation reaction of 2-OV with butyraldehyde. A 1 mm path length cuvette was used, therefore actual ellipticity is 10x of that shown.

In the case of 2-oxoglutarate and butyraldehyde, the ^{1}H NMR spectrum was obtained to verify the carboligation product (5-hydroxy-4-oxooctanoic acid) formed (Figure 4.9). The unique proton chemical shift for the CH-OH functional group at ~4.4 ppm (H$_c$) and ~2.7 ppm (OH) is seen on the NMR spectrum in addition to the other protons.
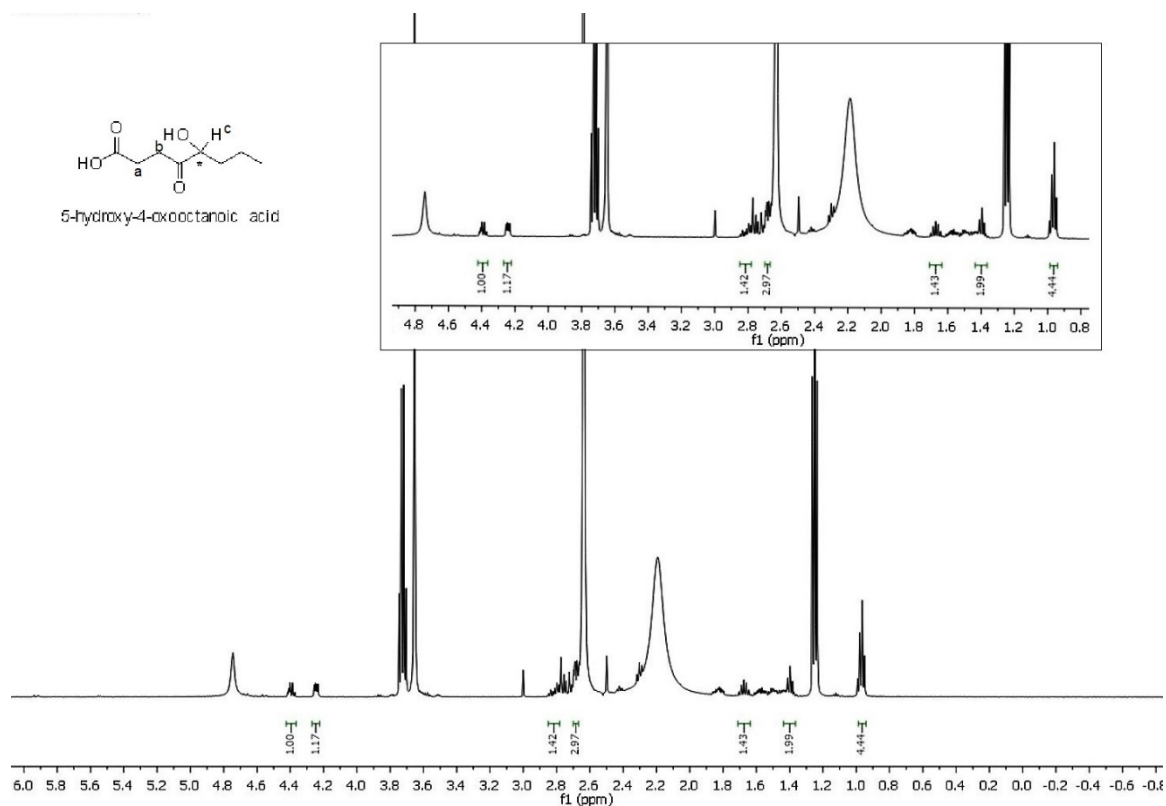
Figure 4.9 ^{1}H NMR spectrum of E1o-ec catalyzed carboligation product of 2-oxoglutarate with butyraldehyde. The large peaks correspond to water (in CDCl$_3$) near ~2.0 ppm and DMSO-d$_6$ near ~2.6 ppm.

Next, the carboxylic acids, 2-ketohexanoic acid and 2-oxo-5-hexenoic acid, were tested with various acceptors. The substrate 2-ketohexanoic acid was tested with glyoxylate, and in this case the (*S*)-enantiomer was formed verified by the (+) CD peak at ~290 nm (Figure 4.10).
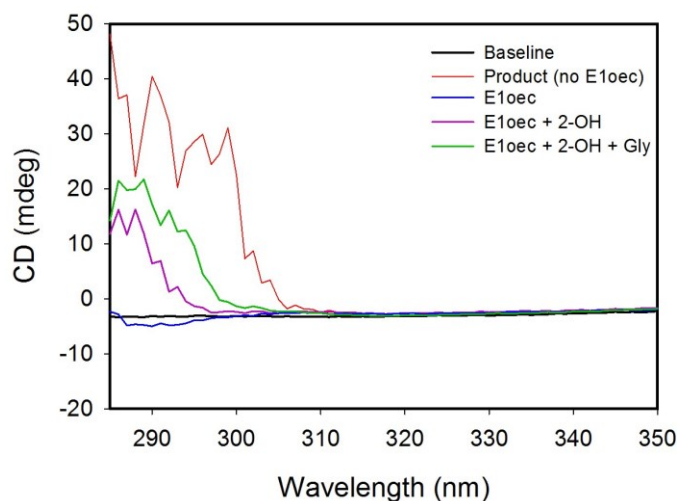
Figure 4.10. E1o-ec catalyzed carboligation reaction with 2-ketohexanoic acid & glyoxylate.

Of all the substrates tested, 2-oxo-5-hexenoic acid was of most interest due to the introduction of the terminal alkene functional group. The resulting carboligation product with glyoxylate, butyraldehyde, and propanal were confirmed by CD spectroscopy (Figure 4.11). Remarkably, the carboligation product with glyoxylate produced the (*S*)-enantiomer as shown by the positive peak at ~280 nm (Figure 4.11, top), while both butyraldehyde and propanal produced the (*R*)-enantiomer with a negative peak at 282 nm (Figure 4.11, middle and bottom).
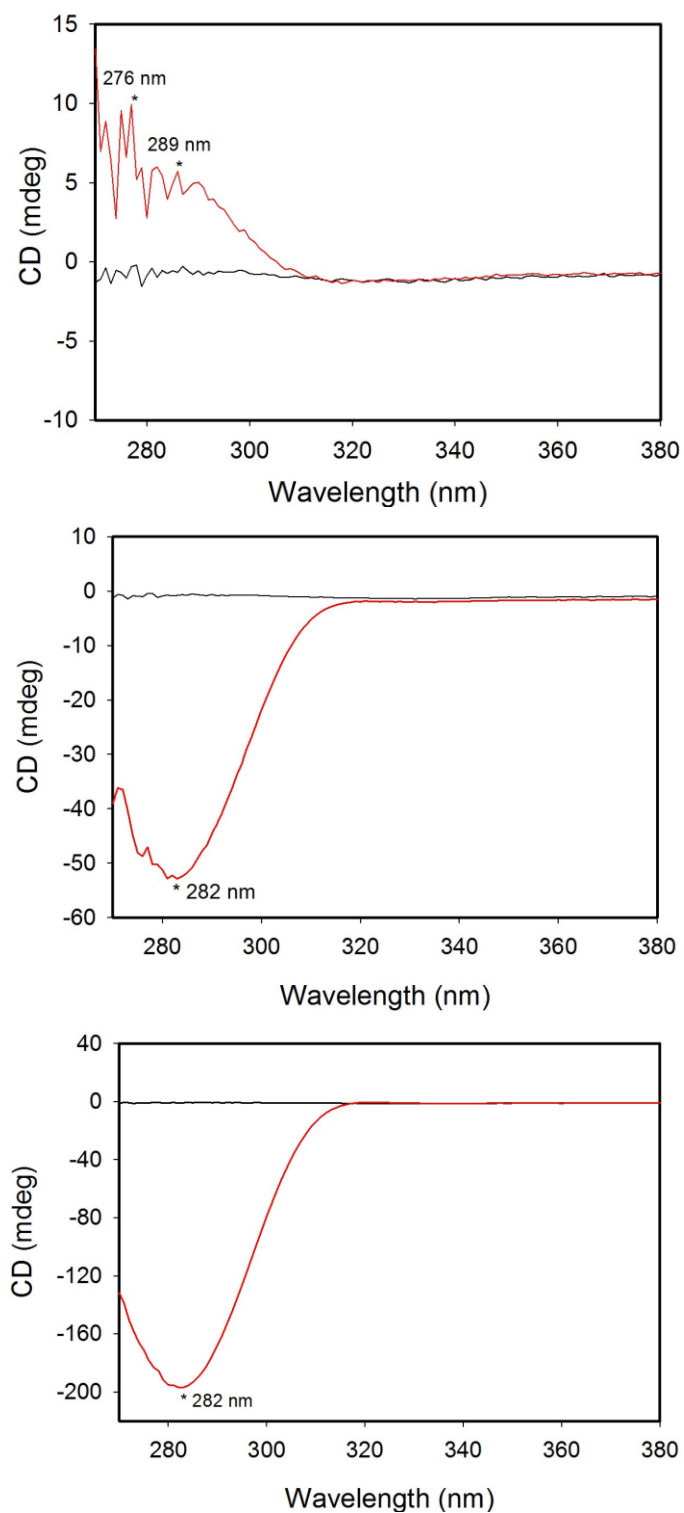
Figure 4.11. CD spectroscopy of E1o-ec catalyzed carboligation reaction with 2-oxo-5-hexenoic acid and various acceptors. (Top) with glyoxylate, (Middle) with butyraldehyde, and (Bottom) with propanal.

4.3.3 Carboligation reaction on an analytical scale with human E1o.

In addition to the above work with E1o-ec, similar initial studies were conducted using E1o-h. For the first time, E1o-h was used to catalyze carboligation reactions and therefore the natural substrate, 2-oxoglutarate, as well as the substrate 2-oxoadipate were tested with the acceptor glyoxylate. First, the carboligation product produced by 2-oxoglutarate and glyoxylate was verified by CD spectroscopy. Similar to the E1o-ec results, E1o-h produced the (R)-enantiomer as indicated by the (-) 279 nm peak (Figure 4.12).
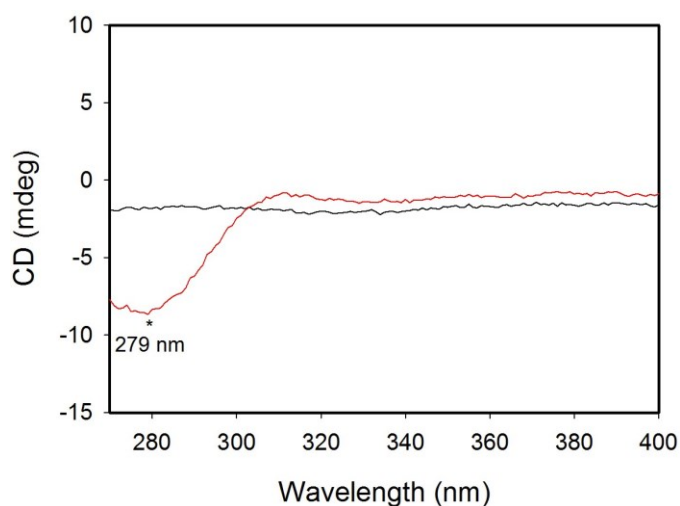
Figure 4.12. Human E1o catalyzed carboligation reaction of 2-OG with glyoxylate. A 1 mm path length cuvette was used, therefore actual ellipticity is 10x greater.

Next, the carboligation product, 2-hydroxy-3-oxohexanedioic acid, was confirmed by ^{1}H NMR spectroscopy (Figure 4.13). Not only is the CH-OH functional group clearly visible (~4.4 ppm for -CH and ~2.75 ppm for -OH), but the other proton peaks at ~2.7 and 2.5 ppm are also visible. For the first time, the carboligation reaction was successfully carried out by E1o-h.
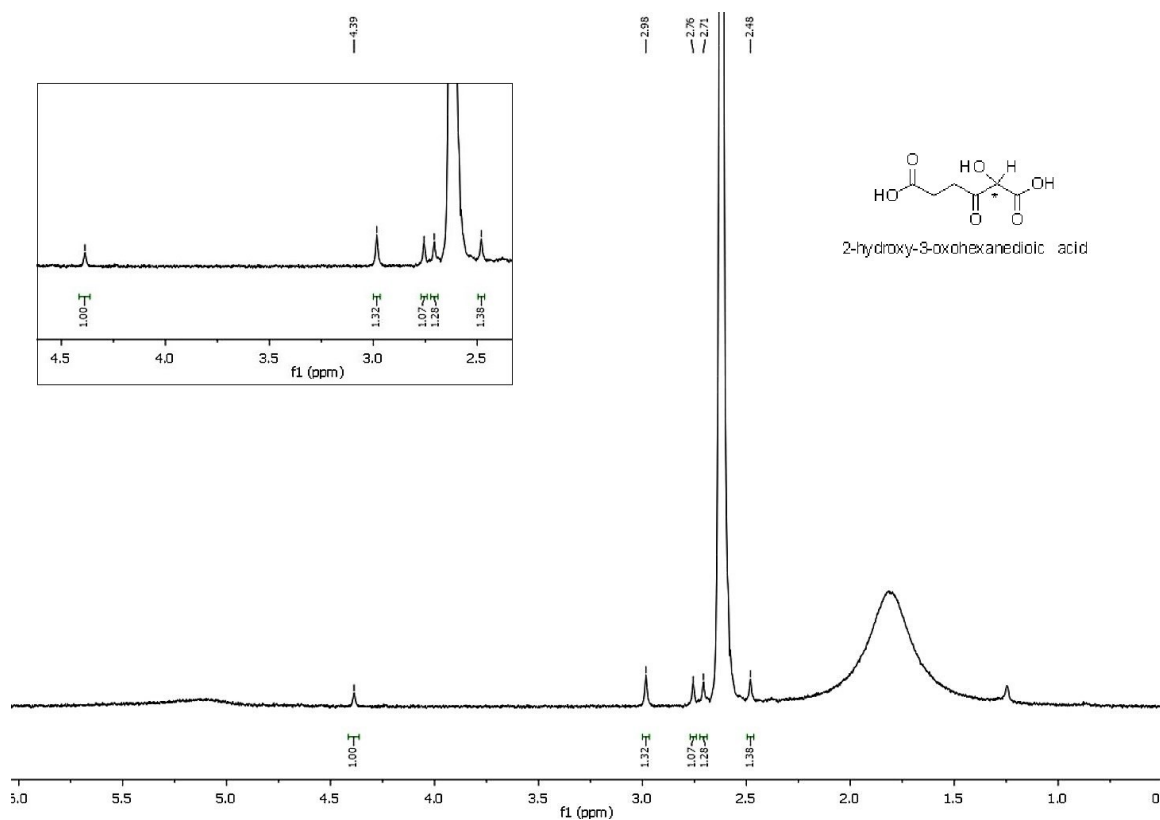
Figure 4.13 ^{1}H NMR spectrum of E1o-h catalyzed carboligation product of 2-oxoglutarate with glyoxylate. The large peaks correspond to water (in CDCl$_3$) near ~1.7 ppm and DMSO-d$_6$ near ~2.6 ppm.

Next, the substrate 2-oxoadipate was used with the acceptor glyoxylate, and in fact human E1o can catalyze the formation of the carboligation product (Figure 4.14). The most obvious difference is that the product formed is the (*S*)-enantiomer proving that a one-carbon difference changes the orientation of the resulting carboligation product. Again, the ^{1}H NMR spectrum was obtained for the carboligation product, 2-hydroxy-3-oxoheptanedioic acid, with visible peaks for the CH-OH functional group (~4.4 ppm for –CH and ~2.78 ppm for –OH) (Figure 4.15).
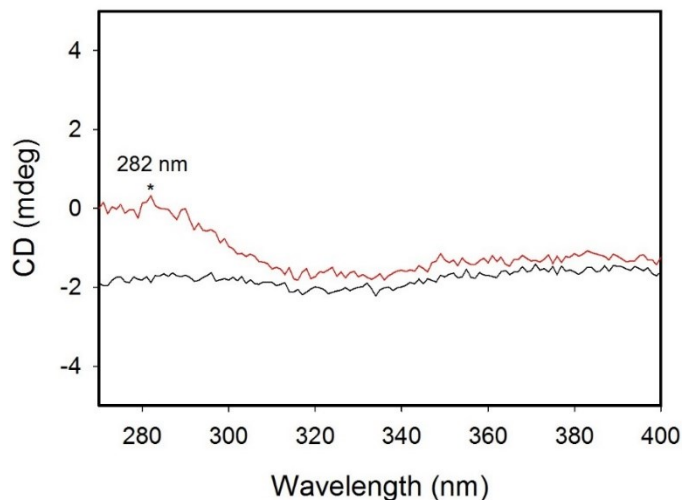
Figure 4.14. Human E1o catalyzed carboligation reaction with 2-oxoadipate and glyoxylate. A 1 mm path length cuvette was used - actual ellipticity is 10x of that shown.
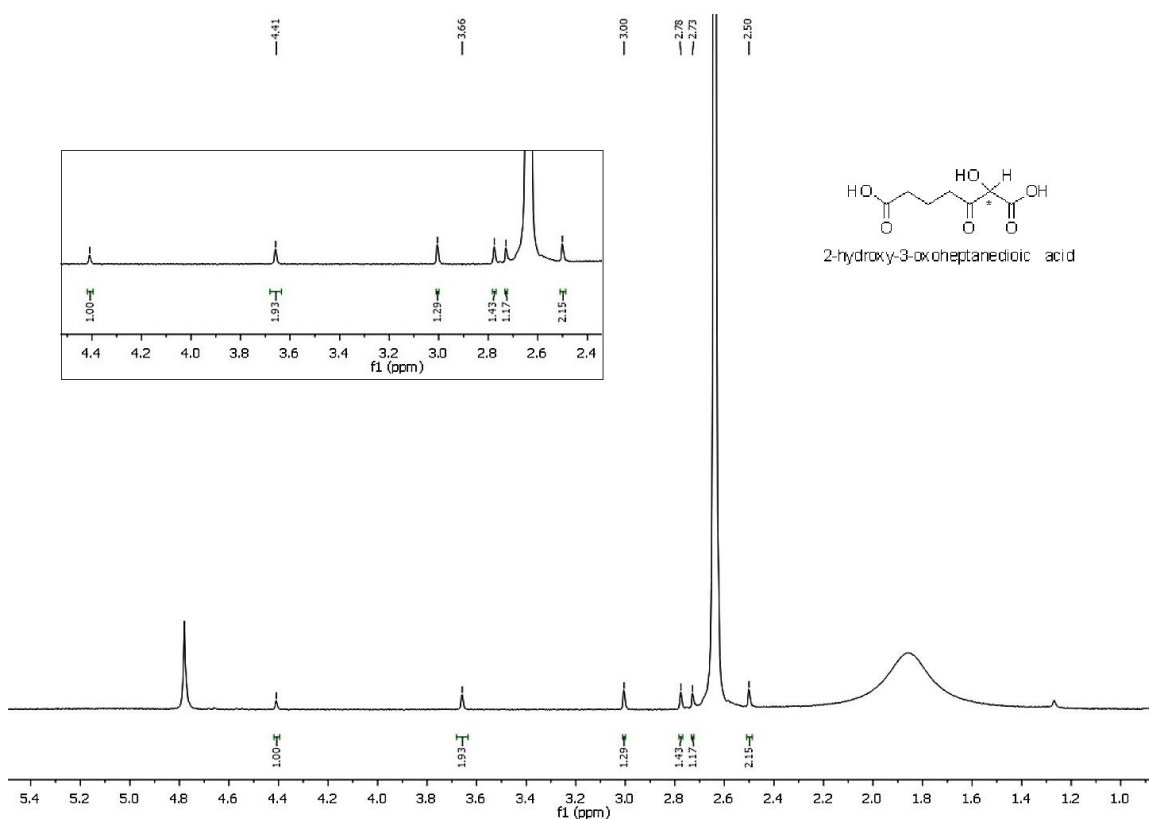
Figure 4.15 ^{1}H NMR spectrum of E1o-h catalyzed carboligation product of 2-oxoadipate with glyoxylate. The large peaks correspond to water (in CDCl$_3$) near ~1.8 ppm and DMSO-d$_6$ near ~2.6 ppm.

4.4 CONCLUSIONS

The E1o-ec and human E1o component of OGDHc were found to successfully catalyzes the formation of acetoin-like products for all the reactions tested as established by CD spectroscopy and ^{1}H NMR spectroscopy. In addition, E1o displays different enantioselectivities in product formation, depending on both substrate and acceptor being used (Table 4.2). For instance, E1o-ec and E1o-h both produce the (*R*)-enantiomer with 2-OG as the substrate and glyoxylate as the acceptor whereas the (*S*)-enantiomer is produced with 2-OA as the donor substrate and glyoxylate as the acceptor. It appears that a one carbon difference on the part of the substrate plays an important role in the E1o binding pocket therefore changing the enantioselectivity. These results suggest that E1o from both *E. coli* and human 2-OGDHc are capable of synthesizing stable chiral intermediates with various functional groups that can be exploited for further chemical synthesis. Overall, this work expands the scope of both carboxylic acid donors and straight chain aldehyde acceptors for their use in carboligation reactions by the E1o component.

Table 4.2 Enantioselectivity of all products produced by E1oec or E1oh.

Substrates	Acceptors	Product	enantioselectivity
2-oxoglutarate	Glyoxylate	1	(*R*)
	Butyraldehyde	2	(*R*)
2-oxoadipate	Glyoxylate	3	(*S*)
2-oxovalerate	Butyraldehyde	4	(*R*)
2-ketohexanoic acid	Glyoxylate	5	(*S*)
2-oxo-5-hexenoic acid	Glyoxylate	6	(*S*)
	Butyraldehyde	7	(*R*)
	Propanal	8	(*R*)

References

1. Reed, L. J. A trial of research from lipoic acid to α-keto acid dehydrogenase complexes. *J. Biol. Chem*. **276**, 38329-38336 (2001).

2. Perham, R. N. Domains, motifs, and linkers in 2-oxo acid dehydrogenase multienzyme complexes: A paradigm in the design of multifunctional protein. *Biochemistry*, **30,** 8501-8512 (1991).

3. Patel, M. S. & Roche, T. E. Molecular biology and biochemistry of pyruvate dehydrogenase complexes. *FASEB J.* **14**, 3224-3233 (1990).

4. Harris, R. A., Bowker-Kenley, M. M., Huang, B. & Wu, P. Regulation of the activity of the pyruvate dehydrogenase complex. *Adv. Enzyme Regul*. **42**, 249-259 (2002).

5. Roche, T. E., Baker, J. C., Yan, X., Hiromasa, Y., Gong, X., Peng, T., Dong, J., Turkan, A., & Kasten, S.A. Distinct regulatory properties of pyruvate dehydrogenase kinase and phosphatase isoforms. *Prog. Nucleic Acid Res. Mol. Biol*. **70**, 33-75 (2001).

6. Hiromasa, Y., Fujisawa, T., Aso, Y. & Roche, T. E. Organization of the cores of the mammalian pyruvate dehydrogenase complex formed by E2 and E2 plus the E3-binding protein and capacities to bind E1 and E3 components, *J. Biol. Chem*. **279**, 6921-6933 (2004).

7. Roche, T. E. & Hiromasa, Y. Pyruvate dehydrogenase kinase regulatory mechanisms and inhibition in treating diabetes, heart ischemia, and cancer, *Cell. Mol. Life Sci*. **64**, 830-849 (2007).

8. Gudi, R., Bowker-Kinley, M. M., Kedishvili, N. Y., Zhao, Y. & Popov, K. M. Diversity of the pyruvate dehydrogenase kinase gene family in humans, *J. Biol. Chem.* **270**, 28989-28994 (1995).

9. Hiromasa, Y., Yan, X. & Roche, T. Specific ion influence on self-association of pyruvate dehydrogenase kinase isoform 2 (PDHK2), binding of PDHK2 to the L2 lipoyl domain, and effects of the lipoyl group-binding site inhibitor, Nov3r. *Biochemistry* **47**, 2312-2324 (2008).

10. Roche, T. E., Hiromasa, Y., Turkan, A., Gong, X., Peng, T., Yan, X., Kasten, S. A., Bao, H. & Dong, J. Essential roles of lipoyl domains in the activated function and control of pyruvate dehydrogenase kinases and phosphatase isoform 1. *Eur. J. Biochem*. **270,** 1050-1056 (2003).

11. Huang, B., Gudi, R., Wu, P., Harris, R. A., Hamilton, J. & Popov, K. M. Isoenzymes of pyruvate dehydrogenase phosphatase: DNA-derived amino acid sequences, expression, and regulation. *J. Biol. Chem*. **273**, 17680-17688 (1998).

12. Brautigam, C. A., Wynn, R. M., Chuang, J. L. & Chuang, D. T. Subunit and catalytic component stoichiometries of an *in vitro* reconstituted human pyruvate dehydrogenase complex. *J. Biol. Chem*. **284**, 13086-13098 (2009).

13. Perham, R. N. (2000) Swinging arms and swinging domains in multifunctional enzymes: Catalytic machines for multistep reactions. Annu. Rev. Biochem. 69, 961−1004.

14. Hansford, R. G., and Zorov, D. (1998) Role of mitochondrial calcium transport in the control of substrate oxidation. Mol. Cell. Biochem. 184, 359−369.

15. Frank, R. A. W., Price, A. J., Northrop, F. D., Perham, R. N., and Luisi, B. F. (2007) Crystal Structure of the E1 Component of the Escherichia coli 2-Oxoglutarate Dehydrogenase Multienzyme Complex. J. Mol. Biol. 368, 639−651.

16. Ricaud, P. M., Howard, M. J., Roberts, E. L., Broadhurst, R. W., and Perham, R. N. (1996) Three-dimensional structure of the lipoyl domain from the dihydrolipoyl succinyltransferase component of the 2-oxoglutarate dehydrogenase multienzyme complex of Escherichia coli. J. Mol. Biol. 264, 179−190.

17. Knapp, J. E., Mitchell, D. T., Yazdi, M. A., Ernst, S. R., Reed, L. J., and Hackert, M. L. (1998) Crystal structure of the truncated cubic core component of the Escherichia coli 2-oxoglutarate dehydrogenase multienzyme complex. J. Mol. Biol. 280, 655−668.

18. Robien, M. A., Clore, G. M., Omichinski, J. G., Perham, R. N., Appella, E., Sakaguchi, K., and Gronenborn, A. M. (1992) Three dimensional solution structure of the E3-binding domain of the dihydrolipoamide succinyltransferase core from the 2-oxoglutarate dehydrogenase multienzyme complex of Escherichia coli. Biochemistry 31, 3463−3471.

19. Patel, M.S. & Korotchkina L.G. The biochemistry of the pyruvate dehydrogenase complex. *Biochem. Mol. Biol. Educ*. **31**, 5-15 (2003).

20. Patel, M. S. & Korotchkina, L. G. Regulation of pyruvate dehydrogenase complex. *Biochem*. *Soc. Trans*. **34**, 217-222 (2006).

21. Kato, M., Wynn, R. M., Chuang, J. L., Tso, S. C., Machius, M., Li, J., Chuang, D. T. Structural basis for inactivation of the human pyruvate dehydrogenase complex by phosphorylation: role of disordered phosphorylation loops. *Structure* **16**, 1849-1859 (2008).

22. Kolobova, E., Tuganova, A., Boulatnikov, I. & Popov, K. M. Regulation of pyruvate dehydrogenase activity through phosphorylation at multiple sites. Biochem. J. 358, 69 -77 (2001).

23. Korotchkina, L. G. & Patel, M. S. Probing the mechanism of inactivation of human pyruvate dehydrogenase by phosphorylation of three sites. J. Biol. Chem. 276, 5731-5738 (2001).

24. Korotchkina, L. G. & Patel, M. S. Site specificity of four pyruvate dehydrogenase kinase isoenzymes toward the three phosphorylation sites of human pyruvate dehydrogenase. J. Biol. Chem. 276, 37223-37229 (2001).

25. Reed, L. J., Damuni, Z. & Merryfield, M. L. Regulation of mammalian pyruvate alpha-keto acid dehydrogenase complexes by phosphorylation-dephosphorylation. *Cur. Top. Cell. Regul.* **27**, 41-49 (1985).

26. Wu, P., Inskeep, K., Bowker- Kinley, M. M., Popov, KI. M. & Harris, R. A. Mechanism responsible for inactivation of skeletal muscle pyruvate dehydrogenase complex in starvation and diabetes. Diabetes 48, 1593-1599 (1999).

27. Holness, M. J., Kraus, A., Harris, R. A. & Sugden, M. C. Targeting upregulation of pyruvate dehydrogenase kinase (PDK)-4 in slow-twitch skeletal muscle underlies the state of modification of the regulatory characteristics of PDK induced by high-fat feeding, Diabetes 49, 775-781 (2000).

28. Kwon, H. S., Huang, B., Unterman, T. G.& Harris, R. A. Protein kinase B-alpha inhibits human pyruvate dehydrogenase kinase-4 gene induction by dexamethasone through inactivation of FOXO transcription factors, Diabetes 53, 899-910 (2004).

29. Patel, M. S. & Harris, R. A. Mammalian α-keto acid dehydrogenase complexes gene regulation and genetic defects, FASEB J. 9, 1164-1172 (1995).

30. Imbard, A., Boutron, A., Vequaud, C., Zater, M., de Lonlay, P., Ogier de Baulny, H., Barnerias, C., Miné, M., Marsac, C., Saudubray, J.-M. & Brivet, M. Molecular

characterization of 82 patients with pyruvate dehydrogenase complex deficiency. Structural implications of novel amino acid substitutions in E1 protein. *Mol. Gen. Metab*. **104**, 507-516 (2011).

31. Patel, K. P., O'Brien, T. W., Subramony, S. H., Shuster, J., and Stacpoole, P. W. The spectrum of pyruvate dehydrogenase complex deficiency: clinical, biochemical and genetic features in 371 patients. *Mol. Genet. Metab*. **106**, 385-394 (2012).

32. Jeoung, N. H., Harris, C. R.& Harris, R. A. Regulation of pyruvate metabolism in metabolicrelated diseases. *Rev. Endocr. Metab. Disord*. **15**, 99-110 (2014).

33. Vander Heiden, M. G., Cantley, L. C.& Thompson, C. B. Understanding the Warburg effect: the metabolic requirements of cell proliferation. *Science **324***, 1029-1033 (2009).

34. Enns, L. & Ladiges, W. Mitochondrial redox signaling and cancer invasiveness. *J. Bioenerg. Biomembr.* **44**, 635-638 (2012).

35. Marin-Hernández, A., Gallardo-Pérez, J. C., Rodriguez-Enriquez, S.& Moreno Sánchez, R. HIF-1alpha modulates energy metabolism in cancer cells by inducing over-expression of specific glycolytic isoforms. *Mini Rev. Med. Chem*. **9**, 1084-1101 (2009).

36. Schulze, A. & Downward, J. Flicking the Warburg switch-tyrosine phosphorylation of pyruvate dehydrogenase kinase regulates mitochondrial activity in cancer cells. *Mol. Cell* **44**, 846-848 (2011).

37. Olenchock, B.& Vander Heiden, M. G. Pyruvate as a pivot point for oncogeneinduced senescence. *Cell* **153**, 1429-1430 (2013).

38. Kaplon, J., Zheng, L., Meissl, K., Chaneton, B., Selivanov, V. A., Mackay, G., van der Burg, S. H., Verdegaal, E. M. E., Cascante, M., Shlomi, T., Gottlieb, E.& Peeper, D. S. A key role for mitochondrial gatekeeper pyruvate dehydrogenase in oncogene-induced senescence. *Nature* **498**, 109-112 (2013)

39. Fujiwara, S., Kawano, Y., Yuki, H., Okuno, Y., Nosaka, K., Mitsuya, H.& Hata, H. PDK1 inhibition is a novel therapeutic target in multiple myeloma. *Br. J. Cancer* **108**, 170-178 (2013).

40. Hur, H., Xuan, Y., Kim, Y. B., Lee, G., Shim, W., Yun, J., Ham, I. H.& Han, S.U. Expression of pyruvate dehydrogenase kinase-1 in gastric cancer as a potential therapeutic Target. *Int. J. Oncol*. **42**, 44-54 (2013).

41. Sutendra, G. & Michelakis, E. D. (2013) Pyruvate dehydrogenase kinase as a novel therapeutic target in oncology. *Front. Oncol*. **3**, 38 (2013).

42. Papandreou, I., Cairns, R. A., Fontana, L., Lim, A. L.& Denko, N. C. HIF-1 mediates adaptation to hypoxia by actively downregulating mitochondrial oxygen consumption. *Cell Metab*. **3**, 187-197 (2006).

43. Kim, J. W., Tchernyshyov, I., Semenza, G. L. & Dang, C. V. HIF-1-mediated expression of pyruvate dehydrogenase kinase: a metabolic switch required for cellular adaptation to hypoxia. *Cell Metab*. **3**, 177-185 (2006).

44. Michelakis, E. D., Sutendra, G., Dromparis, P., Webster, L., Haromy, A., Niven, E., Maguire, C., Gammer, T. L., Mackey, J. R., Fulton, D., Abdulkarim, B., McMurtry, M. S. & Petruk, K. C. Metabolic modulation of glioblastoma with dichloroacetate. *Sci. Transl. Med*. **2**, 31-34 (2010).

45. Lu, C. W., Lin, S. C., Chen, K. F., Lai, Y. Y. & Tsai, S. J. Induction of pyruvate dehydrogenase kinase-3 by hypoxia–inducible factor-1 promotes metabolic switch and drug resistance. *J. Biol. Chem*. **283**, 28106-28114 (2008).

46. Hitosugi, T., Fan, J., Chung, T.-W., Lythgoe, K., Wang, X., Xie, J., Ge, Q., Gu, T.-L., Polakiewicz, R. D., Roesel, J. L., Chen, G. Z., Boggon, T. J., Lonial, S., Fu, H., Khuri, F. R., Kang, S. & Chen, J. Tyrosine phosphorylation of mitochondrial pyruvate dehydrogenase kinase 1 is important for cancer metabolism. *Molecular Cell* **44**, 864-877 (2011).

47. Morrell, J. A., Orme, J., Butlin, R. J., Roche, T. E., Mayers R. M.& Kilgour, E. AZD7545 is a selective inhibitor of pyruvate dehydrogenase kinase 2. *Biochem. Soc. Trans*. **31**, 1168- 1170 (2003).

48. Tuganova, A., Klyuyeva, A. & Popov, K. M. Recognition of the inner lipoyl-bearing domain of dihydrolipoyl transacetylase and of the blood glucose-lowering compound AZD7545 by pyruvate dehydrogenase kinase 2. *Biochemistry* **46**, 8592-8602 (2007).

49. Mayers, R. M., Butlin, R. J., Kligour, E., Leighton, B., Martin, D., Myatt, J., Orme, J. P.& Holloway, B. P. AZD7545, a novel inhibitor of pyruvate dehydrogenase kinase 2 (PDK2), activates pyruvate dehydrogenase *in vivo* and improves blood glucose control in obese (fa/fa) Zucker rats. *Biochem. Soc. Trans*. **31**, 1165-1167 (2003).

50. Aicher, T. D., Anderson, R. C., Gao, J., Shetty, S., Coppola, G. M., Stanton, J.L., Knorr, D.C., Sperbeck, D. M., Brand, L. J., Vinluan, C. C., Kaplan, E. L., Dragland, C., Tomaselli, H.C., Islam, A., Lozito, R. J., Liu, X., Maniara, W.M., Fillers, W. S., DelGrande, D., Walter, R. E. & Mann, W. R. Secondary amides of (R)-3,3,3-trifluoro-

2-hydroxy-2-methylpropionic acid as inhibitors of pyruvate dehydrogenase kinase. *J. Med. Chem*. **43**,236-249 (2000).

51. Baker, J. C., Yan, X., Peng, T., Kasten, S. & Roche, T. Marked differences between two isoforms of human pyruvate dehydrogenase kinase. *J. Biol. Chem*. **275**, 15773-15781 (2000).

52. Tuganova, A. & Popov, K. M. Role of protein-protein interactions in the regulation of pyruvate dehydrogenase kinase activity. *Biochem. J*., **387**, 147-153 (2005).

53. Tuganova, A., Boulatnikov, I. & Popov, K. M. Interaction between the individual isoenzymes of pyruvate dehydrogenase kinase and the inner lipoyl-bearing domain of transacetylase component of pyruvate dehydrogenase complex. *Biochem. J*., **366,** 129-136 (2002).

54. Kato, M., Chuang, J. L., Tso, S.-C., Wynn, R. M. & Chuang, D.T. Crystal structure of pyruvate dehydrogenase kinase 3 bound to lipoyl domain 2 of human pyruvate dehydrogenase complex. *EMBO J.,* **24**, 1763-1774 (2005).

55. Wang, J., Kumaran, S., Zhou, J., Nemeria, N. S., Tao, H., Kakalis, L., Park, Y.-H., Birkaya, B., Patel, M. & Jordan, F. Elucidation of the interaction loci of the human pyruvate dehydrogenase complex E2·E3BP core with pyruvate dehydrogenase kinase 1 and kinase 2 by H/D exchange mass spectrometry and nuclear magnetic resonance. *Biochemistry*, **54**, 69-82 (2015).

56. Korotchkina, L.G., Sidhu, M. S. & Patel, M.S. Characterization of testis-specific isoenzymes of human pyruvate dehydrogenase. *J. Biol. Chem*. **281**, 9688-9696 (2006).

57. Seifert, F., *et al.*, K. Direct kinetic evidence for half-of-the-sites reactivity in E1 component of the human pyruvate dehydrogenase complex through alternating sites cofactor activation. *Biochemistry*, **45**, 12775-12785 (2006).

58. Korotchkina, L.G., & Patel, M.S. Mutagenesis studies of the phosphorylation sites of recombinant pyruvate dehydrogenase. Site-specific regulation. *J. Biol. Chem*. **270**, 14297-14304 (1995).

59. Patel, M.S., Korotchkina, L.G. & Sidhu, S. Interaction of E1 and E3 components with the core proteins of the human pyruvate dehydrogenase complex. *J. Mol. Catal. B. Enzym.* **61**, 2-6 (2009).

60. Liu, T.C., Hong, Y.S., Korotchkina, L.G., Vettakkorumakankav, N. N. & Patel, M.S. Site-directed mutagenesis of human dihydrolipoamide dehydrogenase: role of lysine-54 and glutamate-192 in stabilizing the thiolate-FAD intermediate. *Protein Express Purif*. **16**, 27-39 (1999).

61. Bowker-Kinley, M. M., Davis, W. I., Wu, P., Harris, R. A. & Popov, K. M. Evidence for existence of tissue-specific regulation of the mammalian pyruvate dehydrogenase complex. *Biochem. J.,* **329**, 191-196 (1998).

62. Wynn, R. M., Kato, M., Chuang, J. L., Tso, S.-C., Li, J. & Chuang, D. T. Pyruvate dehydrogenase kinase-4 structures reveal a metastable open conformation fostering robust core-free basal activity. *J. Biol. Chem*. **283**, 25305-25315 (2008).

63. Ravindran, S., Radke, G. A., Guest, J. R. & Roche, T. E. Lipoyl domain-based mechanism for the integrated feedback control of the pyruvate dehydrogenase complex by enhancement of pyruvate dehydrogenase kinase activity. *J. Biol. Chem*. **271**, 653-662 (1996).

64. Yang, D., Gong, X., Yakhnin, A. & Roche, T. E. (1998) Requirements for the adaptor protein role of dihydrolipoyl acetyltransferase in the up-regulated function of the pyruvate dehydrogenase kinase and pyruvate dehydrogenase phosphatase. *J. Biol. Chem.* **273**, 14130-14137 (1998).

65. Patel, M. S. & Korotchkina, L. G. Regulation of mammalian pyruvate dehydrogenase complex by phosphorylation: complexity of multiple phosphorylation sites and kinases. *Exp. Mol. Med.* **33**, 191-197 (2001).

66. Green, T., Grigorian, A., Klyuyeva, A., Tuganova, A. & Popov, K. M. Structural and functional insights into the molecular mechanism responsible for the regulation of pyruvate dehydrogenase kinase 2. *J. Biol. Chem.* **283**, 15789-15798 (2008).

67. Harris, R. A., Popov, K. M., Zhao, Y., Kedishvili, N.Y., Shimomura, Y.& Crabb D.W. A new family of protein kinases - the mitochondrial protein kinases. *Advan. Enzyme Regul.*, **35**, 147-162 (1995).

68. Kukimoto-Niino, M. et al. Inhibitor-bound structures of human pyruvate dehydrogenase kinase 4. *Acta Cryst.* **D67**, 763-773 (2011).

69. Guevara, E. L., Yang, L., Birkaya, B., Zhou, J., Nemeria, N. S., Patel, M.S., and Jordan, F. Global view of cognate kinase activation by the human pyruvate dehydrogenase complex. *Nature Scientific Reports* (in press).

70. Devedjiev, Y., Steussy, C. N., and Vassylyev, D. G. Crystal structure of an asymmetric complex of pyruvate dehydrogenase kinase 3 with lipoyl domain 2 and its biological implications. *J. Mol. Biol.*, **370**, 407-416 (2007).

71. Kato, M., Li, J., Chuang, J. L., and Chuang, D. T. Distinct structural mechanism for inhibition of pyruvate dehydrogenase kinase isoforms by AZD7545, dichloroacetate, and radicicol. *Structure*, **15**, 992-1004 (2007).

72. Ciszak, E. M., Makal, A., Hong, Y. S., Vettaikkorumakankauv, A. K., Korotchkina, L. G., and Patel, M. S. How dihydrolipoamide dehydrogenase-binding protein bind dihydrolipoamide dehydrogenase in the human pyruvate dehydrogenase complex. *J. Biol. Chem.* **281**. 648-655 (2006).

73. Müller, M., Gocke, D., and Pohl, M. Thiamin diphosphate in biological chemistry: exploitation of diverse thiamin diphosphate-dependent enzymes for asymmetric chemoenzymatic synthesis. *FEBS J.* **276**, 2894-2904 (2009).

74. Lindqvist, Y., Schneider, G., Ermler, U., and Sundström, M. Three-dimensional structure of transketolase, a thiamine diphosphate dependent enzyme, at 2.5 A resolution. *EMBO J.* **11**, 2373-2379 (1992).

75. Kaplun, A. et al. Glyoxylate carboligase lacks the canonical active site glutamate of thiamine-dependent enzymes. *Nat. Chem. Biol.* **4**, 113-118 (2008).

76. Brammer, L.A., and Meyers, C.F. Revealing substrate promiscuity of 1-deoxy-D-xylulose 5-phosphate synthase. *Org. Lett.* **11**, 4748-4751 (2009).

77. Mosbacher, T.G., Müller, M., and Schulz, G.E. Structure and mechanism of the ThDP-dependent benzaldehyde lyase from *Pseudomonas fluorescens*. *FEBS J.* **272**, 6067-6076 (2005).

78. Baykal, A., Chakraborty, S., Dodoo, A., and Jordan, F. Synthesis with good enantiomeric excess of both enantiomers of alpha-ketols and acetolactates by two thiamin diphosphate-dependent decarboxylases. *Bioorg. Chem.* **34**, 380-393 (2006).

79. Sergienko, E. A., and Jordan, F. Catalytic acid-base groups in yeast pyruvate decarboxylase. 3. A steady-state kinetic model consistent with the behavior of both wild-type and variant enzymes at all relevant pH values. *Biochemistry* **40**, 7382-7403 (2001).

80. Nemeria, N., Tittmann, K., Joseph, E., Zhou, L., Vazquez-Coll, M. B., Arjunan, P., Hubner, G., Furey, W., and Jordan, F. Glutamate 636 of the Escherichia coli pyruvate dehydrogenase-E1 participates in active center communication and behaves as an engineered acetolactate synthase with unusual stereoselectivity. *J. Biol. Chem.* **280**, 21473-21482 (2005).

81. Patel, H., Shim, D. J., Farinas, E.T., and Jordan, F. Investigation of the donor and acceptor range for chiral carboligation catalyzed by the E1 component of the 2-oxoglutarate dehydrogenase complex. *J. Mol. Catal. B: Enzym.* **98**, 42-45 (2013).

82. Beigi, M., Waltzer, S., Fries, A., Eggeling, L., Sprenger, G. A., and Müller, M. TCA Cycle involved enzymes SucA and Kgd, as well as MenD: Efficient biocatalysts for asymmetric C-C bond formation. *Org. Lett.* **15**, 452-455 (2013).

83. Shim, D. J., Nemeria, N. S., Balakrishnan, A., Patel, H., Song, J., Wang, J., Jordan, F., Farinas, E. T. Assignment of function to histidines 260 and 298 by engineering the E1 component of the Escherichia coli 2-oxoglutarate dehydrogenase complex; substitutions that lead to acceptance of substrates lacking the 5-carboxyl group. *Biochemistry* **50**, 7705-7709 (2011).

84. Nemeria, N. S., Ambrus, A., Patel, H., Gerfen, G., Adam-Vizi, V., Tretter, L., Zhou, J., Wang, J., and Jordan, F. Human 2-oxoglutarate dehydrogenase complex E1

component forms a thiamin-derived radical by aerobic oxidation of the enamine intermediate. *J. Biol. Chem.* **289**, 29859-29873 (2014).

Appendix References:

1. Diggle, S. P. et al. The Pseudomonas aeruginosa 4-Quinolone Signal Molecules HHQ and PQS Play Multifunctional Roles in Quorum Sensing and Iron Entrapment. *Chem. Biol.* **13**, 701–710 (2003).

2. Déziel, E. et al. Analysis of Pseudomonas aeruginosa 4-hydroxy-2-alkylquinolines (HAQs) reveals a role for 4-hydroxy-2-heptylquinoline in cell-to-cell communication. *Proc. Natl. Acad. Sci. U.S.A.* **101**, 1339–1344 (2004).

3. Vial, L. et al. *Burkholderia pseudomallei*, *B. thailandensis*, and *B. ambifaria* produce 4-hydroxy-2-alkylquinoline analogues with a methyl group at the 3 position that is required for quorum-sensing regulation. *J. Bacteriol.* **190**, 5339–5352 (2008).

4. Tam, V. H. et al. Impact of multidrug-resistant Pseudomonas aeruginosa bacteremia on patient outcomes. *Antimicrob. Agents Chemother.* **54**, 3717–3722 (2010).

5. Dubern, J.-F. and Diggle, S. P. Quorum sensing by 2-alkyl-4-quinolones in Pseudomonas aeruginosa and other bacterial species. *Mol Biosyst* **4**, 882–888 (2008).

6. Jimenez, P. N. et al. The multiple signaling systems regulating virulence in Pseudomonas aeruginosa. *J. Microbiol. Mol. Biol. Rev.* **76**, 46–65 (2012).

7. Schertzer, J. W., Brown, S. A., and Whiteley, M. Oxygen levels rapidly modulate *Pseudomonas aeruginosa* social behaviours via substrate limitation of PqsH. *Mol. Microbiol.* **77**, 1527–1538 (2010).

8. Agarwal, A., Kahyaoglu, C., and Hansen, D. B. Characterization of HmqF, a Protein Involved in the Biosynthesis of Unsaturated Quinolones Produced by *Burkholderia thailandensis*. *Biochemistry* **51**, 1648-1657 (2012).

9. Somanathan, R. and Smith, K. M. Synthesis of some 2-alkyl-4-quinolone and 2-alkyl-4-methoxyquinoline alkaloids. *J. Heterocyclic Chem.* **18**, 1077-1079 (1981).

10. Pesci, E.C. et al. Quinolone signaling in the cell-to-cell communication system of *Pseudomonas aeruginosa*. *Proc. Natl. Acad. Sci. USA* **96**, 11229–11234 (1999).

11. Diggle, S.P. et al. The *Pseudomonas aeruginosa* quinolone signal molecule overcomes the cell density-dependency of the quorum sensing hierarchy, regulates rhl-dependent genes at the onset of stationary phase and can be produced in the absence of LasR. *Mol. Microbiol.* **50**, 29-43 (2003).

12. Dietrich, L. E. P., Price-Whelan, A., Petersen, A., Whiteley, M., and Newman, D. K. The phenazine pyocyanin is a terminal signaling factor in the quorum sensing network of Pseudomonas aeruginosa. *Mol. Microbiol* **61**, 1308–1321 (2006).

13. Hoffman, L. R. et al. Selection for Staphylococcus aureus small-colony variants due to growth in the presence of Pseudomonas aeruginosa. *Proc. Natl. Acad. Sci. USA* **103**, 19890–19895 (2006).

14. Meneely, K. M., Barr, E. W., Bollinger, J. M., and Lamb, A. L. Kinetic mechanism of ornithine hydroxylase (PvdA) from *Pseudomonas aeruginosa*: substrate

triggering of O2 addition but not flavin reduction. *Biochemistry* **48**, 4371–4376 (2009).

15. Hodgkinson, J., Bowden, S. D., Galloway, W. R. J. D., Spring, D. R., and Welch, M. Structure-activity analysis of the *Pseudomonas* quinolone signal molecule. *J. Bacteriol.* **192**, 3833–3837 (2010).

16. Jeoung, N. H. Pyruvate dehydrogenase kinases: therapeutic targets for diabetes and cancer. *Diabetes Metab. J.* **39**, 188-197 (2015).

Appendix A.

Quinolone Quorum Sensing – Functional Characterization of the Flavin

Monooxygenase, PqsH, from *Pseudomonas aeruginosa*

A.1 INTRODUCTION

In nature, many bacteria utilize a cell-to-cell communication system known as quorum sensing (QS) to monitor their surrounding population. In the case of the *Pseudomonas* and *Burkholderia* species, quinolone quorum sensing (QQS) is one of the signaling pathways used to determine cell population density as well as regulate expression of QS-dependent genes.[1] The growing number of infections from opportunistic pathogens such as *Pseudomonas aeruginosa* and *Burkholderia cepacia* in elderly and immunocompromised patients, for instance those with HIV or cystic fibrosis, pose a serious health concern.[2,3] Two other *Burkholderia* species, *B. mallei* and *B. pseudomallei*, have also been well characterized as primary animal and human pathogens. Moreover, these bacteria are resistant to many classes of antibiotics further complicating the matter underscoring the need for novel therapeutic approaches.[4]

To date there have been many studies on the isolation and function of a multitude of quinolone molecules specific to both *P. aeruginosa* and *B. thailandensis*.[2,3] Within *P. aeruginosa*, the QQS system consists of 4-hydroxy-2-alkylquinolines (HAQs) in which two quinolones, 4-hydroxy-2-heptylquinoline (HHQ) and 3,4-dihydroxy-2-heptylquinoline (Pseudomonas quinolone signal [PQS]), have been shown to bind a specific transcription factor PqsR, also referred to as MvfR, that upregulates the production of virulence factors and HAQ synthesis by an auto induction mechanism (Figure A.1,

left).[5,6] The final step in the biosynthesis of PQS is the 3'-hydroxylation of the quinolone ring of HHQ catalyzed by the enzyme PqsH, a member of a family of flavin-dependent monooxygenases.[7] Since PQS plays an important part in the *P. aeruginosa* QQS biosynthetic pathway, understanding the role of hydroxylation of QQS molecules by PqsH may aid in finding novel functions.
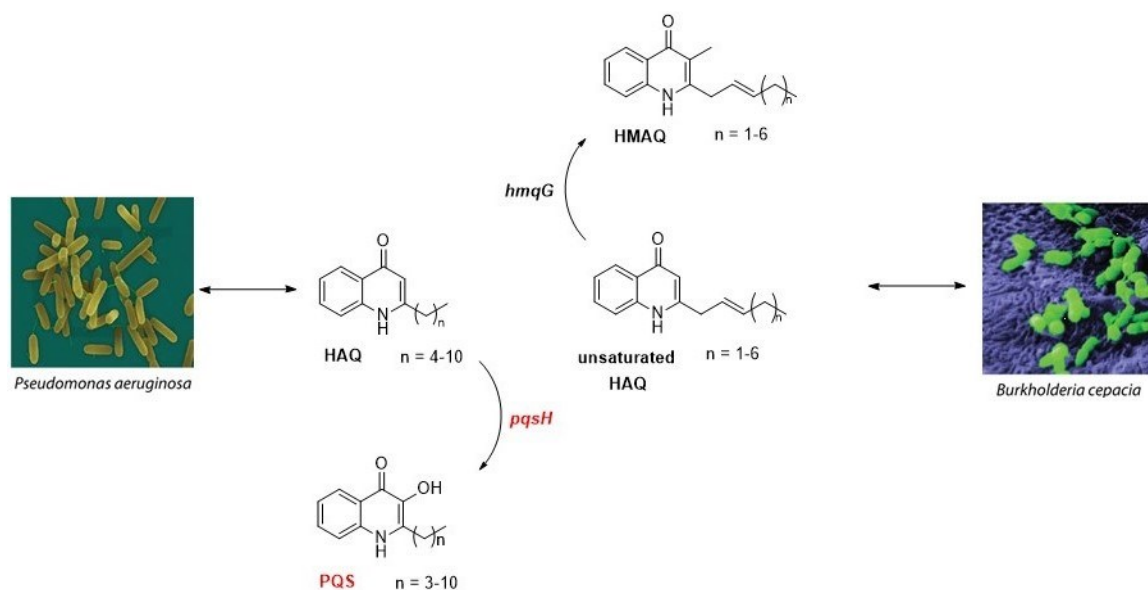
Figure A.1. Quinolone quorum sensing molecules specific to either *Pseudomonas aeruginosa* (left) or *Burkholderia cepecia* (and *B. thailandensis*) (right).

B. thailandensis produces a number of structurally similar quinolones differing by β,γ-unsaturation of the alkyl chain and a 3'-methyl group in which HmqF and HmqG are involved in the biosynthesis of these modifications, respectively.[3,8] These quinolones are referred to as 4-hydroxy-3-methyl-2-alkylquinolines (HMAQs), which are involved in QS within *Burkholderia* (Figure A.1, right).[3] Given the structural similarities between HMAQ and HHQ and PqsH promiscuity towards HHQ analogs with various chain lengths, we

sought to identify if PqsH has the ability to hydroxylate HMAQ molecules produced by *B. thailandensis* (Figure A.2).[3,7] Further investigations through in vitro and in vivo experimentation have established novel PqsH hydroxylation pathways. In this study, we have shown that PqsH has two alternative functions one of which is the conversion of 2-alkyl-4-hydroxyquinolone N-oxides (HQNO) to PQS providing an alternate substrate for the biosynthesis of PQS. The other function involves the hydroxylation of HMAQs from *Burkholderia* that could potentially act as interspecies quorum sensing sabotage.
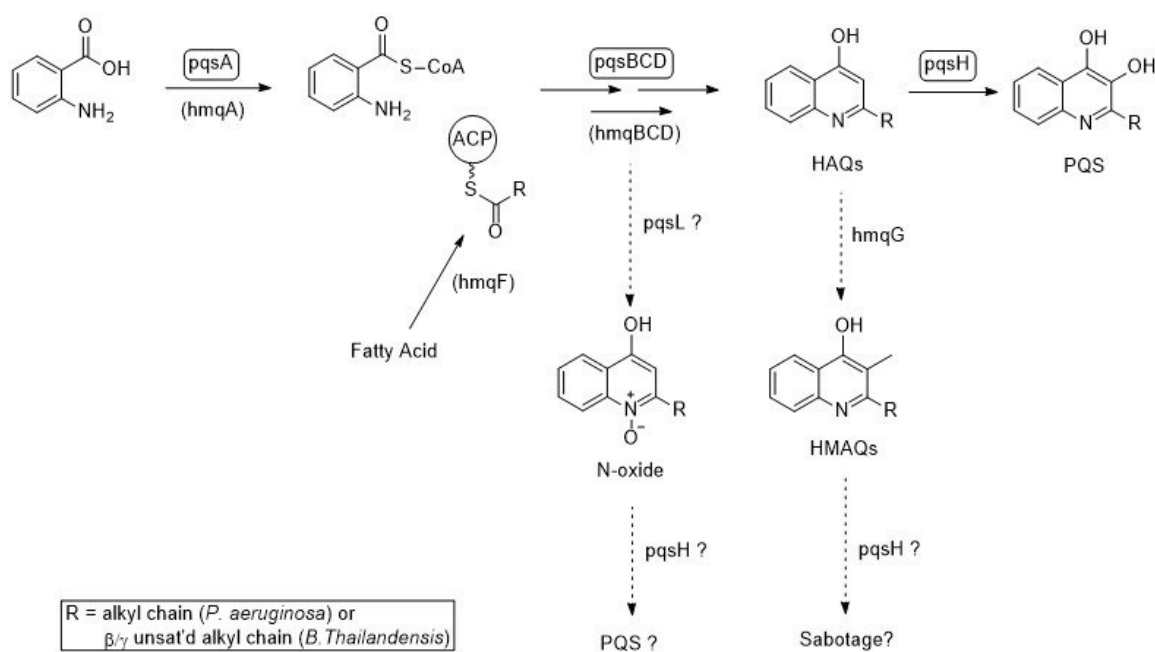
Figure A.2. Biosynthesis of quinolones produced by *P. aeruginosa* and *B. thailandensis* including possible salvage and sabotage pathways by pqsH.

A.2 MATERIALS AND METHODS

A.2.1 Materials. Amylose resin used for maltose binding protein purification was purchased from New England BioLabs. Dithiothreitol (DTT), isopropyl-β-D-thiogalactopyranoside (IPTG), NADH, and FAD were purchased from Affymetrix USB. Vectors (pET 28a and pMAL-C2x) were purchased from Novagen and DE3 cells from Stratagene.

A.2.2 Cloning, Expression and Purification of PqsH. *Bacterial Strains, Plasmids and Overexpression*. The *pqsH* gene was amplified from *P. aeruginosa PA*01 chromosomal DNA and the resulting amplicon was digested and ligated into pET28a to create pET28a-pqsH. The *pqsH* gene was then amplified from pET28a-pqsH and the resulting amplicon was digested and ligated into pMAL-C2x bearing a N-terminally fused maltose-binding protein to create pMAL-C2x-pqsH as done previously by Schertzer and coworkers.[7] The recombinant plasmid *pqsH*-pMAL-C2x was transformed into competent *Ecoli* Arctic Express (DE3) cells (Stratagene, La Jolla, CA) and plated on LB-agar plates supplemented with ampicillin (100 μg/mL) and gentamycin (20 μg/mL) grown at 37 ᵒC overnight. A single colony from the resulting plate was used to inoculate 50 mL LB containing 100 μg/mL ampicillin grown at 37 ᵒC overnight with rapid agitation. Four flasks containing 1 L of LB supplemented with 100 μg/mL ampicillin were then inoculated with 10 mL of saturated culture. The culture was grown to log phase ($OD_{600} = 0.2 - 0.4$) at 37 ᵒC for 1 hour with a decrease in temperature to 15 ᵒC, then induced by the addition of 500 μM iPTG followed by further incubation overnight at 15 ᵒC with rapid agitation. The cells were

harvested by centrifugation at 6900g for 30 min at 4 °C (Beckman JLA 8.100 rotor) and the cell pellets were stored at -20 °C until purification.

Cell Disruption and Purification. Cells were suspended in 40-50 ml buffer A [20 mM Tris (pH 7.5), 1 mM DTT, 0.5 mM EDTA, 10 μM FAD, 100 μM NADH and 200 mM NaCl]. The cells were lysed by sonication using 5" on/ 25" off for 5 min and cell debris was removed by centrifugation at 33000g for 30 – 45 min at 4 °C (Beckman JA 25.50 rotor). The cell lysate was loaded onto an amylose column pre-equilibrated with 5 CV buffer A and washed with 5 CV of the same buffer. The bound protein was eluted with a linear maltose gradient (from 0 to 10 mM) at a flow rate of 1 ml/min. Fractions containing PqsH as determined by SDS-PAGE were pooled followed by buffer exchange into buffer B [20 mM Tris (pH 8.0), 1 mM DTT, 0.5 mM EDTA, 10 μM FAD, 100 μM NADH and 10% glycerol]. The recombinant protein was then concentrated by centrifugation through an Amicon concentrator with a 10 kDa cutoff membrane (Centriprep centrifugal filters, Millipore) and flash-frozen in liquid nitrogen as BB's stored at -80 °C. The resulting soluble PqsH protein product had an apparent molecular mass, determined by SDS-PAGE, in agreement with the mass of 85 kDa deduced from the amino acid sequence.

A.2.3 Synthesis of 2-alkyl-4-quinolone (AHQ) compounds.

Synthesis of AHQs, specifically HHQ, PQS, HQNO and HMAQ, were synthesized as described previously.[9,10,11] (Note: synthesis done by DBH).

A.2.4 Enzyme Activity Assay. In order to investigate PqsH activity towards multiple synthetic quinolone molecules, a standard reaction mixture containing 50 mM Tris (pH

8.0), 10 μM FAD, 300 μM NADH, 150 μM substrate and 8% methanol (v/v) in a final volume of 200 μL initiated upon addition of purified PqsH protein to 5 μM. Reactions were allowed to progress for 24 hrs. at 25°C and were quenched with 600 μL (three volumes) of acidified ethyl acetate (0.01% acetic acid in ethyl acetate). Organic phase was removed and dried via speed vacuum centrifuge followed by resuspension of the dried product in 50 μL 95% methanol + 0.1% formic acid. Reactions were performed in triplicate and resulting products were subjected to HPLC-MS analysis.

A.2.5 Phenotype Assay. Verification of PQS formation from the precursor HQNO was done *in vivo* with the *PA*01 Δ*pqs*A knockout strain. A saturated culture was first made by inoculating 4 mL of LB with a single colony of *PA*01 Δ*pqs*A grown on a LB-agar plate grown overnight at 37°C with rapid agitation. Reactions were completed by diluting 160 μL of saturated culture with fresh LB to 4 mL (25:1 dilution) and a synthetic standard, HQNO or HHQ (control), was added to a final concentration of 50 μM during log phase (OD_{600} = 0.2 – 0.3). All cultures were grown overnight at 37°C with rapid agitation. In order to quantify pyocyanin concentration, 200 μL of saturated culture was spun down at 18000g for 5 min in a microcentrifuge (Beckman Coulter), and absorbance reading of the supernatant at 690 nm was measured at 25°C using a Tecan Infinite M200 spectrophotometer (Tecan Group Ltd.) as described by Dietrich and coworkers.[12] The remaining saturated culture was subjected to quinolone extraction and purification by solid phase extraction (SPE) on a 1 mL, 50 mg C18 column (Silicycle, Quebec City, QC). To the culture, formic acid (FA) concentration was brought to 0.1% and equal parts of methanol + 0.1% FA was added to lyse the cells. After mixing samples, the mixture was

spun at 18000g for 10 min in a microcentrifuge and to the supernatant methanol concentration was diluted to 25% by the addition of 0.1% FA. The SPE C18 columns were then equilibrated with 1 mL methanol and conditioned with 1 mL of 5% methanol + 0.1% FA. Samples were then loaded onto the C18 columns, washed with 1 mL of 5% methanol + 0.1% FA and eluted with 2 x 100 μL of 95% methanol + 0.1% FA. Final elution steps were collected and subjected to HPLC-MS analysis.

A.2.6 Product Analysis and Quantification by HPLC-MS. The separation of the quinolone products isolated from the *in vitro* and *in vivo* assays were performed on a Kinetex C18 column [50.0 mm x 2.10 mm, pore diameter of 100 Å, particle size of 2.6 μm (Phenomenex, Torrance, CA)] connected to an Agilent 1200 series HPLC system (Agilent Technologies Inc., Santa Clara, CA). The column was first equilibrated for 10 min with 10% buffer A [Acetonitrile + 0.1% FA] and 90% buffer B [Water + 0.1% FA]. The following gradient was then applied from 10% A and 90% B to 90% A and 10% B over 12 min, held at 90% A and 10% B for 2 min and brought back to 10% A and 90% B in 2 min with a total run time of 20 min. The separations were conducted at a flow rate of 0.2 mL/min and absorbance was monitored at 260nm. The HPLC eluents were directly infused into the mass spectrometer for analysis performed on a 7.0 T Fourier transform ion cyclotron resonance mass spectrometer (Bruker Daltonics Inc., Billerica, MA), which was externally calibrated with sodium trifluoroacetate clusters (0.1 mg/mL in acetonitrile).

In order to quantify the amount of product produced as a function of time, the elution times of HHQ, HQNO, HMAQ and PQS were established using synthetic standards. A standard curve was first created of known quinolone concentration

individually assessed using the HPLC-MS conditions described above. The quinolone peaks corresponding to a known concentration were integrated and were used to create a standard curve of peak integration versus quinolone concentration. The resulting slope of the curve was then used to determine amount of product formation during a given reaction time. HPLC and MS analysis was performed using Hystar and Apex, respectively, from Bruker Daltonics.

A.2.7 Steady-State Kinetics. In order to investigate enzyme kinetics of PqsH as well as substrate preference, enzyme activity assays were performed under steady-state conditions. Reaction mixtures containing 50 mM Tris (pH 8.0), 10 μM FAD, 2mM NADH, 8% methanol and HQNO (50 – 500 μM) or HMHQ (10 - 150 μM) in a final volume of 200 to 600 μL was initiated upon addition of purified PqsH protein to 5 μM. The reactions were allowed to progress for various times and were quenched with three volumes of acidified ethyl acetate (0.01% acetic acid in ethyl acetate) as described by Schertzer and coworkers.[7] The organic phase was removed and dried via speed vacuum centrifuge followed by resuspension of the dried product in 50 μL 95% methanol + 0.1% formic acid. Reactions were performed in triplicate and resulting products were subjected to HPLC-MS analysis. Quantification of product formation was done as previously described for product quantification by HPLC-MS and was fit to the Michaelis-Menten equation (Origin 9.0, OriginLabs, Northampton, MA).

A.2.8 Inhibition of pqsH by HMHQ and HQNO. Under steady-state conditions, a similar enzyme activity assay to the one described above was used to test if HMHQ and

HQNO were inhibitors versus HHQ for the pqsH hydroxylation reaction. Reaction mixtures contained 50 mM Tris (pH 8.0), 10 μM FAD, 300 μM NADH, 8% methanol, were performed at various concentrations of HHQ (2 – 50 μM) and either HMHQ (2 – 6 μM) or HQNO (2 – 6 μM) in a final volume of 250 μL initiated upon addition of purified PqsH protein to 5 μM. The reactions were allowed to progress for various times and were quenched as well as worked up as described above. All products were resuspended in 300 μL methanol and were assayed for PQS fluorescence ($\lambda_{excitation}$ = 342 nm and $\lambda_{emission}$ = 450 nm) on a Tecan Infinite M200 spectrophotometer.[7] Equation 1 was used to fit the mixed inhibition data for HMHQ and HQNO:

$$v = V_{max} \, [S]/(\alpha[S] + \alpha'K_m) \qquad \textbf{equation A.1}$$

where V_{max} is the maximal velocity, $[S]$ is the concentration of the substrate, K_m is the Michaelis-Menten constant for the substrate, $\alpha = (1 + [I]K_i)$ where K_i refers to the equilibrium constant when inhibitor binds to free enzyme and $\alpha' = (1 + [I]K'_i)$ where K'_i refers to the equilibrium constant when inhibitor binds the enzyme-substrate complex.

A.3   RESULTS AND DISCUSSION

A.3.1 Verification of PQS production by PqsH in the presence of HQNO via HPLC-MS. To examine our hypothesis of PqsH promiscuity towards alternative substrates, we cloned and expressed pqsH with the N-terminally fused maltose binding protein (pMAL-C2x) in Escherichia coli and reconstituted its activity in vitro where product formation was

monitored as done previously.[7] First we examined the ability of PqsH to hydroxylate 4-hydroxy-2-heptylquinoline N-oxide (HQNO) in vitro. PqsH was incubated with FAD, NADH and the substrate HQNO and analyzed by High Performance Liquid Chromatography-Mass Spectrometry (HPLC-MS). We observed the formation of PQS over time, which was verified by high resolution MS and comparison of retention times with a synthetic PQS standard (Figure A.3 (a)). A second product was identified by HPLC-MS with a mass corresponding to a 3,4-dihydroxy-2-heptylquinoline N-oxide intermediate (Figure A.3 (b)). The presence of the 3,4-dihydroxy N-oxide intermediate provides mechanistic evidence of two sequential steps where hydroxylation occurs prior to N-O bond cleavage (Scheme A.1). In a control reaction without either co-factor FAD or NADH, no reaction was observed. In addition to the novel N-O bond cleavage activity of PqsH, we have identified a new precursor of PQS. This is of particular interest since HQNO, although has demonstrated modest antibacterial properties, does not have a known role within QQS.[13] This novel pathway involving quinolone N-oxides as precursors for PQS biosynthesis provides evidence that P. aeruginosa is capable of harnessing more than one QQS molecule for the production of PQS.
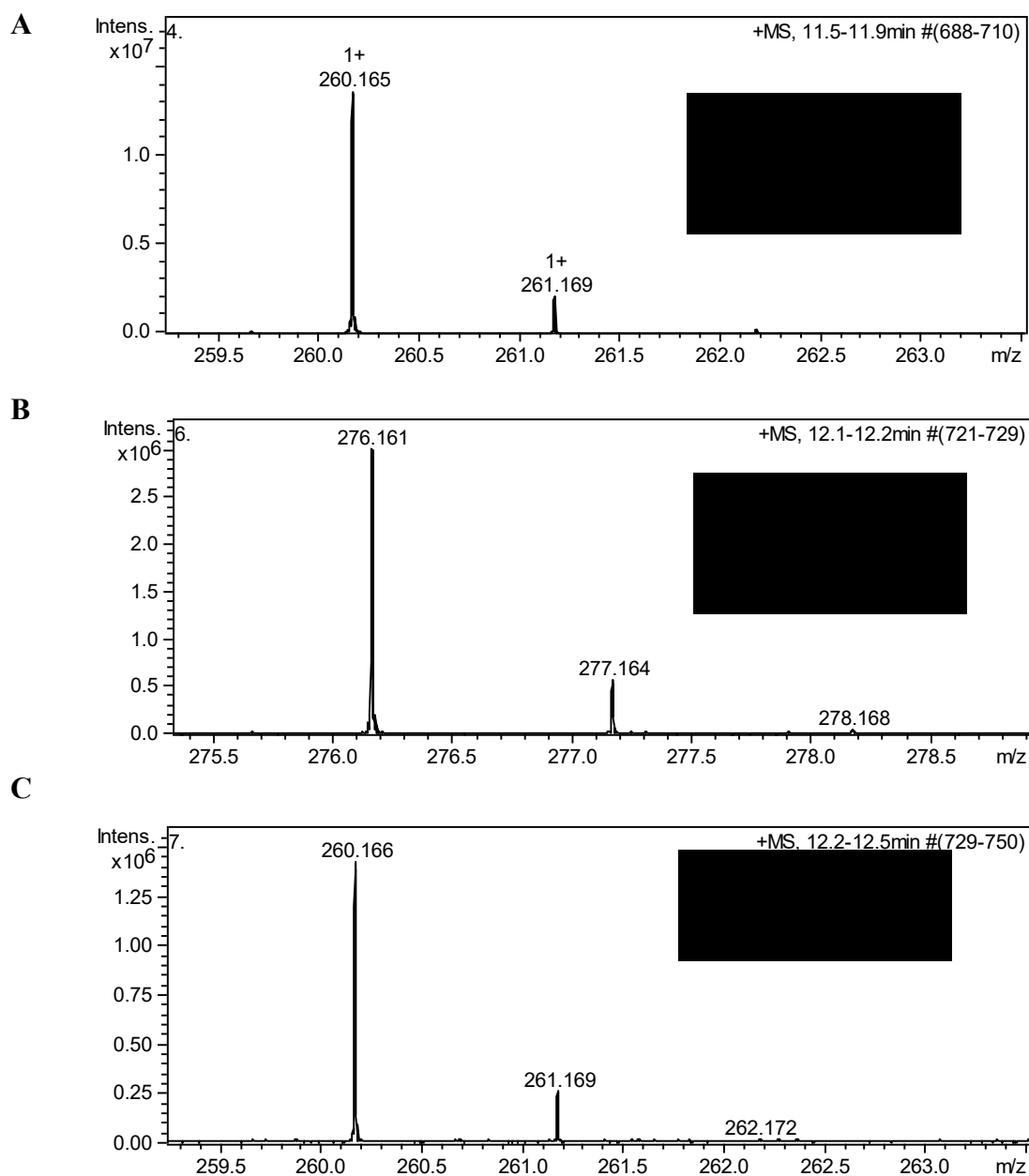
Figure A.3. HPLC-MS analysis of the PqsH protein activity assay with HQNO. (A) MS

characterization of the starting material, HQNO, confirmed by elution time and m/z of the

synthetic standard. (B) MS characterization of the 3,4-hydroxy-2-heptylquinoline *N*-oxide

intermediate. (C) MS characterization of PQS confirmed by elution time and m/z of the

synthetic standard.   Provides confirmation that HQNO is in fact a precursor to PQS formation via a 3,4-hydroxy, N-oxide intermediate. All products observed < 5 ppm error.

Scheme A.1. Hydroxylation of HQNO by PqsH.
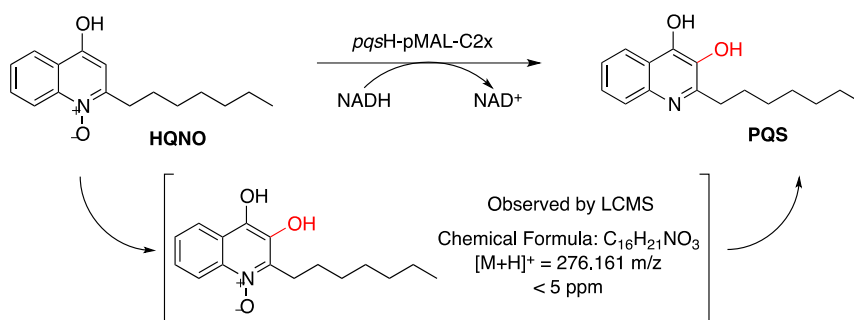
A.3.2 Phenotype Assay via UV/Vis Spectrometry verifies Pyocyanin production with HQNO.   One of the many roles of PQS is to upregulate the synthesis of phenazine pyocyanin (PYO), a known product of the quorum sensing cascade found in *P. aeruginosa*, and has been previously used to document QQS response.[12] In order to confirm PQS production occurs *in vivo* via the mechanism presented above, an *in vivo* assay was conducted where PQS and PYO production was monitored. The HQNO and HHQ (control) synthetic standards were incubated with the PA01 Δ*pqs*A knockout strain, which is unable to produce quinolone molecules, and PYO production was measured spectrophotometrically while PQS concentration was measured via LCMS (Table A.1).

Table A.1. Phenazine pyocyanin *in vivo* assay results.

Substrate	PYO conc.* (µM)	PQS conc. (µM)
HQNO	1.763	63.053
HHQ	6.265	218.664

* Determined by Beer's Law measuring A_{690} and using the extinction coefficient $\varepsilon_{690} = 4,130$ M^{-1} cm^{-1}.

In the case of HQNO, PQS production was observed and reinforced by the PYO concentration found in the culture supernatant. The presence of PQS successfully proves PqsH ability to hydroxylate HQNO *in vivo*.

A.3.3 Verification of the B. Thailandensis specific HMHQ phosphorylation by PqsH via HPLC-MS. Additionally, a potential sabotage pathway via PqsH was discovered due to its ability to hydroxylate 4-hydroxy-3-methyl-2-heptylquinoline (HMHQ) specific to *B. thailandensis* (Scheme A.2).

Scheme A.2. Hydroxylation of HMAQ by PqsH.
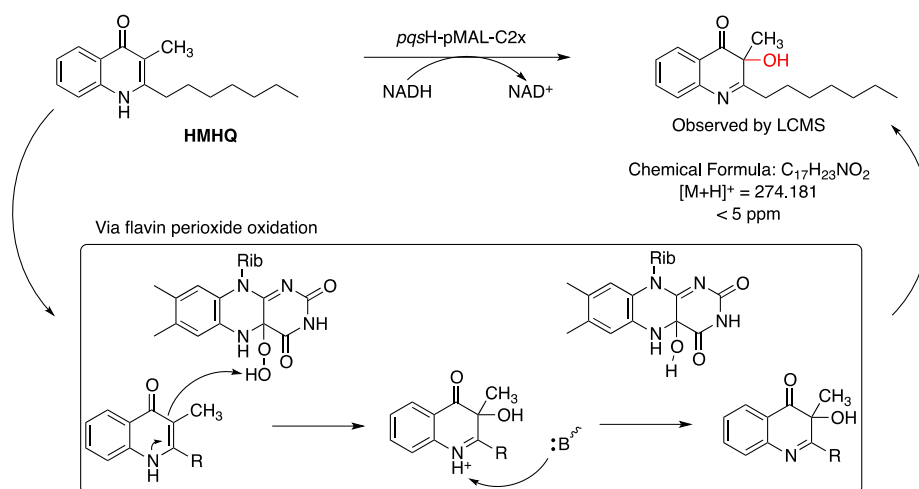
PqsH activity towards HMHQ was assessed as previously done for HQNO in which PqsH was incubated with the proper reagents followed by LCMS (Figure A.4). We observed the formation of a new product with a mass that corresponds to 2-heptyl-3-hydroxy-3-methyl-4-quinolone, which yielded $[M+H]^+$ ions at 274 m/z versus the $[M+H]^+$ ions at 258 m/z for the HMHQ synthetic standard (Figure A.4).
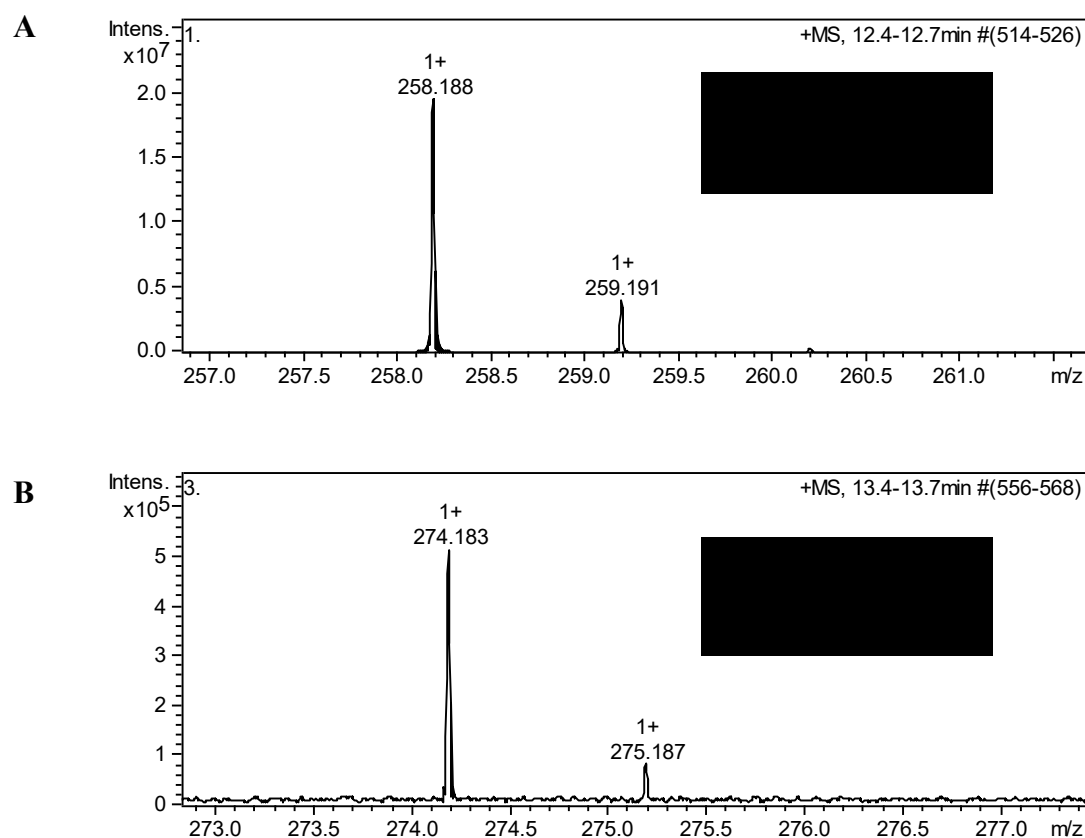
Figure A.4. HPLC-MS analysis of the PqsH protein activity assay with HMHQ. (A) MS characterization of the starting material, HMHQ, confirmed by elution time and m/z of synthetic standard. (B) MS characterization of 3,4-hydroxy-3-methyl-2-heptylquinoline product. Provides confirmation that PqsH can in fact hydroxylate *B. thailandensis* specific quinolone molecules. All products confirmed to < 5 ppm error.

We propose that PqsH hydroxylates HMHQ via a flavin peroxide oxidation mechanism similar to other Flavin monooxygenases.[14] The addition of the hydroxyl group at the 3'-position to the *B. thailandensis* quinolone is intriguing since hydroxylation is unique to *P. aeruginosa*. This modification to the quinolone ring could render the molecule inactive since it has been shown that modifications on the ring effects signaling activity in the *B. thailandensis* QQS system.[15]

A.3.4 Steady-State Kinetics determined for PqsH secondary substrates, HQNO and HMHQ. Since HHQ is the primary substrate of PqsH whereas HQNO and HMHQ are secondary substrates, we determined the steady-state kinetic parameters of these substrates. The kinetic constants were determined by an enzyme activity assay *in vitro* at saturating concentrations (> 5x K_m) of all substrates initiated by the addition of purified *pqsH*-pMAL-C2x to 5 µM (Table A.2).

Table A.2. Steady-state kinetic parameters of PqsH-MBP.

Substrate	k_{cat} (min^{-1})	K_m (µM)	k_{cat}/K_m (M^{-1} min^{-1})
HQNO	0.00210 ±0.00003	9.065 ±1.100	232.1 ± 14.4
HMHQ	0.00602 ±0.00003	7.407 ±1.344	813.3 ± 24.3
HHQ*	2.7 ± 0.1	0.110 ± 0.040	2.4 x 10^7

* As determined by Schertzer et al.[2,3,7,13]

Product formation was then quantified over a period of time by HPLC separation and peak integration in comparison to a standard curve, where data was fitted to the

Michaelis-Menten equation (Figure A.5). The significant difference in catalytic efficiency for both HQNO and HMHQ versus HHQ is due to reduced k_{cat} values, reflecting perturbation of the chemical steps following initial substrate binding.
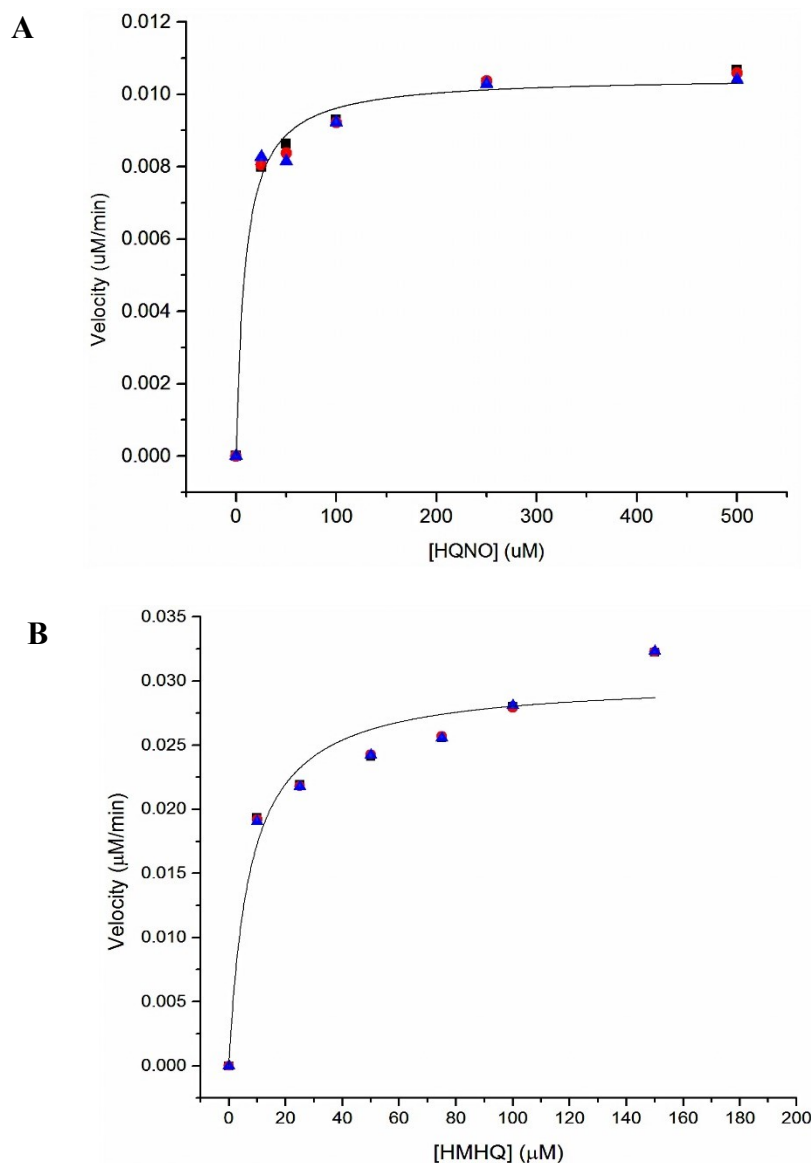
Figure A.5. Steady-State kinetics of HQNO and HMHQ hydroxylation catalyzed by PqsH. (A) Michaelis-Menten curve extrapolated from the data collected with HQNO as the substrate. (B) Michaelis-Menten curve extrapolated from the data collected with HMHQ

as the substrate. Both kinetic studies were done in triplicate were the substrate concentration was varied in the presence of > 5x K_m concentrations of the other substrates. Errors of the derived steady-state parameters shown in Table 1 are standard errors of the Michaelis-Menten equation fit.

A.3.5 Inhibition studies via PQS fluorescence. The studies demonstrated inhibition of PqsH for HHQ, primary substrate, versus HQNO and HMHQ, secondary substrates. Additionally, inhibition studies of PqsH by HMHQ and HQNO were performed in which both HMHQ and HQNO demonstrated mixed inhibition (Figure A.6). In the case of HMHQ, $K_m^{app} < K_m$ suggesting it binds more favorably to the enzyme-substrate complex. As for HQNO, $K_m^{app} > K_m$ suggesting it binds more favorably to free enzyme. These preliminary studies demonstrate that HMAQ and HQNO may not only act as alternate substrates for PqsH but also influence the dynamics of PQS production *P. aeruginosa.*
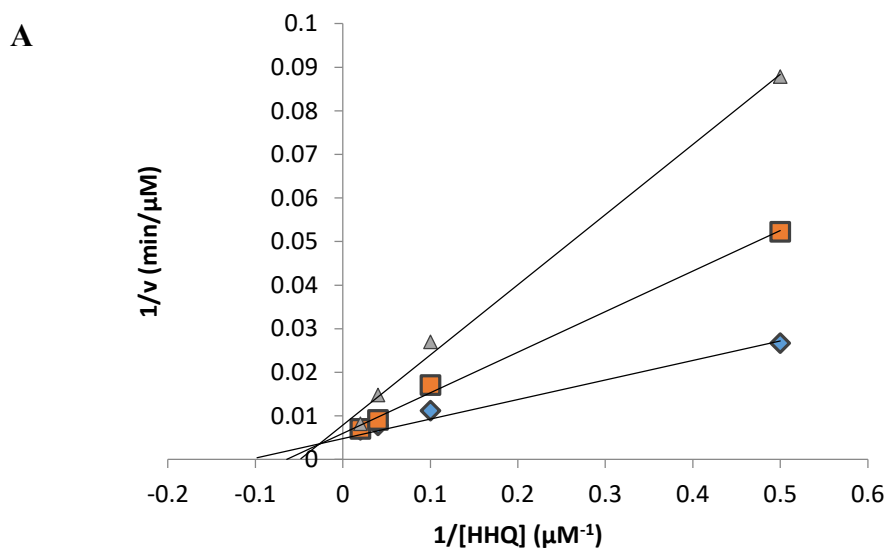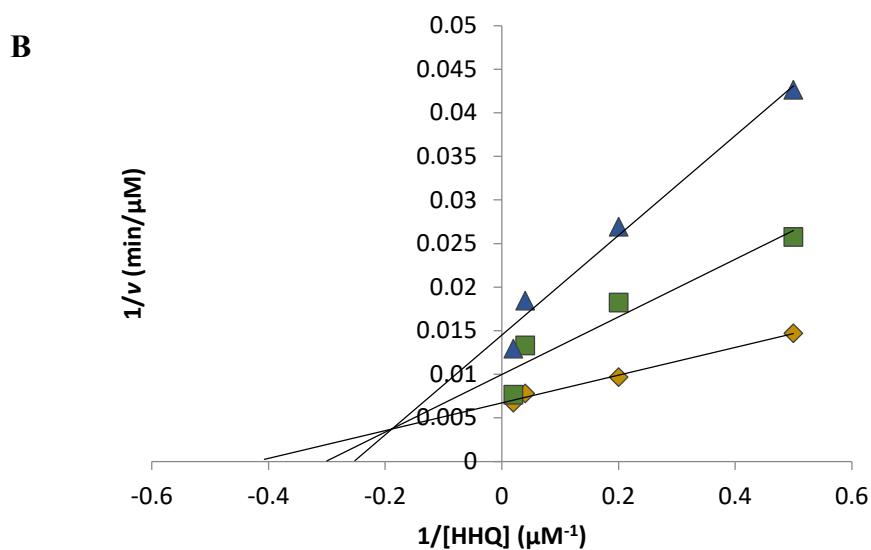
Figure A.6. Inhibition studies of pqsH by HMHQ and HQNO. Activity assays were measured in 50 mM Tris (pH 8.0), 10 μM FAD, 300 μM NADH, 8% methanol as described above in materials and methods. **(A)** Mixed inhibition by HMHQ where initial velocities were measured at 5 μM PqsH protein, 0 μM (◆), 2 μM (▪), and 4 μM (▲) HMHQ, and varying concentrations of HHQ. The data was fit to equation 1 listed above and yielded the following values for HMHQ: $V_{max}^{app} = 146.62 \pm 28.34$ min^{-1}, $K_m^{app} = 0.0568 \pm 0.0109$ μM, $K_i = 1.3533 \pm 0.0503$ μM, and $K_i' = 3.4378 \pm 0.0605$ μM. **(B)** Mixed inhibition by HQNO where initial velocities were measured at 5 μM PqsH protein, 0 μM (◆), 2 μM (▪), and 4 μM(▲) HQNO, and varying concentrations of HHQ. The data fit for HQNO to equation 1 yielded the following values: $V_{max}^{app} = 84.43 \pm 21.95$ min^{-1}, $K_m^{app} = 0.278 \pm 0.035$ μM, $K_i = 0.4333 \pm 0.0049$ μM, and $K_i' = 2.3141 \pm 0.0092$ μM.

A.4 CONCLUSIONS

Until now, the only known pathway for PQS production was the hydroxylation of HHQ by the flavin-dependent monooxygenase PqsH. We have since shown an alternative pathway where QQS *N*-oxide can be converted to PQS providing an alternate precursor for PQS formation (Scheme A.3 (a)). This novel PQS precursor has also provided insight on N-O bond cleavage activity of PqsH in addition to the known hydroxylation activity. Furthermore, we have shown that quinolone molecules unique to the *B. thailandensis* QQS system can undergo hydroxylation via PqsH rendering it a multipurpose enzyme within *P. aeruginosa* (Scheme A.3 (b)).

Scheme A.3. Novel PqsH pathways in (a) *P. aeruginosa* and (b) *B. thailandensis*.
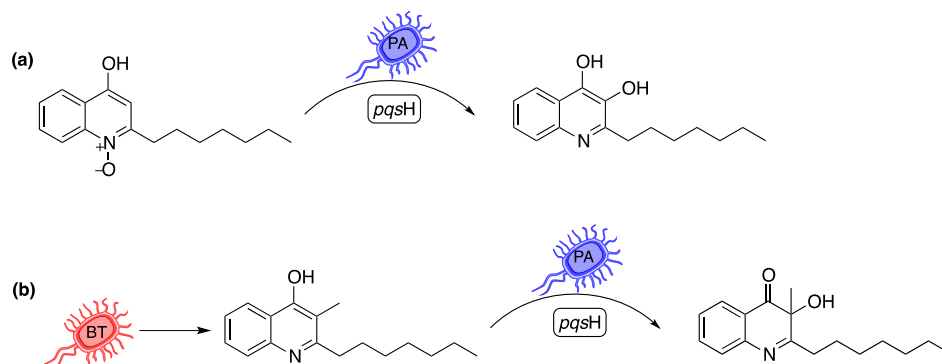
Such a modification specific to *P. aeruginosa* suggests potential interspecies signaling sabotage employed by these bacteria in their environments. Additional mechanistic investigation of the conversion from *N*-oxide quinolone to PQS is currently underway to elucidate the mechanism of N-O bond cleavage by PqsH. The impact of the resulting 2-heptyl-3-hydroxy-3-methyl-4-quinolone on the *B. thailandensis* QQS system through *in vivo* studies is also to be determined in order to establish how effective it is in blocking or attenuating QQS signal.

APPENDIX B. FLUORESCENCE SPECTROSCOPY FROM CHAPTER 2

Table B.1 K_d values for binding of the E2·E3BP-derived domains to PDK1-PDK4 as detected by fluorescence spectroscopy[68].*

K_d (μM)	DANS-L1	DANS-L2S	DANS-L1L2S MS1	DANS-L1L2S MS2	DANS-L3S'	Dapoxyl-L3S'
PDK1	4.43±0.35	17.1±0.94	2.10±0.12	3.62 ±0.25	No binding	No binding
PDK2	0.91±0.08	1.38±0.03	0.89±0.09	0.64±0.09	0.025[a]	2.07 ± 0.06
PDK3	0.62±0.03	1.21±0.06	0.54± 0.05	0.396±0.06	0.103 [a]	No binding
PDK4	0.35±0.06	2.07±0.16	0.27± 0.02	0.397±0.03	5.93 ± 1.06	5.02 ± 0.13

[a] On binding of PDK2 and PDK3 to DANS-L3S', quenching of the DANS-L3S' fluorescence was observed while in others enhancement resulted.

* Fluorescence spectroscopy experiments carried out by Luying Yang.

APPENDIX C. Pyruvate Dehydrogenase Kinase Inhibitors from Chapters 2 and 3
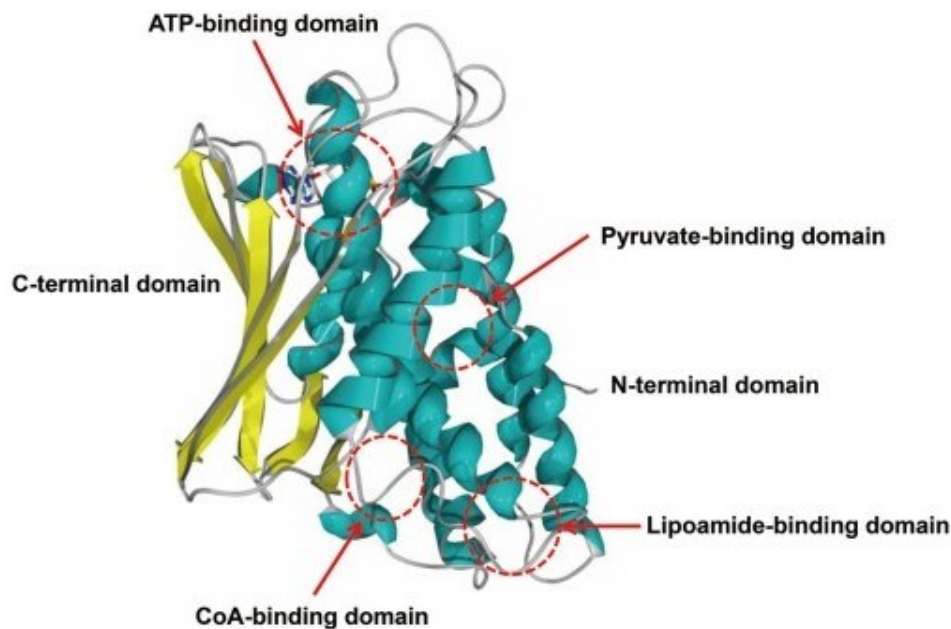
Figure C.1 Allosteric binding domains and substrate binding domains on the pyruvate dehydrogenase kinases (PDKs)[16].
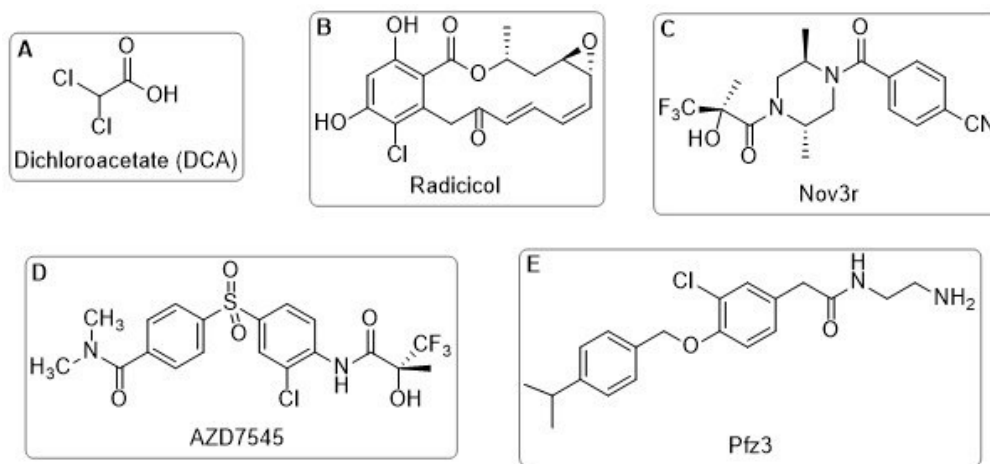
Figure C.2 PDK Inhibitors[16]. (A) DCA, inhibitor of the pyruvate-binding domain. (B) Radicicol, inhibitor of the nucleotide-binding domain. (C) Nov3r, inhibitor of the lipoamide-binding domain. (D) AZD7545, inhibitor of the lipoamide-binding domain. (E) Pfz3, inhibitor of the coenzyme A-binding site.

APPENDIX D.   GENERAL PROTOCOLS FOR CHAPTERS 2 and 3

D1. Plasmid Purification and Site-Directed Mutagenesis

D.1.1 *Materials*

The Wizard® Plus Minipreps DNA purification system was used for purification of DNA (Promega, Madison, WI). The QuikChange® II XL site-directed mutagenesis kit was used (Stratagene, La Jolla, CA). DNA sequencing was done at the Molecular Resource Facility of the New Jersey Medical School (Newark, NJ). E. coli BL21(DE3) cells were from Novagen (EMD Chemicals, Gibbstown, NJ). Primers were from Integrated DNA Technologies, Inc. (Coralville, IA).

D.1.2 *Plasmid Purification*

The Wizard® Plus Minipreps DNA purification kit from Promega was used for plasmid purification based on the protocol provided. Human L1L2S cells (truncated human E2p protein) were spread on the LB agar plate containing 35 μg/ml kanamycin. Single colonies were chosen and grown overnight at 37 °C in 10 ml LB medium containing 35 μg/ml kanamycin followed by the plasmid purification protocol below:

1. Pellet 5-10 ml of cells by centrifugation at 1,400 × g for 10 min. Pour off the supernatant and blot the tube upside-down on a paper towel to remove excess media.

2. Completely resuspend the cell pellet in 400 μl of Cell Resuspension Solution. Transfer the resuspended cells to a 1.5 ml microcentrifuge tube.

3. Add 400 μl of Cell Lysis Solution and mix by inverting the tube 4 times. The cell suspension should clear immediately.

4. Add 400 μl of Neutralization Solution and mix by inverting the tube several times. Alternatively, if using an EndA+ strain, add 800 μl of Neutralization Solution, mix by inverting the tube 4 times and incubate at room temperature for 10 min.

5. Centrifuge the lysate at 10,000 × g in a microcentrifuge for 5 min. If a pellet has not formed by the end of the centrifugation, centrifuge an additional 15 min.

6. Pipet 1 ml of the resuspended resin into each barrel of the Minicolumn syringe assembly. (If crystals or aggregates are present, dissolve by warming the resin to 25-37 °C for 10 min. Cool to 30 °C before use). Thoroughly mix the Wizard® Minipreps DNA Purification Resin before removing an aliquot.

7. Carefully remove all the cleared lysate from each miniprep and transfer it to the barrel of the Minicolumn/syringe assembly containing the resin. No mixing is required at this stage. The resin and lysate should be in contact only for the time it takes to load the Minicolumns.

8. Open the stopcocks and apply a vacuum of at least 15 inches of Hg to pull the resin/lysate mix into the Minicolumn. When the entire sample has completely passed through the column, break the vacuum at the source. *Note: If using an EndA+ strain, add 2 ml of 40% isopropanol/4.2M guanidine hydrochloride solution to each column. Apply a vacuum and continue it for 30 s after all of the solution has flowed through the columns. Note that this solution will flow through the column more slowly than the standard Column Wash Solution. After this wash proceed with the standard column wash procedure (Step 9).*

9. Add 2 ml of the Column Wash Solution (containing 95% ethanol) to the Syringe Barrel and reapply the vacuum to draw the solution through the Minicolumn.

10. Dry the resin by continuing to draw a vacuum for 30 s after the solution has been pulled through the column. Do not dry the resin for more than 30 s. Remove the Syringe Barrel and transfer the Minicolumn to a 1.5 ml microcentrifuge tube. Centrifuge the Minicolumn at 10,000 × g in a microcentrifuge for 2 min to remove any residual Column Wash Solution.

11. Transfer the Minicolumn to a new microcentrifuge tube. Add 50 µl of nuclease-free water to the Minicolumn and wait 1 min. Centrifuge the tube at 10,000 × g in a microcentrifuge for 20 s to elute the DNA. The DNA will remain intact on the Minicolumn for up to 30 min; however, prompt elution will minimize nicking of plasmids in the range of 20kb. For elution of large plasmids (≥10kb), the use of water preheated to 65-70 °C may increase yields. For plasmids ≥20kb, use water preheated to 80 °C.

12. Remove and discard the Minicolumn. DNA is stable in water without addition of buffer if stored at -20 °C or below. DNA is stable at 4 °C in TE buffer. To store the DNA in TE buffer, add 5 µl of 10X TE buffer to the 50 µl of eluted DNA.

13. The concentration of plasmids was measured using $\varepsilon = 0.050$ at 260nm.

D.1.3 *Plasmid Digestion*

For plasmid digestion XhoI and NdeI was used (vector pET-28b, molecular weight 5369 bp). The reaction medium contained in 1 μl buffer # 4, 5 μl purified plasmid, 2 μl distilled water and reaction was started by the addition of 1 μl of NdeI enzyme. The reaction was kept for 4 hours of incubation at 37 ºC followed by the addition of 1 μl of XhoI. The reaction was incubated overnight at 37 ºC and checked by Agarose gel.

D.1.4 *Primer Design*

Primers were designed using the program QuikChange Primer Design from Agilent Technologies. The following are guidelines for primer design:

1. Both mutagenic primers must contain the desired mutation and anneal to the same sequence on opposite strands of the plasmid.

2. Primers ideally should be between 25 and 45 bases in length, with a melting temperature (Tm) of ≥78 °C. Primers longer than 45 bases may be used, however using longer primers increases the likelihood of secondary structure formation, which may affect the efficiency of the mutagenesis reaction.

3. The desired mutation (deletion or insertion) should be in the middle of the primer with ~10–15 bases of correct sequence on both sides.

4. The primers optimally should have a minimum GC content of 40% and should terminate in one or more C or G bases.

5. The received primers and antiprimers were centrifuged for 6 min and dissolved in 100 μl sterilized water which was centrifuged for 10 min. The concentration was measured using molar extinction coefficient (ε) = 0.033 at 260nm.

D.1.5 *Site-Directed Mutagenesis*

Mutagenesis was carried out using the QuikChange® II XL Site-Directed Mutagenesis Kit from Agilent Technologies.

1. Prepare the control reaction as indicated below:

   5 µl of 10× reaction buffer

   2 µl (10 ng) of pWhitescript 4.5-kb control plasmid (5 ng/µl)

   1.25 µl (125 ng) of oligonucleotide control primer #1 [34-mer (100 ng/µl)]

   1.25 µl (125 ng) of oligonucleotide control primer #2 [34-mer (100 ng/µl)]

   1 µl of dNTP mix

   38.5 µl of double-distilled water (ddH2O) to a final volume of 50 µl

   Then add 1 µl of *PfuTurbo* DNA polymerase (2.5 U/µl)

2. Prepare the sample reaction(s) as indicated below:

   5 µl of 10× reaction buffer

   5–50 ng of dsDNA template (1 µl)

   125 ng of oligonucleotide primer #1 (5 µl)

   125 ng of oligonucleotide primer #2 (5 µl)

   1 µl of dNTP mix

   3 µl of QuikSolution

   ddH2O to a final volume of 50 µl

   Then add 1 µl of *PfuTurbo* DNA polymerase (2.5 U/µl)

3. Set up cycling parameters for the site directed mutagenesis method (For the control reaction, use a 5 minute extension time and run the reaction for 18 cycles):

   Segment 1: 1 cycle at 95 ºC for 1 minute

Segment 2: 18 cycles at 95 ºC for 50 seconds, then 60 ºC for 50 seconds, and finally

68 ºC for 1 minute/kb of plasmid length

Segment 3: 1 cycle at 68 ºC for 7 minutes

4. Following temperature cycling, place the reaction on ice for 2 minutes to cool the

    reaction ≤ 37 °C

Dpn I digestion of the amplification products:

1. Add 1 µl of the *Dpn* I restriction enzyme (10 U/µl) directly to each amplification

    reaction.

2. Gently and thoroughly mix each reaction mixture by pipetting the solution up and

    down several times. Spin down the reaction mixtures in a microcentrifuge for 1

    minute and immediately incubate each reaction at 37ºC for 1 hour to digest the

    parental supercoiled dsDNA.

Transformation of XL10-Gold supercompetent cells

1. Gently thaw the XL10-Gold supercompetent cells on ice. For each control and

    sample reaction to be transformed, aliquot 45 µl of the supercompetent cells to

    a *prechilled* 14 ml BD Falcon polypropylene round-bottom tube.

2. Add 2 µl of the β-ME mix provided with the kit to the 45 µl of cells.

3. Swirl the contents of the tube gently. Incubate the cells on ice for 10 minutes,

    swirling gently every 2 minutes.

4. Transfer 2 µl of the *Dpn* I-treated DNA from each control and sample reaction

    to separate aliquots of the supercompetent cells. As an optional control, verify

    the transformation efficiency of the XL10-Gold supercompetent cells by adding

    1 µl of 0.01 ng/µl pUC18 control plasmid (dilute the control provided 1:10 in

high quality water) to a 45 μl aliquot of the supercompetent cells. Swirl the transformation reactions gently to mix and incubate the reactions on ice for 30 minutes.

5. Heat pulse the transformation reactions for 30 seconds at 42 °C and incubate the tubes on ice for 2 minutes.

6. Add 0.5 ml of NZY$^+$ broth preheated to 42 °C and incubate the transformation reactions at 37 °C for 1 hour with shaking at 225–250 rpm.

7. Plate the appropriate volume of each transformation reaction on agar plates containing the appropriate antibiotic for the plasmid vector. For sample mutagenesis: use 35 μg/ml kanamycin LB plates with the following volumes: 1) 5 μl sample + 250 μl NZY$^+$ broth, 2) 50 μl sample + 250 μl NZY$^+$ broth and 3) 250 μl sample. For the mutagenesis and transformation controls, spread cells on LB ampicillin agar plates containing 80 μg/ml X-gal (100 μl from 2 % stock) and 20 mM IPTG (100 μl from 10 mM stock).

8. Incubate the transformation plates at 37 °C for > 16 hours.

Transformation of BL21 (DE3) competent cells

1. Pre-chill two 14-ml BD Falcon polypropylene round-bottom tubes on ice. Preheat SOC medium to 42 ºC.

2. Thaw the cells on ice, gently mix and add 100 μl to each polypropylene tubes.

3. Add 1.7 μl of the β-mercaptoethanol provided with kit to each aliquot of cells.

4. Swirl the tubes gently. Incubate the cells on ice for 10 minutes, swirling gently every 2 minutes. (note: do not need control here so two tubes can be used for sample plasmids)

5. Add 1-50 ng (1 µl) of experimental DNA.

6. Incubate the tubes on ice for 30 minutes.

7. Heat-pulse the tubes in a 42 °C water bath for 45 seconds. The duration of the heat pulse is critical.

8. Incubate the tubes on ice for 2 minutes.

9. Add 0.9 ml pre-heated SOC medium and incubate at 37 °C for 1 hour with shaking at 225-250 rpm.

10. Plate (5 µl+100 µl SOC, 50 µl+100 µl SOC, 150 µl plasmid) the transformation mixture on LB-ampicillin agar plates. Incubate the plates at 37 °C overnight.

Check expression

1. From the above plates, 5 different colonies were chosen and grown overnight at 37 °C in 2 ml LB medium containing 35 µg/ml kanamycin.

2. Inoculate 10 ml LB medium supplemented with 35 µg/ml kanamycin with 0.2 ml overnight culture (50:1 dilution) and incubate for 2 hours at 37 °C.

3. Add 1 mM IPTG to cultures and grow for an additional 4-5 hour at 37 °C.

4. Cells were collected by centrifugation of 1 ml from each sample and stored at -20 °C. The expression was checked by SDS-PAGE.

Cells storage at -80 °C

Overnight culture of 10 ml LB medium containing 35 µg/ml kanamycin (5 tubes) was grown overnight at 37 °C. In small 1.5 ml tubes (3 tubes from each culture), 0.15 ml 70 % sterilized glycerol and 0.85 ml overnight culture was mixed and stored immediately in liquid nitrogen until it is ready to store at -80 °C.

D.2. SDS-PAGE

Determination of the purity of protein fractions from the Ni_{2+} Sepharose 6 fast flow

column or other purification methods were performed by using SDS PAGE as described in

the Mini-PROTEAN® 3 Cell Instruction Manual.

The procedure for gel casting (Mini-PROTEAN® 3 Cell Instruction Manual):

1. For most protein purifications, 12 % Laemmli buffer system was used. 4.0 ml of 30 % acrylamide/ Bis stock solution in 3.35 ml of deionized water, 2.50 ml of 1.5 M Tris-HCl (pH 8.8), 100 µl of 10 % SDS and 50 µl of 10% APS were combined for making resolving gel. For larger proteins (>150 kDa), 7.5 % Laemmli buffer was used. 2.5 ml of 30 % acrylamide/ Bis stock solution and 4.85 ml of deionized water was used with same reagents as the 12 % system.

2. 5.0 µl of TEMED was added into this mixture to initiate polymerization. This solution was added to the preassembled case immediately, and deionized water was overlaid. Then, the cast containing resolving gel solution was solidified for 30 min at room temperature.

3. After 30 min at room temperature, overlaid water was decanted from the cast, and 1.33 ml of 30 % acrylamide/ Bis stock solution in 6.10 ml of deionized water, 2.5 ml of 0.5 M Tris-HCl (pH 6.8), 100 µl of 10 % SDS and 50 µl of 10% APS was combined for making stacking gel.

4. 10.0 µl of TEMED was added into this mixture to initiate polymerization. This solution was poured on the top of solidified resolving gel, and sample combs were

added on the stacking gel for making sample pockets. This cast containing stacking gel solution was solidified for 30 min at room temperature.

Sample preparation:

Protein fractions from columns were diluted to 1-2 µg/ml concentration. From that 5 µl sample was taken and added 50 µl of sample buffer containing 3.8 ml of deionized water, 1.0 ml of 0.5 M Tris-HCl (pH 6.8), 0.8 ml of glycerol, 1.6 ml of 10 % (w/v) SDS, 0.4 ml of 2-mercaptoethanol, and 0.4 ml of 1 % (w/v) bromophenol blue (8.0 ml total volume) and this mixture was heated for 3 min in boiling water bath.

Loading and running samples on SDS-PAGE:

1. 10x electrode (Running) buffer, pH 8.3, was prepared as follows: 30 g/l Tris base, 144 g/l Glycine, and 10 g/l SDS to 1.0 L with dionised water. Dilute 70 ml of 10x running buffer with 630 ml deionized water for one electrophoretic run.

2. 15-20 µl of prepared samples were applied to the gel and allowed to run for 15 min at 100 volts and then for 40 min at 140 volts.

3. The gel was stained with staining solution containing 40 % methanol, 10 % acetic acid and 0.1 % Cooamassie blue R-250 indicator for 15 min and destained with destaining solution (I) containing 50 % methanol and 10 % acetic acid for 10 min and (II) 5 % methanol and 7 % acetic acid for overnight.

D.3. Determination of Protein concentration by Bradford assay

The calibration of Bradford reagent

1. Prepare dye reagent by diluting 1-part Dye Reagent Concentrate (Bio-Rad catalog # 500-0006) with 4 parts deionized water. Filter through Whatman #1 filter (or

equivalent) to remove particulates and store at 4 ℃. Every 2 weeks calibrate the Bradford reagent.

2. Prepare fifteen dilutions of a protein standard (BSA ~2mg/ml), which is representative of the protein solution to be tested. The linear range of the assay for BSA is 0.1 to 0.9 mg/ml.

3. Pipet 50 μl of each standard and sample solution into a clean, dry test tube. Protein solutions are normally assayed in duplicate or triplicate.

4. Add 2.5 ml of diluted dye reagent to each tube and vortex.

5. Incubate at room temperature for at least 5 min and measure absorbance at 595 nm.

6. Plot the absorbance as a function of standard (BSA) concentration to make a calibration curve from which concentration of similarly treated unknown could be determined.

The determination of protein concentration:

1. Appropriately dilute protein (usually 10x or 25x dilution) and pipet diluted protein into clean and dry test tubes to 50 μl of total volume with deionized water.

2. Add 2.5 ml of diluted dye reagent to each tube and vortex.

3. Incubate at room temperature for at least 5 min and measure absorbance at 595 nm.

4. Estimate protein concentration using the linear equation from the calibration of bradford dye reagent.

Elena L. Guevara
elenague@rutgers.edu
Department of Chemistry
73 Warren Street
Newark, NJ 07102

CURRENT POSITION

Rutgers, The State University of New Jersey - Newark, NJ
Graduate Fellow, 2009 – present

EDUCATION

Rutgers, The State University of New Jersey - Newark, NJ
PhD, Chemistry, March 2017

Fordham University - Bronx, NY
BS, Chemistry, May 2009

GRANTS AND AWARDS

Ruth L. Kirschstein Pre-Doctoral National Research Service Award
2015 – 2016
National Institute of General Medical Sciences, National Institute of Health
Grant #: 5F31GM113601-02

Graduate School of Newark, Dissertation Fellow
2014 – 2015 Rutgers, The State University of New Jersey

Minority Biomedical Research Support Program (MBRS), NIH Fellow
2011 – 2013
Rutgers, The State University of New Jersey
Grant #: 5R25GM096161-02

PROFESSIONAL MEMBERSHIPS

Sigma Xi – National scientific research honors society (associate membership)
American Chemical Society – Graduate Student Affiliate
American Association for the Advancement of Science – Member
American Society for Biochemistry and Molecular Biology – Member
American Association of University Women – Member

CONFERENCE PRESENTATIONS

Guevara, E. L., Yang, L., Nemeria, N.S., Jordan, F. Mechanism and Interaction studies of Human PDC with its Kinases [oral presentation]. In: 44th Mid-Atlantic Regional Meeting; 2016 June 9-12; Riverdale, NY.

Guevara, E. L., Nemeria, N.S., Yang, L., Jordan, F. Mechanism and Interactions of Human Pyruvate Dehydrogenase Complex with its Kinase 1 [poster presentation]. In: ASBMB 2016 Annual Meeting; 2016 April 2-6; San Diego, CA.

Leong, F. G., **Guevara E. L.**, Hansen, D. B. Improving the expression and purification of pqsH, a protein involved in quorum-sensing in *Pseudomonas aeruginosa* [poster presentation]. In: 38th ACS Northeast Regional Meeting; 2012 September 30 - October 3; Rochester, NY.

Guevara, E. L., Hansen, D.B. Role of PqsH and its promiscuity towards various quinolone quorum sensing molecules [poster presentation]. In: 244th ACS National Meeting & Exposition; 2012 August 19-23; Philadelphia, PA.

Guevara, E. L., Anand, P., Hansen, D. B. Understanding structural diversity in quinolone quorum sensing molecules across bacterial species [poster presentation]. In: 243rd ACS National Meeting & Exposition; 2012 March 25-29; San Diego, CA.

PUBLICATIONS

Guevara, E. L., Yang, L., Birkaya, B., Zhou, J., Nemeria, N.S., Patel, M.S., Jordan, F. Global view of cognate kinase activation by the human pyruvate dehydrogenase complex [Manuscript accepted in Nature Scientific Reports].

Ciaccio, J. A., **Guevara, E. L.**, Alam, R. & D'agrosa, C. D. Probing the Reactivity of Dimethylsulfoxonium Methylide with Conjugated and Nonconjugated Carbonyl Compounds: An Undergraduate Experiment Combining Synthesis, Spectral Analysis, and Mechanistic Discovery. *J Chem Educ* **87**, 850–853 (2010).